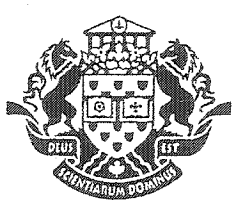

Université d'Ottawa · University of Ottawa

Université d'Ottawa • University of Ottawa

FACULTÉ DES ÉTUDES SUPÉRIEURES ET POSTDOCTORALES

FACULTY OF GRADUATE AND POSTDOCTORAL STUDIES

Valérie GRECO

AUTEUR DE LA THÈSE - AUTHOR OF THESIS

M. Sc. (Microbiology and Immunology)

GRADE - DEGREE

Department of Biochemistry, Microbiology and Immunology

FACULTÉ, ÉCOLE, DÉPARTEMENT - FACULTY, SCHOOL, DEPARTMENT

TITRE DE LA THÈSE - TITLE OF THE THESIS

Functional Analysis of the Role of Conserved Glycine Residues and N-termunus Motifs in the Cell Division Inhibitor MinC from *Neisseria gonorrhoeae*

J.R. Dillon

DIRECTEUR DE LA THÈSE - THESIS SUPERVISOR

CO-DIRECTEUR DE LA THÈSE - THESIS CO-SUPERVISOR

EXAMINATEURS DE LA THÈSE - THESIS EXAMINERS

D. Gray

M. Kozlowski

J.-M. De Koninck, Ph.D.

LE DOYEN DE LA FACULTÉ DES ÉTUDES SUPÉRIEURES ET POSTDOCTORALES

DEAN OF THE FACULTY OF GRADUATE AND POSTDOCTORAL STUDIES

Functional Analysis of the Role of Conserved Glycine Residues and N-terminus Motifs in the Cell Division Inhibitor MinC from *Neisseria gonorrhoeae*

Valerie S. Greco

A thesis submitted to the
School of Graduate Studies and Research
University of Ottawa
In partial fulfillment of the requirements for the
Degree of Master of Science
Department of Biochemistry, Microbiology, and Immunology
Faculty of Medicine

Your file Votre référence
ISBN: 0-494-01482-2
Our file Notre référence
ISBN: 0-494-01482-2

ABSTRACT

MinC is the principle inhibitor of cell division in the Gram negative coccus *Neisseria gonorrhoeae*. Multiple alignment of 28 *minC* homologues from prokaryotic organisms revealed the conservation of four glycines in the C-terminus. Radical mutations of these residues, G138D, G157D, G164S, and G174E, were introduced to $minC_{Ng}$ using site-directed mutagenesis and were expressed heterologously in *Escherichia coli*. Microscopic analysis of cellular morphology revealed abrogation of $MinC_{Ng}$ function as indicated by the inability of the overexpressed protein to induce filamentation, and flow cytometry substantiated these data. The radical mutation of a non-conserved residue was also performed, and no impact on $MinC_{Ng}$ function was observed. Circular dichroism was employed to confirm the preservation of protein structure in all mutants. Using the crystal structure of MinC from *Thermotoga maritima*, the position of the mutations of conserved and non-conserved residues was ascertained. The glycine residues were thus demonstrated to be of paramount importance to protein functionality and their conservation indicates a role for these residues in MinC function among bacterial species. The N-terminus of $MinC_{Ng}$ is not conserved across species, but contains common structural motifs that were similarly mutagenized with moderate effect on the resultant protein as ascertained using similar methodology. Truncations of $MinC_{Ng}$ revealed the necessity of the thirteenth amino acid for division inhibition function. Although the first ten amino acids were not necessary for protein function, the resultant protein was expressed and present in abundance, implicating a role for the extreme N-terminal region in protein stability. Plasmids for $MinC_{Ng}$ localization and purification were also constructed to facilitate future experimentation.

ACKNOWLEDGEMENTS

"None but those who have experienced them can conceive of the enticements of science."(M.W. Shelley, 1818)

A great professor I once had told me that she enjoyed essays and narratives beginning with an appropriately selected quotation. I cannot possibly think of a better way to enthusiastically express my love of research, and my gratitude at having had this opportunity to experiment in the field of molecular microbiology. I could not possibly have chosen a better group of scientists to work with; the sole term "scientist" does not completely describe their roles as colleagues as I also value everyone as dear friends. Jo-Anne has been an excellent supervisor; she was always full of insight and motivation, and was patient and accommodating when my health was poor. Sandra – what can I possibly say? You are among the most sweet and intelligent people I know, and have been so kind in training me in all aspects of bacterial research. Your help has truly been invaluable. Everyone in the laboratory has definitely enhanced my Master's experience. I've never seen Jason have a bad day; he is always willing to help us underlings and "minions". Likewise, Nelson, Marc, and Sudeep have always readily contributed to my knowledge of the other cell division proteins, and I could always count on them to cast a vote in my favour for an action/sci-fi movie when we went to the theatre. Pierre Fabre, under supervision by Sandra and myself, was greatly helpful with this endeavor during his Honours studies. The plant crew, Pat and Ming-Min, were always friendly and helpful in keeping me up to date with their research. The ISSTDR conference was an amazing experience! As for Susan, our discussions over coffee were always welcome, and provided a great venue for the exchange of research ideas; you are a great friend to

me. Dan "the protein man" made all of the purifications possible, and contributes so much to the lab through his friendly, humorous personality. Though I didn't get to know Tatiana well, I sincerely appreciate her continuation of the work that I initiated and I wish her all the best in her future research.

Everyone in BMI has been exceptionally helpful, and I am grateful for all of the friends I've made and for the assistance I've received from the graduate office, the sterilization center, and the Biotechnology Research Institute. I would also like to thank Dr. Filion and Dr. Franks for their assistance with the flow cytometer and fluorescence microscope, respectively, and for tolerating me over the years in my graduate courses. My thesis advisory committee deserves special thanks. Dr. Wright, Dr. Gray, and Dr. Trudeau have been wonderful mentors and have guided me well and contributed many useful ideas for my research.

Many of the professors at the University of Ottawa have had a positive influence on my life and have contributed greatly to my university experience. I would like to thank Dr. Illimar Altosaar for providing me with my first laboratory experience and setting the foundation for my research career. Dr. Doug Johnson has also been extremely supportive of me and has always assisted me, whether it be research or scholarship related. Lorrie Graham was a great professor and a true friend; she believed in me and supported me when my academic career was beginning and others had discouraged me. Other professors that inspired me (and entertained my myriad questions and ideas) include Dr. Thor Arnason, Dr. J. Fenwick, Dr. John Basso and Dr. Jagdeep Sandhu. I couldn't have imagined a more wonderful university experience!

Outside of the lab, I have had a wonderful support network, mainly comprising my near friends and family. My parents have always supported me, financially and

emotionally, and have always encouraged my pursuit of the sciences. Carey has always been someone in which to confide and swap University of Ottawa gossip and stories; I wish her the best experience possible, something akin to what I enjoyed. Wilfred has been exceptional throughout this time, always motivating and encouraging me, providing the proverbial shoulder to cry on, being my *help in doubt and need*, and elevating my mood with his jovial personality. Anna-Maria, you have always been there for me and my university experience wouldn't have been the same without you! And Dave, I love your company and appreciate that you always drag yourself out to Orleans to visit.

Everyone mentioned in this passage is dear to me, has enhanced my life, and will continue to remain dear companions.

"It's funny. Don't ever tell anyone anything. If you do, you start missing everybody."
(J.D. Salinger, 1945)

TABLE OF CONTENTS

LIST OF TABLES

LIST OF FIGURES

LIST OF ABBREVIATIONS

A	alanine
aa	amino acids
AD	activation domain
ATP	adenosine 5'-triphosphate
ATPase	adenosine 5'-triphosphate dephosphorylase
BD	binding domain
bp	base pairs
Bs	*Bacillus subtilis*
BSA	bovine serum albumin
C	cysteine
CD	circular dichroism
D	aspartic acid
dcw	division and cell wall synthesis gene cluster
ddH_20	double distilled water
DNA	deoxyribonucleic acid
dNTP	deoxinucleotide triphosphate
DTT	dithiothreitol
E	glutamic acid
Ec	*Escherichia coli*
EDTA	ethylene diamine tetra-acetic acid
F	phenylalanine
g	gram
G	glycine
GCMBK	gonococcal medium base with Kellogg's supplement
GFP	green fluorescent protein
GTP	guanosine triphosphate
GTPase	guanosine triphosphate dephosphorylase
GST	glutathione S-transferase
H	histidine
I	isoleucine
IPCR	Inverse polymerase chain reaction
IPTG	isopropyl-β-D-thiogalactopyranoside
K	lysine
kb	kilobase pairs
L	leucine
M	methionine
mg	milligram
min	minicell gene cluster, minicell phenotype
MinCCh	Chimeric MinC ($MinC_{Ec}^{1-99}$-$MinC_{Ng}^{103-237}$)
ml	milliliter
mM	millimolar
N	asparagine
NEB	New England Biolabs
Ng	*Neisseria gonorrhoeae*

ng	nanogram
P	proline
PBS	phosphate-buffered saline
PCR	polymerase chain reaction
Q	glutamine
R	arginine
S	serine
SDM	site-directed mutagenesis
T	threonine
TAE	tris-acetate-EDTA buffer
µg	microgram
µl	microlitre
µM	micromolar
µm	micrometer
V	valine
W	tryptophan
X-gal	5-bromo-4-chloro-3-indoyl-β-D-galactoside
Y	tyrosine

1. INTRODUCTION

Cell division is a fundamental process of all living organisms that ensures equipartitioning of genetic and cellular materials between two daughter cells. Bacterial binary fission, which results in the establishment of two equal-sized daughter cells, is no less complex or critical a process than what is observed in eukaryotic organisms. Bacterial growth and viability is dependent on proper and efficient cell division (Adler *et al.*, 1967; de Boer *et al.*, 1988; Lutkenhaus and Adinall, 1997). Bacterial cell division has been studied intensively in model rod-shaped organisms such as *Escherichia coli* (Gram-negative) and *Bacillus subtilis* (Gram-positive), where several mechanisms for proper placement of the division septum to ensure successful cell division have been elucidated. Two complex genetic loci, the *dcw* and *min* gene clusters (de Boer *et al.*, 1988; Yura *et al.*, 1992), encode a number of proteins that have been implicated in midcell site selection and cell division in most prokaryotic species and are currently the subject of much investigation. While these proteins have been highly scrutinized in rod-shaped bacteria, studies of their homologues in round bacteria have been largely neglected. Division in coccal cells remains enigmatic, as no distinct midcell is present in these round cells. Our laboratory has selected the Gram-negative coccus *Neisseria gonorrhoeae* as a model organism to determine the mechanism by which spherical Gram-negative cells divide.

1.1 Cell division in prokaryotes: An overview

Bacteria divide by the process of binary fission. In rod shaped bacteria such as *E. coli* and *B. subtilis*, division occurs with high fidelity at midcell perpendicular to the long

axis to produce two daughter cells of similar size and containing a complete bacterial chromosome (Nanninga and Woldringh, 1985; Figure 1A). Although seemingly simple, this division requires a host of highly specific and perfectly choreographed events to result in two viable cells. Division is essential to the growth and propagation of bacteria; should any link in the division chain falter, reduced viability and cessation of growth will result.

Binary fission relies on a series of events including chromosome replication, segregation of the newly-formed nucleoids, selection of the midcell septation site, invagination of the cytoplasmic membrane at midcell, and synthesis of peptidoglycan to complete the emancipation of one cell from the other. Different bacterial species rely on various mechanisms to achieve cellular division; of particular interest in this discussion is that of the Gram-negative organism.

Cell division is most highly characterized in the Gram-negative rod *E. coli*. After chromosome replication, septation begins almost immediately at a specific cellular location as determined by a complex network of proteins (Donachie, 1993). Cytokinesis, the separation of cytoplasmic compartments, and septation occur together; this requires the coordinated ingrowth of the cell membrane, peptidoglycan, and outer membrane (Donachie, 1993). This process requires the synthesis of peptidoglycan, which is initially covalently bonded between the two cells prior to complete separation (Donachie, 1993). Division occurs in one plane, with the septum forming at midcell, perpendicular to the long axis of the cell (Figure1A). After separation, *E. coli* daughter cells increase in length in one dimension, with elongation proceeding from the pole at which the septum was present in a prior division (Donachie and Begg, 1970). Daughter cells then grow in

Figure 1: Bacterial cell division. A: Rod-shaped bacteria such as *E. coli* divide in one plane parallel to cell poles. A': Electron micrograph of cell division in *E. coli* (www.bio.mtu.edu/campbell/prokaryo.htm). B: *N. gonorrhoeae* divides in alternating, perpendicular planes. Two divisions result in a tetrad of daughter cells. B'1: Electron micrograph of *N. gonorrhoeae* cell division (Dillon laboratory). B'2: Phase contrast micrograph of a *N. gonorrhoeae* tetrad (Dillon laboratory).

A.

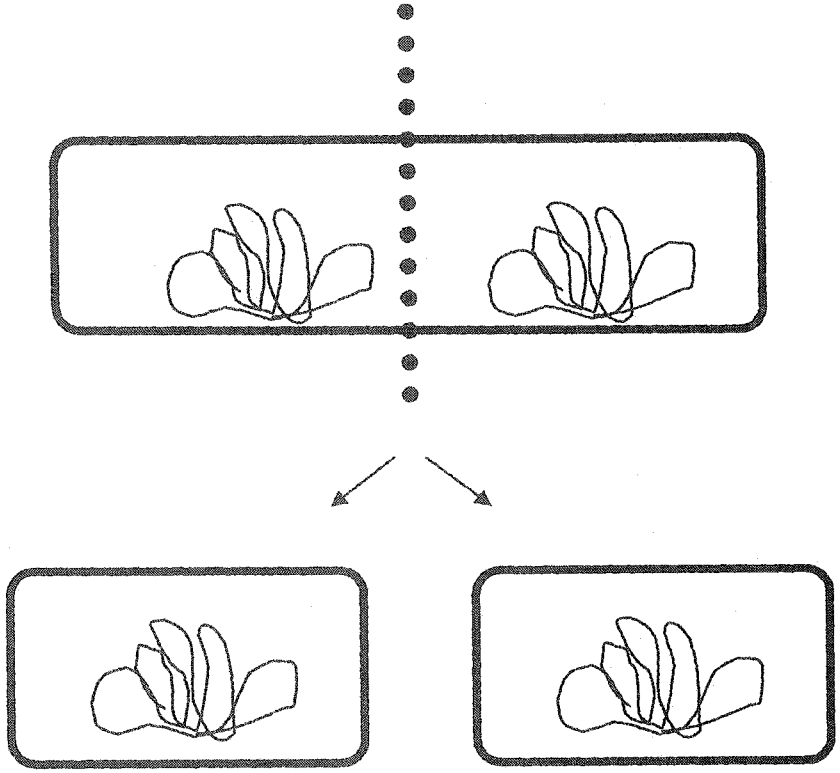

B. 1.

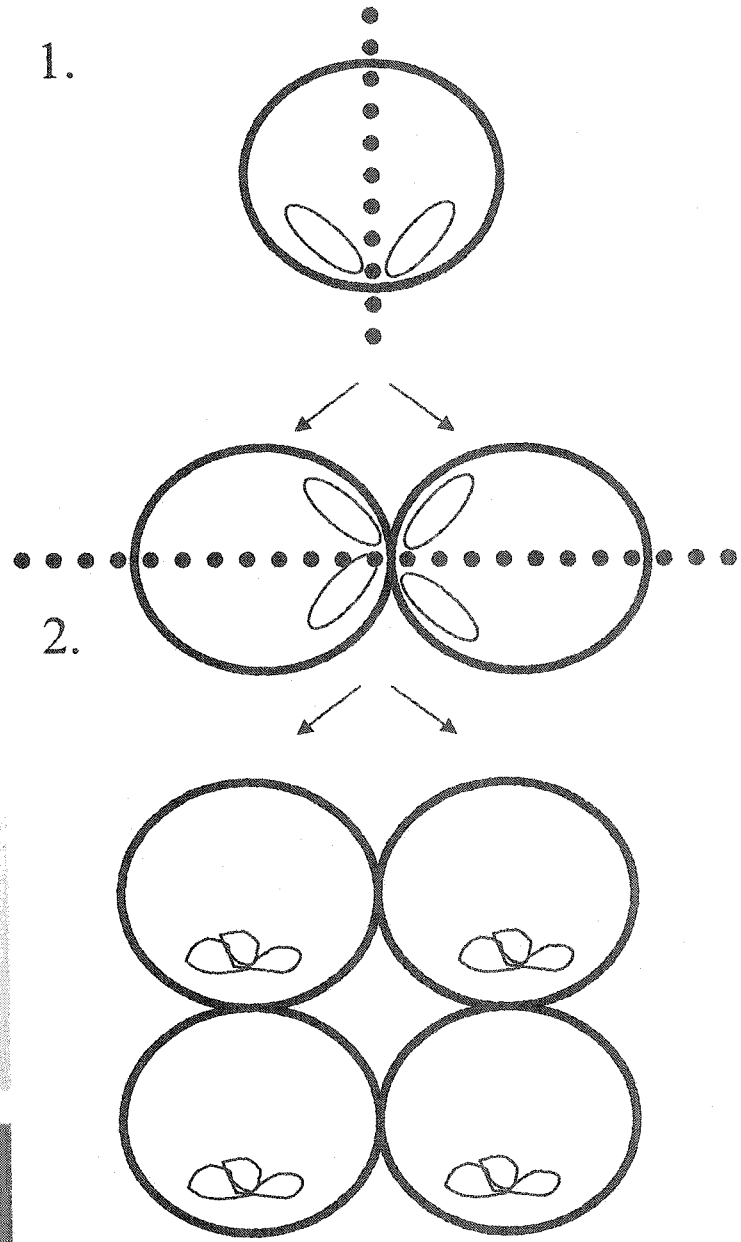

2.

A'.

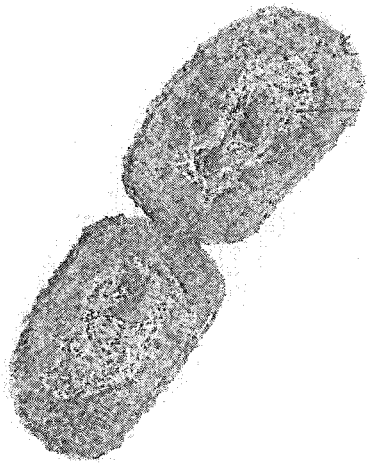

www.bio.mtu.edu/campbell/
prokaryo.htm

B'. 1.

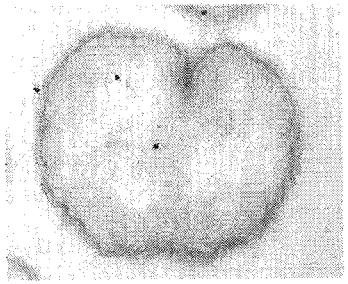

2.

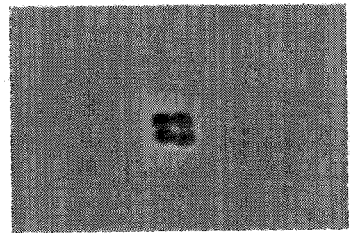

opposite directions, and are then capable of repeating the division process. Subsequent cellular divisions of the daughter cells occur on the same plane.

N. gonorrhoeae also divides by forming a septum in a similar manner as occurs in *E. coli*, however the process varies slightly from that occurring in Gram-negative rods. Division involves asymmetrical invagination of the membrane opposite from the nucleoid (Fitz-James, 1964), and cells grow perpendicular to the invagination. Prior to the complete division of these daughter cells, another division is initiated in a plane perpendicular to the nascent septum (Westling Häggström *et al.*, 1977). This bi-directional growth gives rise to tetrads of gonococcal cells, a phenomenon that is also observed in the case of *N. meningitidis* and *N. pharyngitis* (Westling Häggström *et al.*, 1977). Figure 1B illustrates the growth of *N. gonorrhoeae* through alternating, perpendicular cell divisions; this growth pattern is in marked contrast to that observed in the Gram-negative rod.

1.2 Cell division proteins: the *dcw* cluster

The *dcw* (division and cell wall synthesis) locus has been implicated in cell division and synthesis of peptidoglycan (Yura *et al.*, 1992). The *dcw* cluster in *E. coli* comprises 16 genes located at the 2 min chromosomal region and encodes several proteins that are essential to cell growth and survival (Yura *et al.*, 1992; Ayala *et al.*, 1994; Lutkenhaus and Adinall, 1997; Tamames *et al.*, 2001; Figure 2). These genes are close together, occasionally overlapping, and oriented in one direction (Yura *et al.*, 1992). The *dcw* cluster has homologues identified in 24 bacterial species, and phylogenetic analysis has shown that the relationships between genes in the *dcw* clusters might represent evolutionary events in shape determination and growth in bacteria (Vicente *et al.*, 1998;

Figure 2: Genetic organization of the dcw gene cluster in *E. coli*, *B. subtilis*, and *N. gonorrhoeae*. Adapted from Francis *et al.*, 2000, Tamames *et al.*, 2001, and Snyder *et al.* 2003.

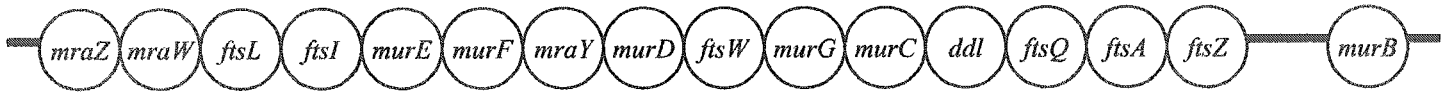

Escherichia coli

Bacillus subtilis

Neisseria gonorrhoeae

Tamames *et al.*, 2001). The order of the *dcw* genes is mostly conserved between species (Figure 2), although organization sometimes varies; in *Helicobacter pylori*, the genes are located at seven different chromosomal locations (Vincente *et al.*, 1998).

One of the most ubiquitous and conserved proteins in the *dcw* gene cluster is FtsZ, a cytoskeletal element and homologue of the eukaryotic tubulin, which forms a ring at the midcell site where septation is to occur and is involved in the cytokinetic event leading to the realization of two separate daughter cells (Bi and Lutkenhaus, 1991; Ayala *et al.*, 1994). FtsZ has intrinsic GTPase activity that is required for self-assembly into protofilaments (FtsZ homopolymers) that subsequently form a contractile ring at midcell prior to cytokinesis (Bi and Lutkenhaus, 1991; Bramhill and Thompson, 1994). The Z-ring, composed of polymerized FtsZ, also serves as a scaffold with which other division-associated proteins such as ZipA, ZapA, FtsA, FtsQ, FtsL, FtsK, FtsI, FtsN, and FtsW associate (Dewar and Dorazi, 2000; Margolin 2001; Margolin, 2003). It is believed that accessory proteins such as ZipA and ZapA serve to bundle the FtsZ protofilaments to form the contractile Z-ring (Margolin, 2003). FtsZ has also been found in chloroplasts where it is essential for organellar division functioning in a manner similar to that observed in prokaryotic organisms (Osteryoung and Vierling, 1995). *E. coli* mutants lacking *ftsZ* formed long, smooth, filamentous cells, while cells over-expressing *ftsZ* from medium copy-number plasmids exhibit the minicell phenotype (Begg and Donachie, 1985). The minicell phenotype is characterized by cell populations that are heterogeneously comprised of small, anucleate cells and elongated, multinucleate rods (de Boer et al., 1988). Extremely high intracellular levels of FtsZ expressed from high copy-number plasmids induce a filamentous phenotype (Begg and Donachie, 1985).

Eight other essential division-associated proteins are encoded by the *E. coli dcw* cluster include FtsA, FtsQ, FtsW, FtsI, FtsK, FtsL, FtsN, and ZipA (Rothfield and Justice, 1997). A complete list of genes encoded by the *dcw* cluster and their genetic order is depicted in Figure 2. FtsA, a protein that associates with the Z-ring early in cell division, is similar in structure to the ATP-binding cytoskeletal eukaryotic protein actin (Sanchez *et al.*, 1994). Other proteins encoded by this region (i.e. the *mur* proteins) are involved in peptidoglycan biosynthesis (Ayala *et al.*, 1994). The *ftsI* gene encodes a penicillin-binding protein that is present in all microbes possessing peptidoglycan cell walls and is essential for cell viability (Curtis *et al.*, 1985). It is involved in peptidoglycan synthesis at the septum during division (Curtis *et al.*, 1985). These proteins, in concert with those encoded by the *minB* locus (see below), enable division site selection, septation, and cytokinesis, resulting in the formation of two daughter cells.

A *dcw* cluster exists in *N. gonorrhoeae* and is comprised of 17 genes including homologues of FtsZ, FtsI, FtsW, and FtsA (Francis *et al.*, 2000; Snyder *et al.*, 2001; Figure 2). The *ftsL* gene is the least conserved *dcw* gene among species, and there is some debate as to whether or not its homologue has been identified in *N. gonorrhoeae* and should be included as an eighteenth gene at this locus (Snyder *et al.*, 2001). Most of the *dcw* genes are involved in cell division, although two genes that are present in the *E. coli dcw* cluster are lacking from the gonococcal cluster and three novel genes are present (Francis *et al.*, 2000). These three genes, *dcaA, dcaB,* and *dcaC* (division cluster competence-associated genes) have been characterized by Snyder *et al.* (2001; 2003) and it has been determined that *dcaA* is involved in natural competence in *N. gonorrhoeae* and is also subject to phase variation. The *ftsI* (*penA*) gene encodes a penicillin-binding protein involved in cell wall synthesis named penicillin-binding

protein 2 (PBP2); alteration in this protein through genetic mutation has been demonstrated to cause decreased susceptibility to penicillin (Sparling *et al.*, 1975; Spratt, 1988).

$FtsZ_{Ng}$ from *N. gonorrhoeae* has also been characterized (Salimnia *et al.*, 2000). It is a 41.5 kDa protein containing the conserved GTP-binding motif of other FtsZ proteins (Salimnia *et al.*, 2000). $FtsZ_{Ng}$ has been shown to be essential for gonococcal cell viability and is functional in *E. coli*, as filamentation results from its heterologous overexpression (Salimnia *et al.*, 2000). GFP-tagged $FtsZ_{Ng}$ localizes at midcell in *E. coli* as has been demonstrated in *E. coli* with native $FtsZ_{Ec}$ (Salimnia *et al.*, 2000).

Regulation of the *dcw* genes is complex and has been intensely studied in *E. coli*. Perfect choreography of division-associated events is essential for the successful generation of two equal-sized daughter cells (Dewar and Dorazi, 2000). Regulation of gene expression occurs at both the transcriptional and post-transcriptional levels (Vicente *et al.*, 1998). The *dcw* genes are transcribed in one direction, although several promoters are present, including at least six promoters for *ftsZ* alone (Aldea *et al.*, 1990; Cam *et al.*, 1996).

Five transcription start sites are found at the 5' end of the *E. coli dcw* cluster as well as three LexA (a repressor of SOS response gene transcription) binding sites (Vicente *et al.*, 1998). Several *cis-* and *trans-* acting signals regulate gene expression from these various promoters (Vicente *et al.*, 1998). The cluster lacks termination signals, allowing for transcription of even the furthest gene downstream, *envA* (Vicente *et al.*, 1998). Gearbox promoters, or promoters that are used for high levels of transcription of genes during periods of slow bacterial growth, are present in the cluster and regulate expression of *ftsA*, *ftsQ*, and *ftsZ* (Aldea *et al.*, 1990, Vicente *et al.*, 1991).

Consequently, the rate of transcription of these genes varies with cell growth; more transcription occurs during periods of slow growth (Aldea *et al.*, 1990). Many of the *dcw* genes are transcribed as polycistronic mRNA, including the *ftsQAZ* transcript (Vicente *et al.*, 1998). Antisense RNA is also transcribed and used to regulate gene expression (Vicente *et al.*, 1998).

Additional regulation of gene expression occurs at the level of mRNA stability; RNAse E sites have been identified (Cam *et al.*, 1996). One such site exists within the *ftsA* transcript that could account for the differences in protein levels of FtsZ and FtsA despite relatively similar levels of transcription. It has also been proposed that FtsA might have an autoregulatory role in repressing gene expression from both *ftsQ* and *ftsA* promoters (Dewar *et al.*, 1989). All of these strategies are employed to carefully coordinate events leading to the division of the bacterial cell.

Our laboratory has investigated the regulation of *dcw* gene transcription in *N. gonorrhoeae* and has determined that complex mechanisms for gene expression exist in this bacterium (Francis *et al.*, 2000). The *dcw* cluster in *N. gonorrhoeae* is divided into four transcriptional units (Francis *et al.*, 2000) as compared to one transcriptional unit in *E. coli* (Yura *et. al.*, 1992). Transcriptional terminators consisting of paired neisserial uptake sequences flank the gonococcal *dcw* cluster, and four internal terminators (three of which contain paired neisserial uptake sequences) have been discovered. A Correia element (a repeated sequence from the gonococcal genome) was also identified as a transcription terminator. Six promoters, some of which are preferentially used under conditions of anaerobiasis, were also identified in the *dcw* cluster; three of these promoters were located upstream of *ftsZ*. It is thus evident that the extreme regulation of *dcw* genes in many bacterial species is essential to complete functionality of the cell

division process. While the *dcw* proteins are essential for the division event, selection of the site at which division should occur is critical and is achieved through the Min system that is both intricate and dynamic.

1.3 Midcell site selection: the *min* locus

The first recognized step in bacterial cell division is the selection of the division site that typically occurs between the two newly-separated nucleoids at midcell (Sullivan and Maddock, 2000; Errington *et al.,* 2003). When the proper midcell division site is selected, two equal-sized, nucleated daughter cells result (Figure 1). In 1967, Adler *et al.* observed populations of *E. coli* cells that were small and anucleate. These miniature cells were subsequently observed and characterized in both Gram-positive and Gram-negative bacteria (Frazer and Curtiss, 1975) and were called minicells. This phenotype was speculated to result from improper division site selection resulting in division occurring at typically neglected potential division sites at the cell poles (Teather *et al.*, 1974). de Boer *et al.* (1988) subsequently characterized a genetic locus in *E. coli* that, when over- or underexpressed resulted in a phenotype characterized by the presence of long, multinucleate cells and smaller anucleate cells (minicells). This locus, the *minB* (minicell) locus, encodes three proteins, MinC, MinD, and MinE, which are responsible for determination of division site placement in *E. coli* (de Boer *et al.,* 1989). Several mutations in the *minB* locus give rise to cells that exhibit the minicell phenotype (Adler *et al.,* 1967; Jaffe *et al.*, 1988).

MinC and MinD comprise the principal proteins that inhibit cell division while MinE imparts topological specificity (determines the cellular location) to the site at which septation will occur (de Boer *et al.,* 1989). Deletion of the *minB* locus in *E. coli*

resultes in the minicell phenotype since no control is exerted over division site selection and polar sites are utilized (de Boer *et al.*, 1989). Overexpression of *E. coli* MinC ($MinC_{Ec}$) together with *E. coli* MinD ($MinD_{Ec}$) or sufficiently high concentrations of $MinC_{Ec}$ alone (i.e. 25X naturally occurring intracellular levels) results in cellular filamentation (multinucleate, aseptate cells reaching lengths in excess of 6X the wild-type cell length) due to the inability of the bacterium to divide at both midcell and polar sites (de Boer *et al.*, 1989, Donachie, 1993). Consequently, $MinC_{Ec}$ function can be ascertained morphologically as the ability to induce filamentation in bacteria when expressed from a high copy-number plasmid.

In *E. coli*, placement of the division septum is partially determined by the location of the nucleoid, the region of the cell containing the bacterial chromosome (Sun and Margolin, 2001). Additional regulation of midcell site selection is performed by the *minB*-encoded proteins (de Boer et al., 1989). The Min proteins are the principal determinants of where the Z-ring will form and where the cell will consequently divide (de Boer *et al.*, 1989). Homologues of $MinC_{Ec}$, $MinD_{Ec}$, and $MinE_{Ec}$ have been identified in many prokaryotic organisms (Varley and Stewart, 1992; Ramirez-Arcos *et al.*, 2001a), however Gram-positive bacteria such as *Bacillus subtilis* lack a functional $MinE_{Ec}$ homologue and subsequently utilize a different protein, DivIVA, in the determination of proper septal placement (Cha and Stewart, 1997). Other prokaryotes lack a *min* system, and their mechanisms of cell division site selection remain largely enigmatic. FtsZ from *E. coli* ($FtsZ_{Ec}$), self-assembles by hydrolyzing GTP to form a ring at the site of septation, and constitutes the primary structure facilitating the cytokinetic event leading to cell division (Hu *et al.*, 1999). MinC is the principle inhibitory protein of cell division in rod-shaped bacteria. $MinC_{Ec}$ prevents septation by promoting the

depolymerization of $FtsZ_{Ec}$ which forms the cytoskeletal ring at midcell during the septation event (Hu *et al.*, 1999).

Overexpression of $MinC_{Ec}$ results in cellular filamentation as cell division is prevented at all potential division sites, including the proper site at midcell (de Boer *et al.*, 1989). In the absence of $MinC_{Ec}$, the minicell phenotype is observed as division is permitted at all potential division sites due to lack of $FtsZ_{Ec}$ polymer destabilization, resulting in a heterogeneous population of elongated cells and small minicells that lack chromosomal material (de Boer *et al.*, 1989).

$MinD_{Ec}$ is an ATPase that dimerizes when bound to ATP in the cytosol and has a molecular mass of approximately 30 kDa (de Boer *et al.*, 1989; de Boer *et al.*, 1992; Hu *et al.*, 2003; Lackner *et al.*, 2003; Lutkenhaus and Sundaramoorthy, 2003). It recruits $MinC_{Ec}$ in the cytosol and moves to the cell membrane where it interacts with phospholipids (Hu *et al.*, 2002; Hu *et al.*, 2003; Lackner *et al.*, 2003; Lutkenhaus and Sundaramoorthy, 2003). It has been hypothesized that the $MinC_{Ec}$-$MinD_{Ec}$ interaction brings the N-terminal domain of $MinC_{Ec}$ in close proximity to $FtsZ_{Ec}$ to enable depolymerization and prevent Z-ring formation at polar sites (Johnson *et al.*, 2002).

$MinE_{Ec}$, the smallest of the Min_{Ec} proteins with a molecular mass of only 10 kDa, is the topological specificity factor that ensures division is inhibited at incorrect, non-polar sites while permitting division at midcell by relieving inhibition by $MinC_{Ec}$ (Shih *et al.*, 2002). $MinE_{Ec}$ comprises two domains, a small N-terminal domain that interacts with $MinC_{Ec}$-$MinD_{Ec}$, and a C-terminal domain that imparts topological specificity for the alleviation of division inhibition at midcell (de Boer *et al.*, 1989; Zhao *et al.*, 1995). $MinE_{Ec}$ dimerizes through interaction between central portions of the molecules (Pichoff *et al.*, 1995). Overexpression of $MinE_{Ec}$ results in minicell formation as division is

permitted to occur at cell poles (de Boer *et al.*, 1989; Pichoff *et al.*, 1995). The Min system, in association with other accessory proteins, achieves proper cell division in *E. coli*, and homologues to these proteins have subsequently been established in a number of other bacterial species including *N. gonorrhoeae* by our laboratory (Ramirez-Arcos et. al, 2001, Errington *et al.*, 2003).

The Min proteins from *E. coli* have been shown to be dynamic, oscillating from pole to pole to prevent septation at polar division sites (Meinhardt and de Boer, 2001). In the current model of cell division in *E. coli* (Figure 3), $MinD_{Ec}$ dimerizes in the presence of ATP. This $MinD_{Ec}$-ATP complex binds a $MinC_{Ec}$ dimer in the cytosol and recruits it to the membrane, forming a tube-like structure originating at a cell pole and elongating towards midcell (Hu *et al.*, 2003; Lackner *et al.*, 2003; Shih *et al.*, 2002; Lutkenhaus and Sundaramoorthy, 2003). At the membrane, $MinC_{Ec}$ inhibits $FtsZ_{Ec}$ polymerization, preventing cell division (Hu *et al.*, 1999). $MinE_{Ec}$ occurs both in the cytosol and as a ring-like complex. A $MinE_{Ec}$ dimmer interacts with the MinCD complex to stimulate the release of $MinC_{Ec}$ from the $MinD_{Ec}$ and cause ATP hydrolysis which subsequently releases $MinD_{Ec}$ from the membrane and initiates oscillation (Hu *et al.*, 2003). Additionally, $MinE_{Ec}$ forms a ring at midcell which is also dynamic, occluding $MinC_{Ec}$ division inhibition at the proper septation site (Shih *et al.*, 2002). $MinE_{Ec}$ causes the dissociation of $MinD_{Ec}$, leading to its own local destabilization and it moves towards the higher concentration of $MinD_{Ec}$ that has been displaced to the other cell half in a wave-like pattern (Meinhardt and de Boer, 2001). The dissociated $MinC_{Ec}$ and $MinD_{Ec}$ oscillate to the opposite pole of the cell where the process is repeated, effectively lowering the concentration of the division inhibitor $MinC_{Ec}$ at midcell and allowing for $FtsZ_{Ec}$ ring formation to occur and initiate the cytokinetic event which will lead to the

Figure 3: Proposed model of the Min cell division system in *Escherichia coli*. Dimeric MinD-ATP recruits dimeric MinC to the membrane where it inhibits FtsZ polymerization. A tubule-like MinCD structure forms at a polar region of the cell and elongates towards midcell. MinE initiates hydrolysis of MinD-bound ATP and displaces MinC; MinD dissociates from the phospholipid. The monomers oscillate to the other end of the cell and repeat this process; the midcell concentration of MinC remains low enough to allow FtsZ to form the cytokinetic ring.

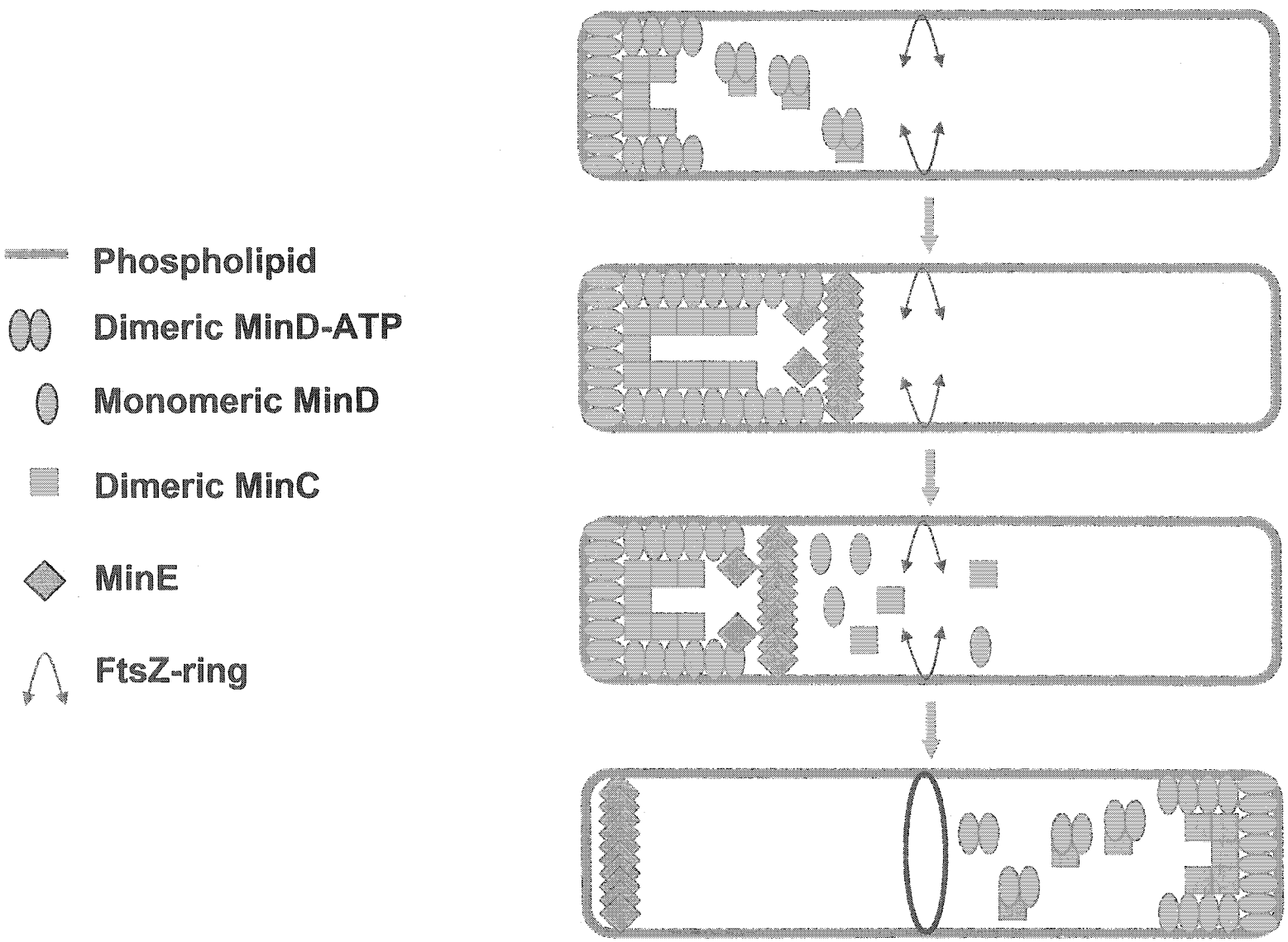
Phospholipid
Dimeric MinD-ATP
Monomeric MinD
Dimeric MinC
MinE
FtsZ-ring

formation of two separate daughter cells. The ATPase activity is essential to the oscillation of these proteins, but the exact mechanism of the oscillation is unknown. It is assumed that $MinD_{Ec}$ dissociates more rapidly from the membrane than $MinE_{Ec}$, enabling the remaining $MinE_{Ec}$ to inhibit the reformation of the $MinCD_{Ec}$ complex at that site (Lutkenhaus and Sundaramoorthy, 2003). Other factors including changes in the membrane and polar nucleation sites may contribute to the reformation of the $MinCD_{Ec}$ complex at the opposite pole (Lutkenhaus and Sundaramoorthy, 2003). A proposed model of cell division is shown in Figure 3.

It has recently been demonstrated that the *E. coli* Min proteins are associated with helical structures that extend between the two cell poles (Shih *et al.*, 2003). The structures are present at both poles of the cell, although the Min_{Ec} proteins are concentrated at one end and then oscillate to the opposite pole. These investigations show that the helical structure might act as a scaffold for the Min_{Ec} proteins, or that it serves as a nucleation site for the synthesis of more helices containing the Min_{Ec} proteins. It is unclear at this time if the coils are composed entirely of Min_{Ec} proteins or if other unidentified scaffolding proteins are involved. The $MinE_{Ec}$ ring appears to be a part of the coiled array that moves towards the polar zone and promotes oscillation of the $MinCD_{Ec}$ complex to the opposite pole.

1.4 Division in Gram-positive cells

Cell division in *B. subtilis*, a Gram-positive, rod-shaped, sporulating soil bacteria (Krieg and Holt, 1984), has been investigated by numerous laboratories. Following the discovery of the *min* locus in *E. coli,* homologues to the $minC_{Ec}$ and $minD_{Ec}$ genes in the *divIVB* locus were discovered (Levin *et al.,* 1992; Varley *et al.,* 1992). No homologue to

$MinE_{Ec}$ was detected, however another gene, *divIVA*, encodes a non-homologous protein that imparts topological specificity to the $MinC_{Bs}$ and $MinD_{Bs}$ complex (Cha and Stewart, 1997). $DivIVA_{Bs}$ is encoded by a different genetic locus from the min_{Bs} and dcw_{Bs} genes. The *dcw* cluster of *B. subtilis* contains homologues of the *E. coli dcw* genes with the inclusion of sporulation-specific genes (Daniel and Errington, 1993; Daniel *et al.* 1996). Organization and transcription of the *dcw* genes are similar between these species, although some genes including *murC, murF*, and the *ddl* genes are located elsewhere on the *B. subtilis* chromosome (Daniel and Errington, 1993; Figure 2).

In contrast to the Min_{Ec} proteins, the Min proteins and DivIVA proteins of *B. subtilis* do not appear to oscillate (Edwards and Errington, 1997, Marston *et al.,* 1998). $DivIVA_{Bs}$ is instead concentrated primarily at the cell poles during vegetative growth, forming a polar cap, and at the division site (Edwards and Errington, 1997, Marston *et al.,* 1998). It retains $MinC_{Bs}$ and $MinD_{Bs}$ at nascent cell poles following division, although $MinC_{Bs}$ and $MinD_{Bs}$ can be recruited in the absence of $DivIV_{Bs}$ (Marston and Errington, 1999). $MinC_{Bs}$ and $MinD_{Bs}$ perform the same division inhibition role as observed in *E. coli* (Edwards and Errington, 1997). It has recently been demonstrated that the Min_{Bs} system is not required for placement of the $FtsZ_{Bs}$ ring at midcell during vegetative growth, indicating that other proteins might be involved in cell division during this phase of the *B. subtilis* life cycle (Migocki *et al.*, 2002; Harry and Lewis, 2003). Additional differences in cell division between *E. coli* and *B. subtilis* exist because of the asymmetrical division that occurs in *B. subtilis* during sporulation (Levin and Losick, 1996).

Few studies of division in Gram-positive cocci have been initiated. It has been shown that the Gram-positive cocci examined to date possess fewer *dcw* genes than *E.*

coli, indicating that essential cell-division associated genes must be located elsewhere on the chromosome (Pucci *et al.*, 1997). In *Streptococcus pneumoniae*, the *dcw* cluster is divided, with *dcw* genes found at three chromosomal locations (Massida *et al.*, 1998). A genetic locus has been identified in *S. pneumoniae* that has five novel open reading frames (*ylmD, ylmE, ylmF, ylmG*, and *ylmH*) and a homologue of $divIVA_{Bs}$ (Massida *et al.*, 1998; Fadda *et al.*, 2003). Insertional inactivation of these genes results in abnormal cellular phenotypes characterized by chain formation of unseparated cells, altered cell diameter, irregular margins, and unclosed division septa (Fadda *et al.*, 2003). *ylmH* null cells experience cell lysis (Fadda *et al.*, 2003). *divIVA* homologues have also been identified in a number of Gram-positive cocci (Fadda *et al.*, 2003). The order of genes among Gram-positive organims is conserved among all species that have been examined (Pucci *et al.*, 1997; Massida *et al.*, 1998). No homologues of the Min proteins have been identified in Gram-positive cocci. Further research is necessary to determine the precise mechanism by which these cells divide.

1.5 The Min system in *N. gonorrhoeae*

N. gonorrhoeae divides in alternating, perpendicular planes and exhibits asymmetric invagination at the division site (Westling-Häggström *et al.*, 1977; Figure 1B). Prior to the discovery of the *min* genes in *N. gonorrhoeae* by our laboratory, it was widely believed that cocci had no requirement for a *min* system. In *N. gonorrhoeae*, the *min* genes are encoded by a 27 kb cluster comprising 17 genes, three of which are *minC*, *minD*, and *minE* homologues (Ramirez-Arcos *et al.*, 2001a). Our laboratory is currently involved with the thorough examination of each of these proteins, including the division inhibitor $MinC_{Ng}$. Our laboratory has demonstrated that overexpression of gonococcal

MinC ($MinC_{Ng}$) and gonococcal MinD ($MinD_{Ng}$) in the heterologous background of *E. coli* is capable of inducing filamentation, indicating the cross-complementation of these proteins and providing a suitable *E. coli* background for laboratory manipulations and research. Insertional inactivation of gonococcal $MinC_{Ng}$ prevents division in gonococci, leading to reduced viability, abnormal morphology, and cell lysis (Ramirez-Arcos *et al.*, 2001a). Similarly, $MinD_{Ng}$ insertionally-inactive mutants exhibit aberrant division in *N. gonorrhoeae* (Szeto *et al.*, 2001). Heterologous expression of either $MinC_{Ng}$ or $MinD_{Ng}$ in *E. coli* induces extreme filamentation, demonstrating that the functionality of these proteins as inhibitors of cell division is conserved across species (Ramirez-Arcos *et al.*, 2001a; Szeto *et al.*, 2001). A study of $MinC_{Ng}$ by Greco (2001) revealed that replacement of conserved residue R136 with a stop codon resulted in production of a non-functional protein as indicated by the inability of transformants to form filaments. It has also been demonstrated that expression of $ftsZ_{Ng}$, $ftsE_{Ng}$, and the min_{Ng} genes is regulated by environmental factors including anarobiosis, pH, and the presence of isoleucine and urea (Ramirez-Arcos *et al.*, 2001b). $MinC_{Ng}$ self-interaction and interaction with $MinD_{Ng}$ has not been demonstrated using the yeast two-hybrid system (unpublished data), thus a chimeric MinC containing the N-terminal domain of $MinC_{Ec}$ (amino acids 1-99) and the N-terminal domain of $MinC_{Ng}$ (amino acids 103-237) was constructed and shown to be capable of interaction with $MinC_{Ng}$ (Ramirez-Arcos *et al.*, 2003).

We also showed that $MinD_{Ng}$ and $MinE_{Ng}$ are capable of oscillation in various *E. coli* backgrounds using green fluorescent protein (GFP)-labeled $MinD_{Ng}$ and GFP-labeled $MinE_{Ng}$. $MinE_{Ng}$ formed a ring at midcell in addition to oscillating, and required the presence of $MinD_{Ng}$ *in cis* for oscillation to occur (Ramirez-Arcos *et al.*, 2002).

These proteins oscillated in round *E. coli rodA*$^-$ mutants, thus it is speculated that similar results would be seen in *N. gonorrhoeae*. Gonococcal cell division is asymmetric, with a preliminary invagination of the cell membrane occurring opposite the nucleoid (Fitz-James, 1964); the $MinCD_{Ng}$ complex oscillates perpendicular to this cleft to prevent division and the two opposite ends of the cell when expressed in *E. coli* backgrounds (Ramirez-Arcos *et al.*, 2002). Once the primary division has taken place, the oscillation changes planes, enabling another division to occur perpendicular to the original division plane, resulting in tetrad formation (Figure 4). The intracellular localization of $MinC_{Ng}$ and whether or not it oscillates with the other Min_{Ng} proteins remains to be discovered. This dynamic behaviour is currently the subject of much investigation.

1.6 MinC: The principle inhibitor of cell division

MinC is the principle inhibitor of cell division in prokaryotes. In *E. coli*, MinC is composed of 231 amino acids having a molecular weight of 26.3 kDa (de Boer *et al.*, 1989). The N- and C-terminal domains of MinC are separated by a hypervariable linker (Cordell *et al.*, 2001). The N-terminal domain of $MinC_{Ec}$ has been shown to interact with $FtsZ_{Ec}$ and the C-terminal domain with $MinD_{Ec}$ (Hu and Lutkenhaus, 2000). In *E. coli*, amino acids 1 to 99 comprise the N-terminal domain, 100 to 124 the linker region, and 125-231 the C-terminal domain (Hu and Lutkenhaus, 2000). Protein stability determinants are located in the C-terminal region between amino acids 160 and 231 (Sen and Rothfield, 1998). Nonsense and missense mutations *minC*25, *minC*27, *minC*28, *minC*36, and *minC*37 render the resultant proteins susceptible to Lon protease (Sen and Rothfield, 1998; Table 1). Several other missense and nonsense mutations that result in $MinC_{Ec}$ non-functionality have been recognized to date (Table 1). Inactivity of $MinC_{Ec}$

Table 1: $MinC_{Ec}$ mutations resulting in the minicell phenotype.

Mutation	Name	Phenotype	Source
G10D	minC19	Minicell, Lon protease stable	Labie *et al.* 1990, Sen and Rothfield, 1998
P47L	minC24	Minicell, Lon protease stable	Mulder *et al.* 1992, Sen and Rothfield, 1998
61Stop(TGA)	minC3	Minicell	Labie *et al.* 1990, Mulder *et al.* 1992
85Stop(TAA)	minC30	Minicell	Mulder *et al.* 1992
117Stop(TAA)	minC23	Minicell	Mulder *et al.* 1992
142Stop(TAA)	minC22	Minicell	Mulder *et al.* 1992
D160N; G161K	minC32	Minicell	Mulder *et al.* 1992
G161E*	minC17	Minicell	Labie *et al.* 1990
G171S*	minC25	Minicell, Lon protease sensitive	Mulder *et al.* 1992, Sen and Rothfield, 1998
G171D*	minC18	Minicell	Labie *et al.* 1990
R172L	minC34	Minicell	Mulder *et al.* 1992
R172C	minC35	Minicell	Mulder *et al.* 1992
A173V	minC27	Minicell, Lon protease sensitive	Mulder *et al.* 1992, Sen and Rothfield, 1998
G176R	minC28	Minicell, Lon protease sensitive	Mulder *et al.* 1992, Sen and Rothfield, 1998
A177V	minC31	Minicell	Mulder *et al.* 1992
A177T	minC33	Minicell	Mulder *et al.* 1992
183Stop(TAA)	minC5	Minicell	Labie *et al.* 1990
S196F	minC20	Minicell	Labie *et al.* 1990, Mulder et al. 1992
202Stop(TGA)	minC29	Minicell	Mulder *et al.* 1992
206Stop(TAA)	minC26	Minicell	Mulder *et al.* 1992
216Stop(TGA)	minC16	Minicell	Labie *et al.* 1990
Nonsense (C-terminal truncation)	minC36	Lon protease sensitive	Sen and Rothfield, 1998
Nonsense(C-terminal truncation)	minC37	Lon protease sensitive	Sen and Rothfield, 1998

* Indicates conserved glycine residue

Figure 4: Proposed model of cell division in *Neisseria gonorrhoeae.* Invagination occurs opposite the replisome; the MinD and MinE interact and oscillate perpendicular to the replisome to inhibit division at cell ends. Following one round of division, the complex oscillates perpendicular to the previous division site, inhibiting division at these ends of the cell. The result is a tetrad of equal-sized daughter cells. Adapted from Ramirez-Arcos *et al.*, 2002).

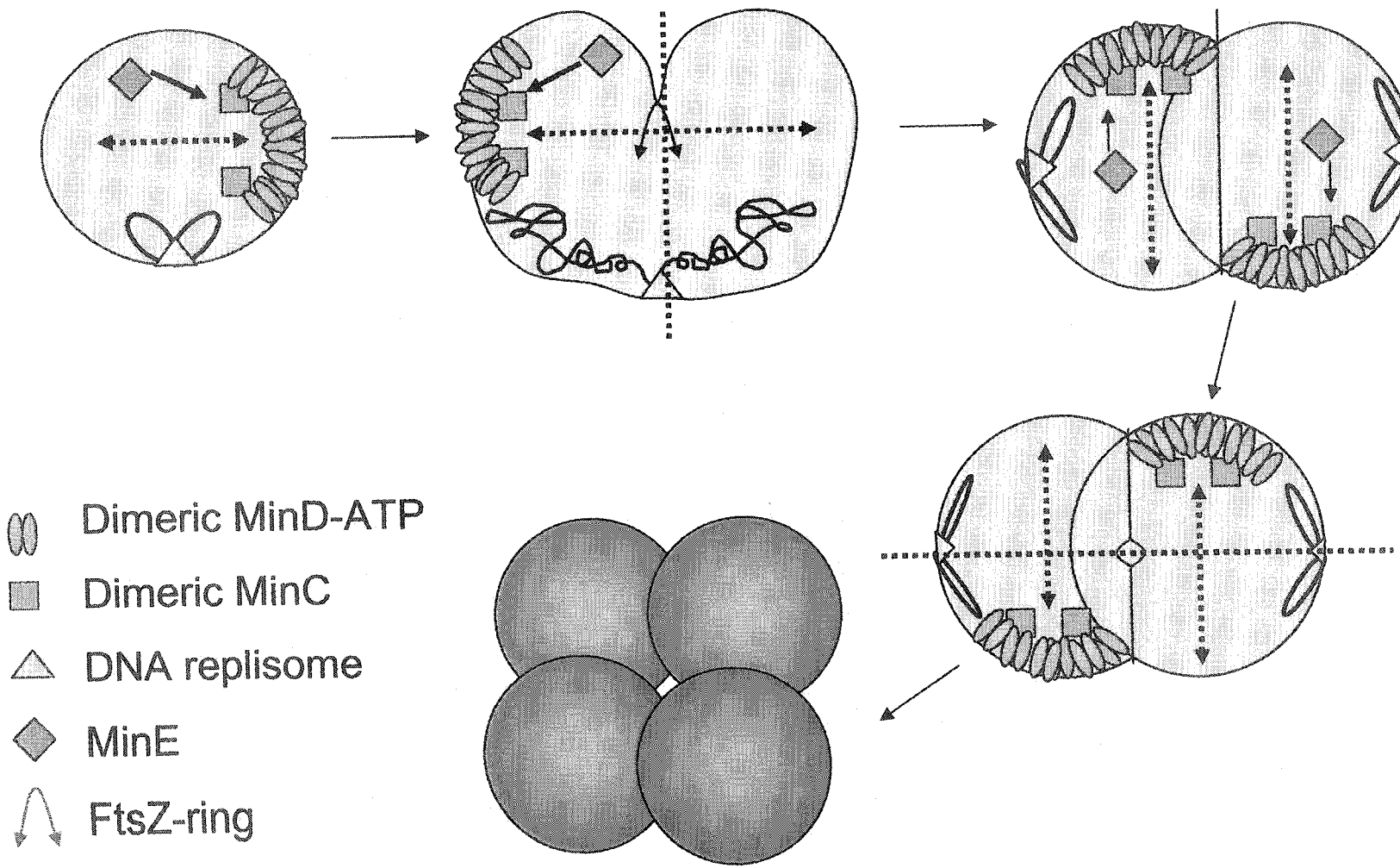
Dimeric MinD-ATP
Dimeric MinC
DNA replisome
MinE
FtsZ-ring

is determined morphologically by the presence of minicells, indicating lack of inhibition of cell division at the cell poles. The majority of mutations studied have been located in the C-terminal region of $MinC_{Ec}$.

The crystal structure of MinC from the thermophilic bacterium *Thermotoga maritima* ($MinC_{Tm}$) has recently been determined (Cordell *et al.*, 2001). This protein contains an N-terminal domain composed of two alpha-helices and five β-strands and a C-terminal domain composed of fifteen beta-strands, twelve of which form a right-handed β-helix that possesses A, B, and C surfaces (Cordell *et al.*, 2001; Figure 5). The hydrophobic A-face was proposed to be the surface responsible for homodimerization of $MinC_{Tm}$ (Cordell *et al.*, 2001). The core of the β-helix is primarily hydrophobic and consists of small, aliphatic amino acids with short side chains. A flexible linker that is hypervariable among species connects these two domains. The N-terminal domain is speculated to be responsible for interaction with $FtsZ_{Tm}$, (Cordell *et al.*, 2001). The surface responsible for $MinD_{Tm}$ interaction has not yet been elucidated. $MinC_{Tm}$ has been determined to be a dimer in solution and aggregates to form a homotetramer (Cordell *et al.*, 2001). Preliminary gel filtration studies of purified $MinC_{Ng}$ from our laboratory have determined that $MinC_{Ng}$ also forms a dimer in solution (unpublished data). The importance of conserved residues and their implicated role in protein-protein interactions will be the subject of the present investigation.

Figure 5: Three-dimensional structure of a MinC dimer from *T. maritima*. Adapted from Cordell *et al.*, 2001; A, B, and C surfaces of the C-terminus β-helix as designated by Cordel *et al.*

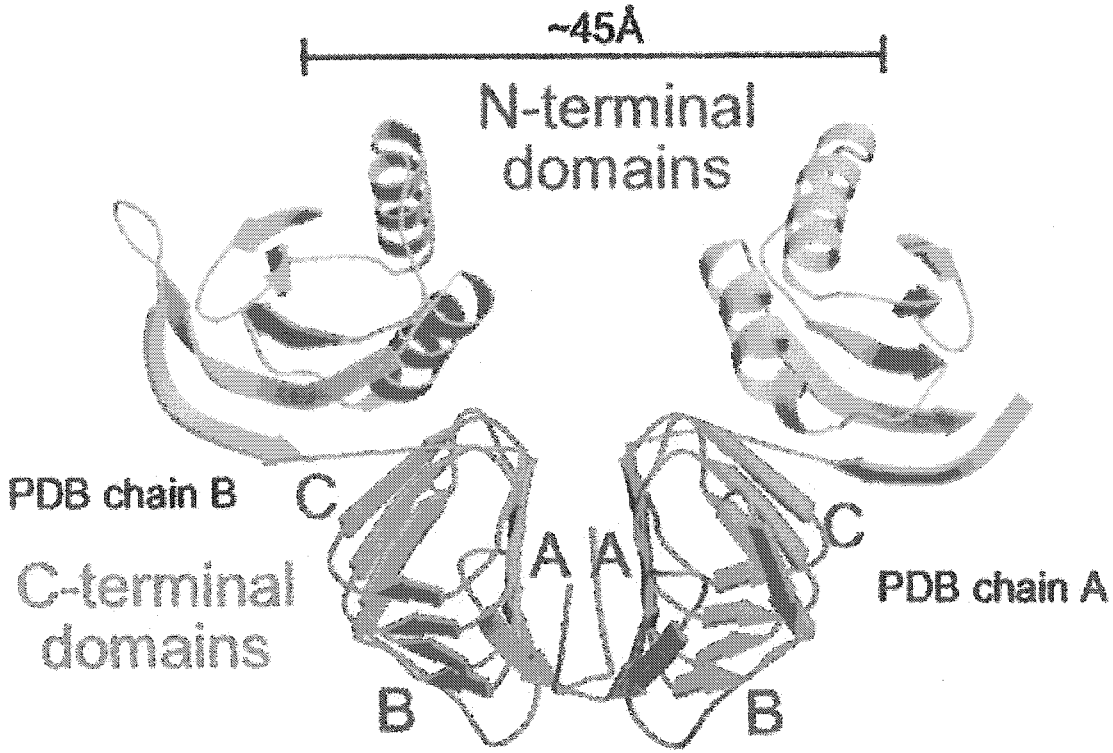
~45Å
N-terminal
domains
PDB chain B
C
C-terminal
domains
A
A
C
PDB chain A
B
B

1.7 Rationale, hypothesis, and objectives

1.7.1 Rationale

Antimicrobial resistance in *N. gonorrhoeae*

The sexually-transmitted infection gonorrhea, caused by *N. gonorrhoeae*, is second in prevalence only to chlamydial infection as a cause of sexually transmitted infections and is a substantial cause of morbidity world-wide (www.cdc.gov). After a 13 year decline, the incidence of gonorrhea has increased dramatically in North America, rising 9% in the United States and 8% in Canada between 1997 and 1998 (www.cdc.gov; www.hc-sc.gc.ca). Strains of *N. gonorrhoeae* resistant to antimicrobial agents have been documented and are increasing in prevalence, challenging efforts to combat the disease (Johnson and Morse, 1988; Ison, 1996; Ison *et al.*, 1998; Sefton, 2002). Resistance to single and multiple antibiotics is a global phenomenon; while the prevalence of resistance to one antimicrobial might wane with the increased use of a different agent, resistance to the latter rapidly ensues (Johnson and Morse, 1988; Sefton, 2002).

Both chromosomal and plasmid-mediated resistance to penicillin and tetracycline in *N. gonorrhoeae* isolates has been well documented (Morse *et al.*, 1986; Johnson and Morse, 1988; Sefton, 2002). Resistance to other antibiotics such as fluoroquinolones also occurs (Knapp *et al.*, 1997; Sefton, 2002). For example, in Canada, both chromosomal and plasmid-mediated resistance to tetracycline has been documented since 1986, but the frequency of these resistances has been declining since 1994 with the decrease in treatment of uncomplicated gonococcal infections with doxycycline for concomitant chlamydial infection (Greco *et al.*, 2003). Resistance to penicillins by production of plasmid-encoded β-lactamases has also been declining steadily since

penicillins are no longer used to treat gonococcal infections (Greco *et al.*, 2003). Consequently, in recent years, resistance to fluoroquinolones among gonococcal isolates in Canada has been rising with the increased use of ciprofloxacin (Sarwal *et al.*, 2003). Third-generation cephalosporins (i.e. cefixime and ceftriaxone) are currently used to treat gonorrhea and azythromycin is typically administered concurrently to control any potential chlamydial co-infection (Health Canada, 1998). However, cefixime-resistant isolates of *N. gonorrhoeae* were recently identified in China (Ye *et al.*, 2002); spread of these resistant strains will ultimately reduce the arsenal of antimicrobial agents with which *N. gonorrhoeae* infection can be treated.

Due to the rapid increase in the number of multi-drug resistant strains of *N. gonorrhoeae* it has become pertinent to initiate a search for novel antimicrobial compounds to control gonococcal infection. Components of the bacterial division apparatus present an attractive target for the development of new antimicrobial compounds since proper cellular division is necessary for the survival and propagation of the organism. Furthermore, the division machinery is not currently targeted by any commercially-available antibiotics. Typical antimicrobials previously used to treat gonococcal infection target the 30 S or 50S ribosome, cell wall biosynthesis machinery, DNA gyrase, or metabolic pathways (Johnson and Morse, 1988; Fox *et al.*, 1997). It is subsequently unlikely that modern strains of *N. gonorrhoeae* will be resistant to compounds that target the division apparatus as no antimicrobial to date has exploited interruption of cell division as a candidate for antimicrobial interference. In order to develop novel chemotherapeutic agents that inhibit cell division it is necessary to have a fundamental knowledge of the proteins involved in bacterial cell division.

Molecular analysis of $MinC_{Ng}$

MinC interacts with other components of the division machinery, such as FtsZ and MinD, as has been demonstrated in *E. coli*, and its structure is important for its function as a division inhibitor in *N. gonorrhoeae*. Both the N- and C-terminal domains play unique and critical roles in the division process, and through characterization of these domains through mutagenesis and truncation analyses it will become possible to understand the significance of conserved glycine residues (G138, G157, G164 and G174 in $MinC_{Ng}$), thus contributing to the understanding of the division process in round bacteria.

The C-terminal domain of $MinC_{Ng}$ is highly-conserved and contains four completely conserved glycine residues; these residues must therefore be critical to protein function across species. Glycines are of specific interest, as they have been implicated in protein flexibility, protein-protein interactions, and positioning of other residues (Alix *et al.*, 2001; Heinrichs and Baker, 1997; Sprinzak and Margalit, 2001; Lo Leggio and Larsen, 2002). Site-directed mutagenesis of conserved residues has been employed to ascertain the necessity of conserved residues in many bacterial and eukaryotic proteins including the bacterial 50S peptidyl transferase and ADP-glucose pyrophosphorylase (Cooperman *et al.*, 1995 and Ballicora *et al.*, 2003, respectively). These data proved that conserved residues, in the cases of these two proteins, were imperative to protein function. In the present study, mutagenesis of conserved residues will be performed to ascertain their necessity to protein function and potentially determine their roles within the protein.

The N-terminal domain is not conserved, but contains structural motifs that should be necessary for protein-protein interaction and function. Disruption of critical

residues within these motifs should cause loss of protein function, possibly by abrogation of certain protein-protein interactions. Site-directed mutagenesis will be a useful tool for the disruption of α-helical motifs in the N-terminal domain of $MinC_{Ng}$ by targeting semi-conserved residues as discussed above.

Truncation of N-terminus residues is also expected to result in loss of protein functionality. C-terminus truncated mutants of $MinC_{Ec}$ are non-functional (Jaffe *et al.*, 1988; Sen and Rothfield, 1998; Table 1), and it is thus reasoned that loss of a certain portion of the N-terminus should have the same effect. The 10^{th} amino acid of $MinC_{Ec}$ is suspected to be essential to protein function as indicated by loss of division inhibition function of the *minC19* mutant (Table 1) in which an aspartic acid is substituted for a glycine residue at position 10 (corresponding to gonococcal position 13; Labie *et al.*, 1990). It is thus expected that a certain portion of the N-terminus of $MinC_{Ng}$ is essential for protein function; loss of the 13^{th} amino acid should be deleterious to the function of this protein.

The long-term goal of the present research is to characterize $MinC_{Ng}$ at the molecular level through structural and functional analysis. Investigation of cell division proteins may lead to the discovery of novel antimicrobial targets for the treatment and prevention of bacterial infection.

1.7.2 Hypothesis

N- and C-terminal domains of MinC from N. gonorrhoeae must play unique roles during the cell division process in this Gram-negative coccus. The C-terminus of MinC is highly similar across species and contains five completely conserved residues including four

glycines. Alteration of these glycine residues will prevent division inhibition by these $MinC_{Ng}$ mutants. Similarly, it is anticipated that substitution of key residues contained within conserved structural motifs of the N-terminus and truncation of the extreme N-terminus residues will result in abrogation of protein function.

1.7.3 Objectives

Objective #1: Functional analysis of the C-terminus of $MinC_{Ng}$ and localization of $MinC_{Ng}$ in *E. coli* and *N. gonorrhoeae*.

1.A. Mutagenesis of conserved glycine residues: Residues G138, G157, G164, and G174 of $MinC_{Ng}$ are completely conserved among bacterial species. Site-directed mutagenesis of these residues will be performed to elucidate their role in protein function. Introduction of a radical mutation in a non-conserved residue will act as a control to determine the importance of a non-conserved amino acid.

1.B. $MinC_{Ng}$ functionality assays: $MinC_{Ng}$ mutants will be studied in terms of functionality as determined by the ability to inhibit cell division using both phase contrast microscopy and flow cytometry.

1.C. Quantitation of mutant $MinC_{Ng}$ mutant expression in *E. coli* PB103: Western blot analysis will be used to confirm the expression of these mutants to ensure that lack of division inhibition functionality does not result from lack of $MinC_{Ng}$ expression.

1.D. $MinC_{Ng}$ purification and circular dichroism (CD) analysis: Native and mutant $MinC_{Ng}$ will be purified by nickel affinity chromatography by constructing 6X histidine fusion plasmids. Purified proteins will be submitted for CD analysis to confirm that the secondary structure of the proteins is not affected by site-directed mutagenesis of conserved residues.

1.E. Determination of protein-protein interactions between $MinC_{Ng}$ mutant and $MinD_{Ng}$. A chimeric MinC containing the N-terminus of $MinC_{Ec}$ and the C-terminus of $MinC_{Ng}$ used by our laboratory for yeast two-hybrid analyses will have a neutral mutation introduced in a non-conserved residue to determine the impact on protein-protein interaction.

1.F. Localization of $MinC_{Ng}$ in *E. coli* PB103: Plasmids for the localization of $MinC_{Ng}$ in both native and heterologous environments will be constructed. Future experiments using these plasmids will enable the determination of the intracellular location of $MinC_{Ng}$ and whether or not the protein oscillates in live native and heterologous cells using fluorescence microscopy.

<u>Objective #2:</u> Structural and functional analysis of the N-terminus of $MinC_{Ng}$

2.A. Mutagenesis of structurally-significant amino acids and truncation of N-terminus amino acids: Alteration of important amino acids L35 and L68 in the N-terminus α-helices of $MinC_{Ng}$ using SDM should indicate if these residues are critical for protein function. Residues from the extreme N-terminus of $MinC_{Ng}$ (10 and 13 aa) will be eliminated to determine which amino acids are necessary for function and which are superfluous.

2.B. $MinC_{Ng}$ functionality assays: Both phase contrast microscopy and flow cytometry will be employed to determine if mutant and truncated $MinC_{Ng}$ proteins are functional.

2.C. Quantitation of $MinC_{Ng}$ expression: Western blot analysis will be used to confirm the expression levels of $MinC_{Ng}$ mutant proteins in *E. coli* PB103.

2.D. Determination of protein-protein interaction among $MinC_{Ec}$ C-terminal domains: Plasmids will be constructed to determine whether or not C-termini of $MinC_{Ec}$ alone are capable of self interaction and interaction with $MinD_{Ec}$. These results can be used to test protein-protein interactions of N-terminus $MinC_{Ng}$ mutants using a chimeric MinC containing the N-terminus of $MinC_{Ng}$ and C-terminus of $MinC_{Ec}$.

2.E. Construction of a glutathione S-transferase (GST) fusion vector: Based on information obtained from other bacterial species, it is expected that $MinC_{Ng}$ will interact with $MinD_{Ng}$ and $FtsZ_{Ng}$, and potentially other proteins involved in the cell division process. It is additionally possible that novel proteins that have not been previously implicated in cell division play a role in this process in *N. gonorrhoeae*. Since yeast two-hybrid methodology has proven inefficient at establishing $MinC_{Ng}$ interactions, the GST-pulldown assay will be useful in determining protein-protein interactions; a plasmid will be constructed in the present study to facilitate GST-pulldown assays in the future.

MATERIALS AND METHODS

Overview

Several methodologies will be employed to investigate the $MinC_{Ng}$ protein in these studies. Site-directed mutagenesis, gene truncation, and other standard molecular biological techniques will be employed in the construction of plasmids for this research. The functionality of proteins encoded by these constructs will be ascertained using a morphological assay performed in *E. coli*. The ability of MinC to induce filamentation when expressed from a high copy-number vector is indicative of its functionality as an inhibitor of cell division (de Boer *et al.*, 1989), and mutants in this study will be evaluated for $MinC_{Ng}$ function on this basis by phase contrast microscopy when expressed heterologously in *E. coli*. Flow cytometry will also be employed to quantitate the number of filamentous and standard-sized cells within transformant populations; this is a novel technique for which a protocol will be established in the course of this investigation. Together, flow cytometric and morphological analysis using phase contrast microscopy will demonstrate the functionality of each site-directed and truncated $MinC_{Ng}$ mutant. Western blot analysis will confirm the expression of each protein investigated.

Purification of $MinC_{Ng}$ will be performed using nickel affinity chromatography. This procedure involves the construction of fusion vectors in which the protein of interest ($MinC_{Ng}$) is fused to a 6X histidine tag at either the N- or C- terminus (Novagen, 2002). Proteins from cell lysate bearing the 6X his tag bind nickel-treated sepharose beads in a column and are eluted by competition with varying concentrations of imidazole (Novagen, 2002). Purified protein is then analyzed using circular dichroism

spectroscopy (CD). CD is a technique that is used to evaluate protein secondary structure based upon characteristic absorption spectra produced by certain structures when a protein is exposed to left- and right-circularly polarized light (Greenfield and Fasman, 1969). This technique is used to confirm that the secondary structure of $MinC_{Ng}$ proteins is not altered by mutagenesis of single amino acids.

To study the localization and dynamics of Min proteins, green fluorescent protein (GFP) fusions will be employed (Meinhardt and de Boer, 2001; Ramirez-Arcos *et al.*, 2002). Fluorescence microscopy of live cells shows the intracellular location of these fusion proteins, and repeated photography of these cells at specific time intervals demonstrates their movement within the cell. In this study, the plasmids for such research will be constructed; low copy-number plasmids will be created to obtain a more accurate representation of $MinC_{Ng}$ localization when the protein is expressed at levels close to those of the native levels in *N. gonorrhoeae*.

Finally, a plasmid for the performance of glutathione S-transferase (GST) pull-down assays will be constructed containing a *gst-min*C_{Ng} fusion gene. The GST-labelled $MinC_{Ng}$ will be passed through an affinity column and be eluted with any interacting proteins that can subsequently be identified by Western blot and nuclear magnetic resonance (NMR) analyses in future experiments.

2.1 Bacterial strains and growth conditions

Strains and plasmids used for this study are presented in Table 2. *E. coli* DH5α was the host used for cloning. *E. coli* PB103 (wild-type) was used for expression studies. *E. coli* cells were grown at 37°C for 16-24 hours with agitation in Luria-Bertani (LB) broth

Table 2. Strains and plasmids used in this study.

Strains/Plasmids	Relevant Genotype	Source/Reference
Strains		
E.coli DH5α	[*sup*E44Δ*lac*U169 (80*lacZ*Δ*M*15) *hsd*R17 *rec*A1 *end*A1 *gyr*A96 *thi*-1 *rel*A1]	Gibco-BRL
E.coli PB103	*dad*R1 *trp*E61 *trp*A62 *tna*-5 *purB*$^+$	Ramirez-Arcos *et al.*, 2001[a]
E.coli C41	B F *dcm ompT hsdS* (r_B m_B) gal λ(DE3) and containing at least one additional uncharacterized mutation	Miroux and Walker, 1996[b]
S. cerevisiae SFY526	*MAT*a *ura3-52 his3-200 ade2-101 lys2-801 trp1-901 leu2-3 112 can*^{r} *gal4-542 gal80-538 URA3::GAL1*$_{UAS}$-*GAL1*$_{TATA}$-*lacZ*	Clontech
N. gonorrhoeae CH811	Auxotype (A)/ serovar (S)/ plasmid content (P) : Non-requiring (NR)/IB/plasmid free	Picard and Dillon, 1989
N. gonorrhoeae F62	ASP: Proline-requiring (Pro)/IB/2.6	West and Clark, 1989
Plasmids[c]		
pUC18	Amp^{R}P$_{lac}$	Amersham Pharmacia
pSR2	Amp^{R}P$_{lac}$::*minC*$_{Ng}$	Ramirez-Arcos *et al.* 2001
pSR12	Amp^{R}P$_{lac}$::GFP-*minC*$_{Ng}$	Unpublished data
pSR15	Amp^{R}P$_{lac}$::GFP-*minDE*$_{Ng}$	Unpublished data
pSR13	Amp^{R}P$_{lac}$:: *minDE*$_{Ng}$-GFP	Unpublished data
pSR24	Amp^{R}P$_{lac}$::*minC*(MinCCh: MinC$_{Ec}^{1-99}$-MinC$_{Ng}^{103-237}$)	Ramirez-Arcos *et al.* 2003
pSR32	Amp^{R}P$_{lac}$::*minC*$_{Ec}$	Ramirez-Arcos *et al.* 2003
pFP20	Kan^{R}P$_{lac}$ oriJRD5	Pagotto *et al.* 2000
pVG4	Amp^{R}P$_{lac}$::*minC*$_{Ng}$(G138D)	Greco, 2001
pVG6	Amp^{R}P$_{lac}$::*minC*$_{Ng}$(G157D)	Greco, 2001
pVG8	Amp^{R}P$_{lac}$::*minC*$_{Ng}$(G164S)	This study
pVG10	Amp^{R}P$_{lac}$::*minC*$_{Ng}$(G174E)	This study
pPF1	Amp^{R}P$_{lac}$::*minC*$_{Ng}$(E144I)	This study
pVG12	Kan^{R}P$_{lac}$::GFP-*minC*$_{Ng}$ oriJRD5	This study
pVG13	Kan^{R}P$_{lac}$::GFP-*minDE*$_{Ng}$ oriJRD5	This study
pVG14	Kan^{R}P$_{lac}$:: *minDE*-GFP$_{Ng}$ oriJRD5	This study
pVG15	Amp^{R}P$_{lac}$::*minC*$_{Ng}$(L35P)	This study
pVG16	Amp^{R}P$_{lac}$::*minC*$_{Ng}$(L68P)	This study
pVG17	Amp^{R}P$_{lac}$::*minC*$_{Ng}^{11-237}$	This study
pVG18	Amp^{R}P$_{lac}$::*minC*$_{Ng}^{14-237}$	This study
pGAD4T4	Amp^{R}P$_{ADH1}$[d]::*gal4* (AD)[e]	Clontech

pSRAD-C	$Amp^R P_{ADH1}$::*gal4* (AD)-*min*C_{Ec}	Ramirez-Arcos *et al.* 2003
pSRAD-D	$Amp^R P_{ADH1}$::*gal4* (AD)-*min*D_{Ec}	Szeto *et al.* 2001
pGADminD	$Amp^R P_{ADH1}$::*gal4* (AD)-*min*D_{Ng}	Szeto *et al.* 2001
pGBT9	$Amp^R P_{ADH1}$::*gal4* (BD)[f]	Clontech
pSRBD-C	$Amp^R P_{ADH1}$::*gal4* (BD)-*min*C_{Ec}	Ramirez-Arcos *et al.* 2003
pSRBD-D	$Amp^R P_{ADH1}$::*gal4* (BD)-*min*D_{Ec}	Szeto *et al.* 2001
pGBT9minD	$Amp^R P_{ADH1}$::*gal4* (BD)-*min*D_{Ng}	Szeto *et al.* 2001
pSRBD-Ch	$Amp^R P_{ADH1}$::*gal4* (BD)-*minC*($MinC_{Ec}^{1-99}$-$MinC_{Ng}^{103-237}$)	Ramirez *et al.*, 2003
pPF2	$Amp^R P_{ADH1}$::*gal4* (BD)-*minC*($MinC_{Ec}^{1-99}$-$MinC_{Ng}^{103-237}$) E144I	This study
pGAD*min*C_{Ec}C	$Amp^R P_{ADH1}$::*gal4* (AD)-*minC*($MinC_{Ec}^{103-231}$)	This study
pGBT*min*C_{Ec}C	$Amp^R P_{ADH1}$::*gal4* (BD)-*minC*($MinC_{Ec}^{103-231}$)	This study
pET30a	$Kan^R P_{lac}$::*lacI*^{q}::6XHis	Novagen
pHLCC	$Kan^R P_{lac}$::*lacI*^{q}::*min*C_{Ng}-6XHis	Unpublished data
pET30aG138D	$Kan^R P_{lac}$::*lacI*^{q}::*min*C_{Ng}(G138D)-6XHis	This study
pET30aG157D	$Kan^R P_{lac}$::*lacI*^{q}::*min*C_{Ng}(G157D)-6XHis	This study
pET30aG164S	$Kan^R P_{lac}$::*lacI*^{q}::*min*C_{Ng}(G164S)-6XHis	This study
pET30aG174E	$Kan^R P_{lac}$::*lacI*^{q}::*min*C_{Ng}(G174E)-6XHis	This study
pET30aCh	$Kan^R P_{lac}$::*lacI*^{q}:: *minC*($MinC_{Ec}^{1-99}$-$MinC_{Ng}^{103-237}$)-6XHis	This study
pGEX-4T-3	$Amp^R P_{tac}$::*lacI*^{q}::GST	Amersham Biosciences
pVAL2	$Amp^R P_{tac}$::*lacI*^{q}::GST-*min*C_{Ng}	This study

a) Gift from P. de Boer
b) Gift from J.E. Walker
c) All pVG- plasmids, pVAL2, pGAD*min*C_{Ec}C, and pGBT*min*C_{Ec}C plasmids constructed by Valerie Greco. Other plasmids constructed by: Sandra Ramirez (pSR-, pSRAD-C, pSRAD-D, pSRBD-C, pSRBD-D, and pSRBD-Ch); Pierre Fabre (pPF1 and pPF2); Hui Li (pHLCC); Franco Pagotto (pFP20); Dan Tessier (pET30aG138D, pET30aG157D, pET30aG164S, pET30aG174E, and pET30aCh); Jason Szeto (pGADminD and pGBT9minD)
d) P_{ADH1}: Yeast promoter, which regulates expression of *gal4*
e) Encodes for the activation domain (AD) of GAL4
f) Encodes for the DNA-binding domain (BD) of GAL4

(Difco, Detriot, MI), supplemented with 100 μg of ampicillin (Amp)/ml, 50 μg of kanamycin (Kan)/ml, and/or 40 μm IPTG, when required (antibiotics from Sigma-Aldrich, St. Louis, MO). All IPTG inductions were performed by diluting 5 ml overnight (16-20 hour) culture in 500 ml LB broth and incubating for 3 hours at 37°C with agitation. For $MinC_{Ng}$ localization studies, cultures were grown at both room temperature (~25°C) and 37°C both with and without agitation for 16-24 hours. Transformants were selected on LB agar containing the aforementioned antibiotics for selection.

Saccharomyces cerevisiae strain SFY526 (Clontech, Palo Alto, CA) was used in yeast two-hybrid assays to examine protein-protein interactions. Yeast was grown at 30°C on yeast extract-peptone-adenine-dextrose (YPAD; Clontech) medium, or on the appropriate synthetic dropout (SD) media to select for transformants, as outlined in the Clontech Yeast Two-Hybrid Manual (Clontech Laboratories Inc, 1999).

N. gonorrhoeae strains CH811 and F62 were grown on GC Medium Base (GCMB; Difco) augmented with 1% Kellogg's defined supplement (GCMBK; Kellogg, 1963; Dillon, 1983) which contains 10 mM $MgCl_2$, and 0.042% $NaHCO_3$. Cells were grown at 35°C for 18 to 24 hours in a humid incubator with 5% CO_2.

Both *E. coli* and *N. gonorrhoeae* strains were preserved at –70°C in Brain-Heart Infusion broth (BHI; Difco) containing 20% glycerol.

2.2 Polymerase chain reaction (PCR) and Inverse PCR (IPCR)

Oligonucleotide primers used for PCR and IPCR in this study are listed in Table 3. Primers were designed in the laboratory using Primer Designer (Scientific and Education

Table 3. Oligonucleotide primers used for PCR reactions in this study.

Primer	Sequence (5'→ 3')[a]	Restriction Endonuclease Site	Product
min10	5' GCG CCT GCA GAT GAT GGT TTA TAT AAT 3'	*Pst*I	*minC*$_{Ng}$ 5' end
min12	5' GCG CGC GAA TTC ATG ATG GTT TAT ATA AT 3'	*Eco*RI	*minC*$_{Ng}$ 5' end
min29	5' GCG CGG ATC CCA AAC AAT TAC TCT GAG CC 3'	*Bam*HI	*minC*$_{Ng}$ 3' end
min29*Sal*I	5' GCG CGT CGA CCA AAC AAT TAC TCT GAG CC 3'	*Sal*I	*minC*$_{Ng}$ 3' end
EcCh1up	5' GCG CGA ATT CAC GCC GGT CAC AAA AAC GCG	*Eco*RI	C-terminus *minC*$_{Ec}$
EcMinCdown	5' 5' GCG CGG ATC CTC AAT TTA ACG GTT GAA CGG 3'	*Bam*HI	
CNg-up	5' GCG CAC TAG TCA TTC GGA AAA TGT TAA AG 3'	*Spe*I	C-terminus *minC*$_{Ng}$
HLC-2	5' GCG CCA TAT GAT GGT TTA TAT AAT TGA ATG 3'	*Nde*I	*minC*$_{Ng}$ 5' end
HLC-3	5' GCG CAA GCT TCT CTG AGC CAA TTG CAC TG 3'	*Hin*DIII	*minC*$_{Ng}$ 3' end
minCG138-1	5' ACC GAT CAG CAG GTT TAT GCC 3'[b]	*Sau*3A	*minC*$_{Ng}$ G138D
minCG138-2	5' ACG GAC AGG GGA TGT AAT CAA 3'	None	
minCG157-1	5' CAG GAC GCG GAA TTG ATT GCA 3'	*Hga*I	*minC*$_{Ng}$ G157D
minCG157-2	5' GCT GAC CGC CCC CGT AAC AAT 3'	None	
minCG164-1	5' GAT TCG AAT ATG CAT ATT TAT 3'	*Taq*Iα	*minC*$_{Ng}$ G164S
minCG164-2	5' TGC AAT CAA TTC CGC CCC CTG 3'	None	
minCG174-1	5' AGA GAT CGT GCT TTG GCC GGC 3'	*Sau*3A	*minC*$_{Ng}$ G174E
minCG174-2	5' CAT CGG CGC ATA AAT ATG CAT 3'	None	
minCE144-1	5' GCC ATC GAT GGC GAT TTG ATT GTT ACG 3'	*Cla*I	*minC*$_{Ng}$ E144I
minCE144-2	5' ATA AAC CTG ACC GGT ACG GAC AGG 3'	None	

minCL35P-1	5' GAT GTG CCG GTC AAA TTG GGC 3'	*Hpa*II	*minC*$_{Ng}$ L35P
minCL35P-2	5' TTC CAA ATC AAA CAA GTC TGA TTG 3'	None	
minCL68P-1	5' GCT GCA CCG GTT TCG TTG TTT CG 3'	*Hpa*II	*minC*$_{Ng}$ L68P
minCL68P-2	5' AAG ATC CAA AGA CTC GGG ATA AT 3'	None	
Trunc1	5' GCG CAC GAA TTC GAT GAT AAA GTC GAC AA 3'	*Eco*RI	*minC*$_{Ng}^{11-237}$
Trunc2	5' GAG CAC GAA TTC GAT GAC AAA GAT GGA CG 3'	*Eco*RI	*minC*$_{Ng}^{14-237}$
Trunc3	5' GCG GAC GAA TTC GAT GAA GTC GAC AAA GA 3'	*Eco*RI	*minC*$_{Ng}^{12-237}$
Trunc4	5' GAG CAC GAA TTC GAT GTC GAC AAA GAT GG 3'	*Eco*RI	*minC*$_{Ng}^{13-237}$
GFP-1	5' GCG CGG TAC CGC TGT GGT ATG GCT GTG C 3'	*Kpn*I	GFP-*minC*$_{Ng}$; GFP-*minDE*$_{Ng}$
GFP-2	5' GCG CCT GCA GTT ACT CTG AGC CAA TTG C 3'	*Pst*I	GFP-*minC*$_{Ng}$
GFP-3	5' GCG CCT GCA GCT ATA CCT TTT TCT GTT CCG 3'	*Pst*I	GFP-*minDE*$_{Ng}$
GFP-4	5' GCG CGA ATT CAA TAC GCA AAC CGC CTC TCC 3'	*Eco*RI	*minDE*$_{Ng}$-GFP
GFP-5	5' GCG CGG TAC CTT ACT TGT ACA GCT CGT CC 3'	*Kpn*I	*minDE*$_{Ng}$-GFP

a) Restriction endonuclease sites are underlined
b) Mutagenized codons are indicated in bold

Software, Durham, NC) and were synthesized by the University of Ottawa Core DNA Sequencing and Synthesis Facility (formerly University of Ottawa Biotechnology Research Institute). All PCR reactions were carried out in the Perkin Elmer GenAmp PCR System 9600 Thermocycler (Perkin Elmer, Wellesly, MA) as follows: 3 minutes at 94°C; 30 cycles of denaturation for 15 seconds at 94°C, annealing for 15 seconds at temperatures varying from 48°C to 53°C (depending on the primer pair used), and extension for 1 to 7 minutes at 72°C (depending on the expected product size; 1 minute/kb); 5 minutes at 72°C; and hold at 4°C. The PCR reactions were carried out in a final volume of 100 µl containing the following reagents: 75.5 µl of double distilled H_2O (ddH_2O), 10 µl of 1X PCR Buffer containing 1.5 mM $MgCl_2$ (Roche Diagnostics, Laval, QUE), 2 µl dNTPs (100mM; Boehringer Mannheim, Laval, QUE), 1 µl of each primer (0.2 µg/ml), 0.5 µl of *Taq* DNA polymerase for PCR amplifications (Roche Diagnostics) or *Pfu* DNA polymerase (Stratagene, La Jolla, CA) for IPCR amplifications, and 10 µl of template DNA. Template DNA was prepared from a 1:50 dilution of plasmid DNA recovered by miniprep. *N. gonorrhoeae* CH811 and *E. coli* PB103 cell suspensions were prepared by diluting cells from overnight cultures in ddH_2O. Cell concentrations were adjusted to ~1 X 10^9 cells using the McFarland Equivalence Turbidity Standard 0.5 (Remel, Lenexa, KA) to provide chromosomal DNA templates for PCR. Concentration of the plasmid DNA templates was determined spectrophotometrically using the GeneQuant RNA/DNA calculator model #80-2103-98 (Amersham Pharmacia, Piscataway, NJ) and adjusted to 0.01 µg/ml with ddH_2O for IPCR reactions.

2.3 Plasmids and plasmid constructs

2.3.1 $MinC_{Ng}$ site-directed mutagenesis (SDM) constructs

SDM was employed to mutagenize conserved N- and C-terminus residues of $minC_{Ng}$ to enable the structural analysis of this protein. All SDM constructs were prepared by IPCR from the pSR2 template ($minC_{Ng}$ in pUC18; Ramirez-Arcos *et al.*, 2001a; Table 2). pSR2 was harvested from DH5α transformants using the QIAgen HiSpeed Miniprep Kit (QIAgen, Mississauga, ONT) as directed by the manufacturer (QIAgen, 2003). Mutated $minC_{Ng}$ encoding for G138D, G157D, G164S, G174E, E144I, L35P, and L68P were created using primer pairs minCG138-1/minCG138-2, minCG157-1/minCG157-2, minCG164-1/minCG164-1, minCG174-1/minCG174-2, minCE144-1/minCE144-2, minCL35-1/minCL35-2, and minCL68-1/minCL68-2 (Table 3). Figure 6 indicates the positions where the primers anneal to $minC_{Ng}$. Each primer pair contains one primer that introduces a novel restriction site to $minC_{Ng}$; these sites are listed in Table 3 and mutagenized codons are indicated. Introduction of novel restriction sites facilitates screening of plasmids prior to DNA sequencing. Figure 7 graphically outlines the IPCR process. Figure 8 provides an overview of the construction of site-directed mutant $minC_{Ng}$ plasmids.

All PCR products in this study were cleaned using the QIAquick PCR purification kit (QIAgen) according to manufacturer's protocols (QIAgen, 2002) using the Sorvall® MC 12V centrifuge (Sorvall, Guelph, ONT). Products of all PCR, IPCR, restriction digests, and other manipulations were screened by electrophoresis using the Bio-Rad Power Pac 300 (Bio-Rad Laboratories, Mississauga, ONT) on 1% agarose gel (made with TAE buffer; Sambrook *et al.* 1980) at 100 V for 1 hour and visualized by

Figure 6: DNA sequence of MinC from *N. gonorrhoeae*. The start of the sequences to which mutagenic primers anneal are indicated with labeled arrows. The start and stop codons are highlighted in bold font and are underlined. Nucleotide numbering corresponds to that of the NCBI $minC_{Ng}$ sequence (accession number AF345908); the first and last nucleotides of the $minC_{Ng}$ gene are indicated (1 and 711).

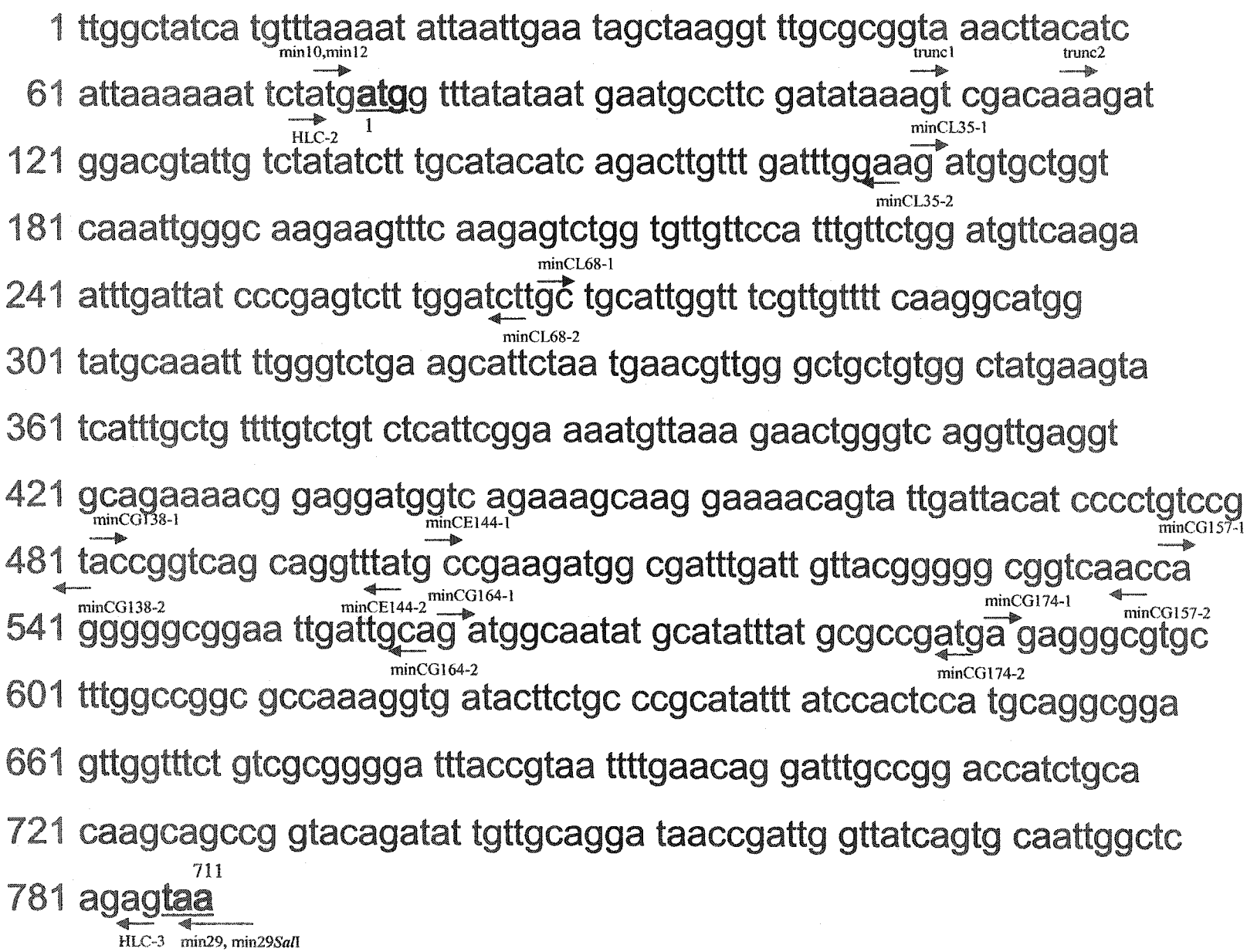
1 ttggctatca tgtttaaaat attaattgaa tagctaaggt ttgcgcggta aacttacatc
min10,min12
trunc1
trunc2
61 attaaaaaat tctatgatgg tttatataat gaatgccttc gatataaagt cgacaaagat
HLC-2
1
minCL35-1
121 ggacgtattg tctatatctt tgcatacatc agacttgttt gatttggaag atgtgctggt
minCL35-2
181 caaattgggc aagaagtttc aagagtctgg tgttgttcca tttgttctgg atgttcaaga
minCL68-1
241 atttgattat cccgagtctt tggatcttgc tgcattggtt tcgttgtttt caaggcatgg
minCL68-2
301 tatgcaaatt ttgggtctga agcattctaa tgaacgttgg gctgctgtgg ctatgaagta
361 tcatttgctg ttttgtctgt ctcattcgga aaatgttaaa gaactgggtc aggttgaggt
421 gcagaaaacg gaggatggtc agaaagcaag gaaaacagta ttgattacat cccctgtccg
minCG138-1
minCE144-1
minCG157-1
481 taccggtcag caggtttatg ccgaagatgg cgatttgatt gttacggggg cggtcaacca
minCG138-2
minCE144-2
minCG164-1
minCG174-1
minCG157-2
541 gggggcggaa ttgattgcag atggcaatat gcatatttat gcgccgatga gagggcgtgc
minCG164-2
minCG174-2
601 tttggccggc gccaaaggtg atacttctgc ccgcatattt atccactcca tgcaggcgga
661 gttggtttct gtcgcgggga tttaccgtaa ttttgaacag gatttgccgg accatctgca
721 caagcagccg gtacagatat tgttgcagga taaccgattg gttatcagtg caattggctc
711
781 agagtaa
HLC-3
min29, min29SalI

Figure 7: Inverse polymerase chain reaction of pSR2 to generate *minC*$_{Ng}$ mutant plasmids. Mutagenic primers were used to amplify pSR2 containing wild-type *minC*$_{Ng}$. Plasmids were then ligated and transformed into *E. coli* DH5α for screening.

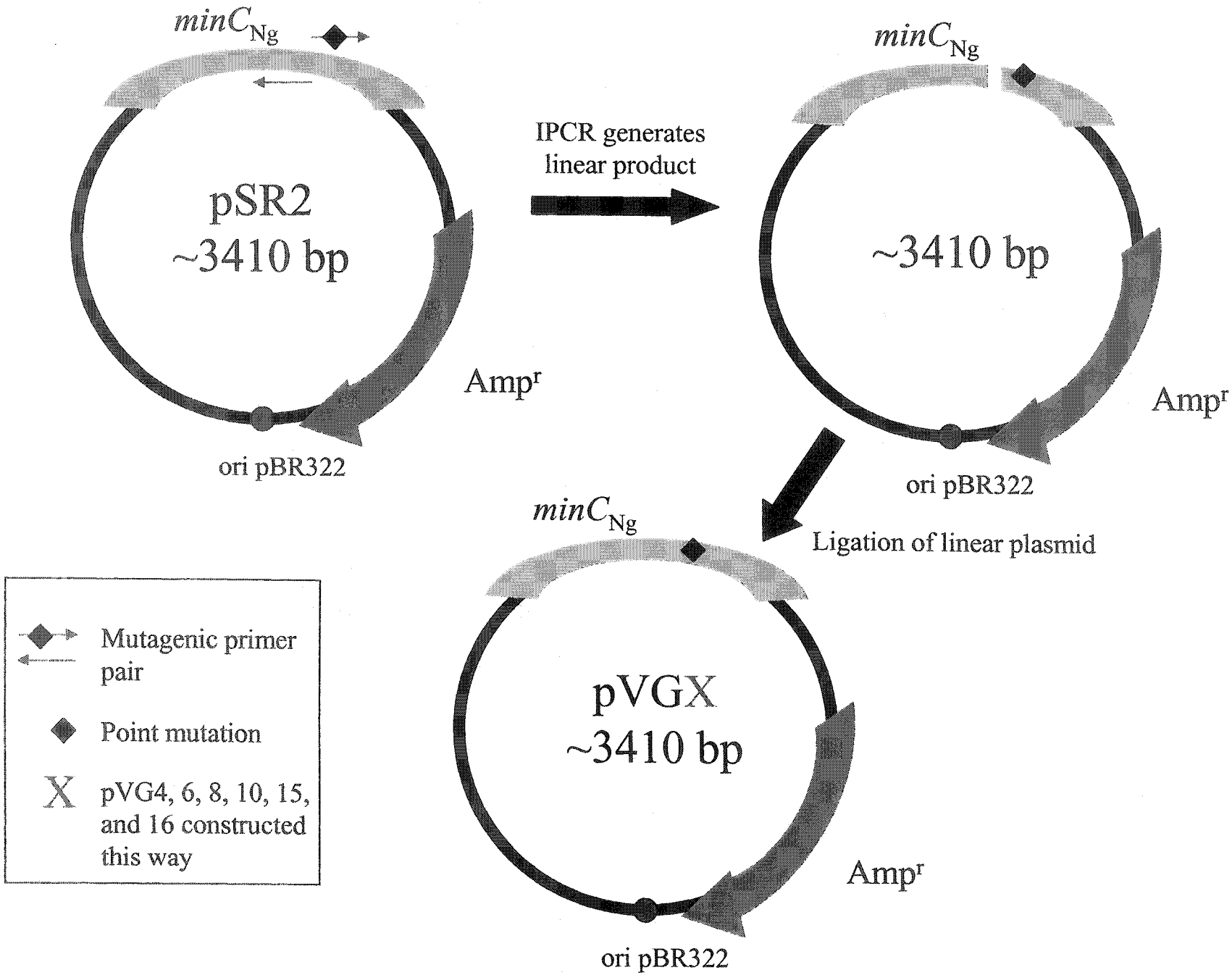
minC Ng
pSR2
~3410 bp
Amp r
ori pBR322
IPCR generates
linear product
minC Ng
~3410 bp
Amp r
ori pBR322
Ligation of linear plasmid
minC Ng
pVGX
~3410 bp
Amp r
ori pBR322
Mutagenic primer pair
Point mutation
X
pVG4, 6, 8, 10, 15, and 16 constructed this way

Figure 8: Overview of the construction of site-directed mutant *min*C_{Ng}-containing plasmids. pVG4, pVG6, pVG8, pVG10, pVG15, and pVG16 were created in this manner.

Overview of site-directed mutagenesis procedure

Inverse PCR of *minC*$_{Ng}$-containing pSR2 with mutagenic primers containing novel restriction sites

↓

Phosphorylation and ligation of linear mutagenized plasmid

↓

Transformation of $CaCl_2$-competent *E. coli* DH5α with circular plasmid

↓

Selection of transformants on LB agar containing ampicillin

↓

Screening of transformant colonies for ~3.4 kb plasmids by "cracking"; positive colonies are subcultured and mutagenized plasmids are recovered by miniprep

↓

Amplification of *minC*$_{Ng}$ from mutagenized plasmids determined positive by cracking

↓

Digestion of *minC*$_{Ng}$ amplicons with specific restriction endonucleases to screen for the introduction of mutations

↓

DNA sequencing for confirmation of introduction of mutation; if not present, another amplicon with a novel restriction endonuclease digestion pattern is sequenced

↓

Confirmed plasmid is used to transform *E. coli* PB103 for morphological analysis (phase contrast microscopy and flow cytometry) and protein expression (Western blot)

staining with ethidium bromide (10 μg/mL) and destaining in ddH_20 for 10 min. DNA size markers used in this study include the 1 Kb Plus DNA Ladder, Low DNA Mass™ Ladder, and Supercoiled DNA Ladder (Invitrogen, Burlington, ONT). Gels were photographed in the MultiImage Light Cabinet using the Alpha Imager 1220 software file version 5.04 (Alpha Innotech, San Leandro, CA).

The IPCR products were linear pSR2 variants containing the desired mutations in $minC_{Ng}$. These linear plasmids were phosphorylated in a 37 μl reaction including 1X T4 DNA ligase buffer (Invitrogen), 15 μl linear plasmid DNA (from 10 μl digested plasmid DNA prepared by miniprep), and 2 μl of T4 polynucleotide kinase (New England Biolabs (NEB), Beverly, MA). This reaction was incubated at 37°C for 20 minutes followed by the addition of 3 μl T4 DNA ligase (Invitrogen). This mixture was then incubated for 18 hours at 16°C. Plasmids pVG4, pVG6, pVG8, pVG10, pPF1, pVG15, and pVG16 (Table 2) were generated in this manner, respectively.

The entire ligation mixtures were used to transform $CaCl_2$ competent *E. coli* DH5α cells using the heat shock method (Sambrook *et al.*, 1980). Transformed cells were incubated for 16 to 24 hours at 37°C and screened for recombinant plasmids using a "cracking" method (Ramirez-Arcos *et al.*, 2001a). Cracking involves the suspension of individual transformant colonies in 25 μl ddH_2O followed by the addition of 25 μl of a 1:9 cracking buffer (0.2 ml 0.5 M EDTA (pH 8), 0.1 g SDS, 0.005 g bromophenol blue, 1.0 ml glycerol, and 7.8 ml ddH_2O):1 M NaCl solution. Colonies positive for a recombinant plasmid (i.e. containing bands corresponding to the size of the expected, 3.4 kb supercoiled product as compared to the supercoiled DNA marker) were selected and subcultured on LB agar containing ampicillin. Plasmids from these colonies were

purified using the QIAgen HiSpeed Miniprep Kit (QIAgen) according to the manufacturer's instructions (QIAgen, 2003) and resuspended in 50 µl ddH_20. This protocol for colony selection and plasmid harvesting was used in the creation of all constructs in this study.

Plasmids were screened for the introduction of mutations in *minC*$_{Ng}$ by PCR amplification of *minC*$_{Ng}$ using primer pair min10/min29 (Table 3; Figure 6) and restriction digestion of the purified amplicon. Each site-directed mutation introduced a novel restriction site in the mutated *minC*$_{Ng}$ that was not present in wild-type *minC*$_{Ng}$, such as *Sau3*AI in pVG4. It was thus possible to screen for *minC*$_{Ng}$ mutants by examining the restriction endonuclease digestion patterns of the transformants as compared to that of the wild-type *minC*$_{Ng}$ from pSR2. Digestion took place in 20 µl reactions including 1X buffer, 2 µl of the *minC*$_{Ng}$ amplicons, and 1 U of the appropriate restriction endonuclease. A *Sau*3AI (Invitrogen) site was generated in pVG4 (*minC*$_{Ng}$G138D), *Hga*I (NEB) in pVG6 (*minC*$_{Ng}$G157D), *Taq*Iα (NEB) in pVG8 (*minC*$_{Ng}$G164S), *Sau*3AI in pVG10 (*minC*$_{Ng}$G174E), *Cla*I (NEB) for pPF2 (*minC*$_{Ng}$E144I), and *Msp*I (NEB) in pVG15 (*minC*$_{Ng}$L35P) and in pVG16 (*minC*$_{Ng}$L68P); these enzymes were used to screen the plasmids. All buffers for these reactions were supplied with the enzymes from the manufacturers. Digests were electrophoresed on 2% agarose gels and stained with ethidium bromide for visualization.

DNA sequencing of entire *minC*$_{Ng}$ amplicons from positive clones was performed by the University of Ottawa Core DNA Sequencing and Synthesis Facility using the Applied Biosystems 373A Sequencer (Perkin Elmer). This sequencer uses the

dideoxy chain termination method of DNA sequencing (Slatko, 1994). This sequencing ensured the absence of frameshift mutations and the fidelity of the amplifications.

2.3.2 N-terminus truncations

Truncations of the N-terminus of *minC*$_{Ng}$ were performed to ascertain the effect of these mutations on protein function when heterologously expressed in *E. coli*. These plasmids were constructed by amplifiying *minC*$_{Ng}$ from pSR2 using a primer pair whose forward primer annealed downstream from the beginning of the gene to eliminate the desired number of amino acids from the N-terminus of the protein. Plasmids pVG17 and pVG18, were constructed by using the Trunc1 and Trunc2 primers, respectively, in combination with the min29 primer (Table 3; Figure 6). Primers included the *Eco*RI and *Bam*HI sites for use in cloning. Amplicons were digested with *Eco*R1 (NEB) and *Bam*HI (NEB), cleaned, and ligated in 20 µl reactions containing 12 µl amplicon, 2 µl similarly digested pUC18 plasmid (Amersham Pharmacia, Piscataway, NJ), 2 µl 10X buffer (NEB), 2 µl ddH20, and 2 µl of appropriate enzyme. The vector:insert ratio necessary for ligation was determined by comparison of relative concentrations of digested pUC18 and *minC*$_{Ng}$ amplicon using the Low Mass™ DNA Ladder (Invitrogen) and a 1:9 ratio was ligated based on band intensity and size of the vector and insert. Constructs were transformed into *E. coli* DH5α and screened for the presence of plasmids by cracking methods. Positive colonies were subcultured on LB agar containing ampicillin and plasmids from these subcultures were purified as described above. Plasmids were then submitted for DNA sequencing of the *minC*$_{Ng}$ gene.

2.3.3 pET30a-*minC*$_{Ng}$ constructs

pET30a (Novagen, Madison, WI) was used to construct *minC*$_{Ng}$-6XHis fusions for protein purification by nickel affinity chromatography. Purified wild-type MinC$_{Ng}$ was used for antibody preparation (Ramirez-Arcos *et al.*, 2001a) and circular dichroism analysis of protein structure. The plasmid pHLCC containing a C-terminus fusion of *minC*$_{Ng}$-6XHis (Table 2) was previously constructed in our laboratory. C-terminus fusions with G138D, G157D, G164S, G174E, and chimeric MinC (amino acids 1-99 of MinC$_{Ec}$ fused to amino acids 103-237 of MinC$_{Ng}$) were constructed for purification. Mutant *minC*$_{Ng}$ sequences were PCR-amplified from plasmids pVG4, pVG6, pVG8, pVG10, and pSR24 using primer pair HLC-2/HLC-3 (Table 3). Fragments were digested with enzymes *Nde*1 (NEB) and *Hin*DIII (NEB) that were selected in order to maintain the reading frame of the fusion protein. Products were cleaned and ligated into similarly-digested pET30a. Plasmids were transformed by heat shock methodology into *E. coli* DH5α and selected on LB agar containing kanamycin. Colonies were screened for plasmids by cracking methods and positive colonies were subcultured, purified, and confirmed by DNA sequencing of the fusion region. Resultant recombinant plasmids were named pET30aG138D, pET30aG157D, pET30aG164S, pET30aG174E, and pET30aCh (Table 2). Confirmed plasmids were then transformed into by heat shock into *E. coli* C41 for protein expression and purification experiments.

2.3.4 GFP-Min$_{Ng}$ fusions

GFP-Min$_{Ng}$ fusions were constructed for localization studies of the gonococcal Min proteins in bacterial cells by fluorescence microscopy. An overview of the construction

of these plasmids is shown in Figure 9. Amplicons containing *gfp-minC*$_{Ng}$, *gfp-minDE*$_{Ng}$, and *minDE*$_{Ng}$-*gfp* were amplified from plasmids pSR12 (derived from pDSW207), pSR15 (derived from pDSW207), and pSR13 (derived from pEGFP; Clontech, Palo Alto, CA; Table 2), respectively, using primer pairs GFP-1/GFP-2, GFP-1/GFP-3, and GFP-4/GFP-5 (Table 3). pDSW207 (Weiss *et al.*, 1999) is derived from pTrc99A (Pharmacia, Piscataway, NJ). These amplicons were digested with *Kpn*I (NEB)/*Pst*I (NEB), *KpnI*/*Pst*I, and *Eco*RI/*Kpn*I, respectively, cleaned, and ligated into similarly digested and cleaned pFP20 (Pagotto *et al.*, 2000; Table 2), a low copy-number shuttle vector for *N. gonorrhoeae* and *E. coli*, using the aforementioned techniques. *E. coli* DH5α was transformed with these plasmids and colonies were selected on LB agar containing kanamycin. Colonies were screened for recombinant plasmids by cracking methods and these plasmids were recovered and verified by restriction digestion with the aforementioned, appropriate enzymes. The QIAgen HiSpeed Midiprep Kit (QIAgen) was used to recover plasmids according to the manufacturer's protocol (QIAgen, 2001) in a final elution volume of 500 µl using Buffer EB (provided with the QIAgen HiSpeed Midiprep Kit). Plasmids were named pVG12 (*gfp-minC*$_{Ng}$), pVG13 (*gfp-minDE*$_{Ng}$), and pVG14 (*minDE*$_{Ng}$-*gfp*).

2.3.5 pGEX-MinC$_{Ng}$ construct

In future work, GST-pulldown assays will be used by other researchers in our laboratory to screen for suspected and novel protein-protein interactions of MinC$_{Ng}$. To facilitate these future studies, a *gst-minC*$_{Ng}$ fusion-containing construct is required, thus pVAL2 containing this fusion was constructed. PCR was used to amplify *minC*$_{Ng}$ from a *N.*

Figure 9: Construction of *gfp*-fusion plasmids. Fusions were amplified from plasmids previously constructed in the laboratory and ligated into low copy number shuttle vector pFP20.

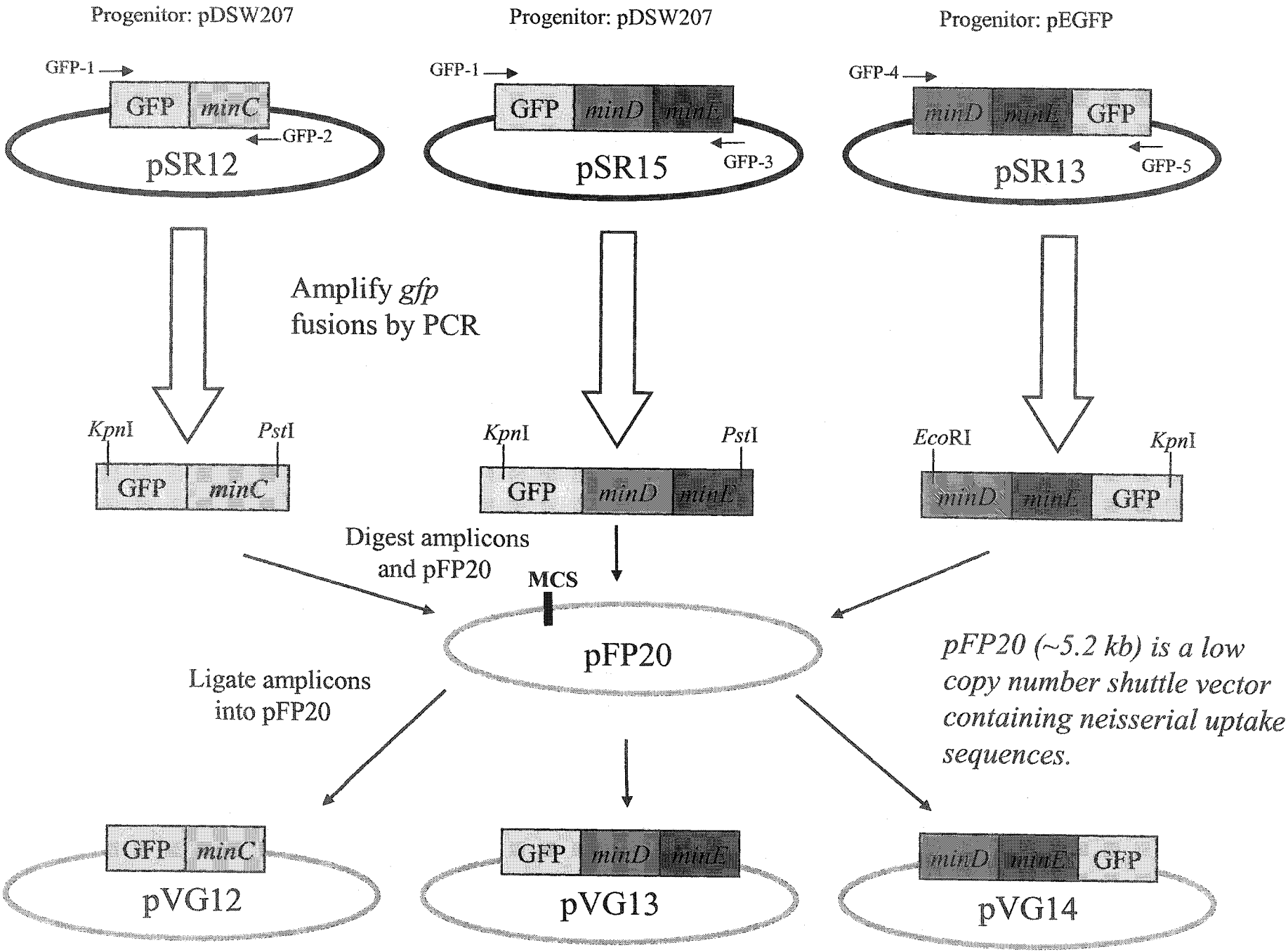
Progenitor: pDSW207
Progenitor: pDSW207
Progenitor: pEGFP
GFP-1
GFP
minC
GFP-2
pSR12
GFP-1
GFP
minD
minE
GFP-3
pSR15
GFP-4
minD
minE
GFP
GFP-5
pSR13
Amplify gfp fusions by PCR
KpnI
PstI
GFP
minC
KpnI
PstI
GFP
minD
minE
EcoRI
KpnI
minD
minE
GFP
Digest amplicons and pFP20
MCS
pFP20
Ligate amplicons into pFP20
pFP20 (~5.2 kb) is a low copy number shuttle vector containing neisserial uptake sequences.
GFP
minC
pVG12
GFP
minD
minE
pVG13
minD
minE
GFP
pVG14

gonorrhoeae CH811 cell suspension (0.5 McFarland turbidity) using primers min12/min29*SalI* (Table 3). Both pGEX-4T-3 (Amersham Biosciences, Baie D'Urfe, QUE; Table 2) and the amplicon were digested with *Eco*RI and *Sal*I (NEB), cleaned, and ligated. Plasmids were then transformed into *E. coli* DH5α and selected on LB agar containing ampicillin. Recombinant plasmids were screened by cracking methods, and positive colonies were subcultured and purified by miniprep (QIAgen). The presence of the *minC*$_{Ng}$ insert in recombinant plasmids was verified by restriction endonuclease digestion with *Eco*RI and *Sal*I. Plasmids that released the insert (720 kb) were submitted for DNA sequencing of the *minC*$_{Ng}$ gene; the fusion site was verified to be in frame.

2.4 Fixed cells and microscopy

The induction of filamentation indicating the inability to form proper septa at midcell in *E. coli* has been used as an indicator of MinC functionality (de Boer *et al.*, 1989; Hayashi *et al.*, 2001; Hu and Lutkenhaus, 2003). Visualization of cells expressing *minC*$_{Ng}$ mutants is necessary to ascertain if the MinC$_{Ng}$ protein is functional using cellular morphology as an indicator. Since MinC$_{Ng}$ is functional when heterologously expressed in *E. coli* (Ramirez-Arcos *et al.*, 2001a), overexpression of MinC$_{Ng}$ results in filamentation since division is inhibited. When a MinC$_{Ng}$ mutant is non-functional as a division inhibitor, filamentation will not occur and a wild-type cellular morphology will be seen.

Wild-type *E. coli* PB103 $CaCl_2$ competent cells were divided into 50 µl aliquots and were transformed as previously described with 2 µL of the following plasmids: pUC18 (negative control), pSR2 (*minC*$_{Ng}$, positive control), pVG4, pVG6, pVG8,

pVG10, pVG15, pVG16, pVG17, pVG18, pPF1, and pPF2. Transformed cells were recovered and fixed with 6% formaldehyde (Sigma® Chemical, ST. Louis, MO) and 0.2% glutaraldehyde (Fisher Chemical, Nepean, ONT) using the protocol described by Ramirez-Arcos *et al* (2001a). This method involves washing transformed cells three times with phosphate buffered saline (PBS) followed by fixation with 6% formaldehyde and 0.2% glutaraldehyde in PBS for 45 minutes. Cells were then washed an additional three times in PBS and resuspended in variable volumes of 100 µl to 500 µl of PBS (pH 7) depending on the size of the bacterial pellet in order to assure equivalent amounts of cells per slide. Fixed cells (10 µl) were then adhered to 0.01% polylysine pre-treated cover slips. Cover slips were then placed onto clean slides containing 10 µl drops of 50% (v/v) glycerol and sealed with transparent nail enamel.

Since no significant morphological differences were observed in cells with or without the addition of 40 µM or 100 µM IPTG, all expression assays were conducted without induction and were repeated at least three times. Ten microscopy fields, each containing a minimum of 100 cells, were analyzed to determine percentage of filaments or normal-sized short rods.

Cells were visualized by phase contrast microscopy using a Zeiss Axioskop microscope (Zeiss X100 oil immersion objective 100-w HBO lamp; Carl Zeiss Canada, Toronto, ONT) under the 100X oil emersion objective. Images were obtained using a Sony Power HAD 3CCD Color Video Camera (model DX 950) and Image Analysis Software version 6.0 (Northern Eclipse, Mississauga, ONT).

2.5 Flow Cytometry

Flow cytometry was used to discriminate the percentage of filamentous cells (>10 μm) and wild-type-sized rods (2-5 μm) within the whole population of *E. coli* cells as a quantitative indicator of $MinC_{Ng}$ functionality. Novel flow cytometry protocol was developed by S. Ramirez-Arcos and V. Greco in concert with representatives from Beckman Coulter for use in the present study. Cells expressing $MinC_{Ng}$ and the mutant variants were suspended in 1 ml of filter sterilized PBS to reduce the presence of background particles. Transformants were analyzed using a Beckman Coulter® Epics XL-MCL flow cytometer (Beckman Coulter, Mississauga, ONT) at a voltage and gain of 50 and 1.0, respectively, for side scatter, and 127 or 459 and 1.0 for forward scatter, respectively. Event retrieval was set to 300 seconds and a maximum of 100,000 cells. Data retrieval and analysis was done using EXPO32 ADC XL 4 Color software and EXPO32 v.1.2 software (Beckman Coulter), respectively. Gate A was created around wild-type sized rods using PB103 transformed with pUC18 as a negative control. Gate B was created around the population of larger cells, presumed to be filamentous, as determined using PB103 transformed with pSR2 expressing wild-type $MinC_{Ng}$ as a positive control for filamentous cells. The percentage of cells within each gate was calculated as the percentage of total gated cells within each gate to exclude background noise and particulate matter. Exact size of filaments could not be ascertained using this instrument. Each sample was subjected to flow cytometric analysis three times, and a second set of transformants was likewise analyzed.

2.6 SDS-PAGE and Western blot analysis

SDS-PAGE was used to determine relative levels of protein expression, the presence of purified proteins, and for Western blot analysis (to confirm $MinC_{Ng}$ expression). Competent cells of *E. coli* PB103 were distributed into 50 µl aliquots and were separately transformed with 2 µl of the following plasmids by heat shock: pUC18, pSR2, pPF1, pVG4, pVG6, pVG8, pVG10, pVG15, pVG16, pVG17, and pVG18. Plasmids had been previously prepared by miniprep and concentrations ranged from ~80 µg/ml to ~300 µg/ml. Transformants were prepared for Western blot analysis by suspension in 1 ml PBS (pH 7.0). The suspensions were then centrifuged for 5 minutes at room temperature at 12,000 rpm and the supernatant discarded. The pellet was then resuspended in 500 µl PBS (pH 7.0) with 100 µl loading buffer (10 ml of loading buffer contains: 0.5 mL 1 M Tris pH 8.0, 1 ml 1 M DTT [0.77g DTT in 5 ml sodium acetate 0.01 M (pH 5.2)], 2 ml 10% SDS, 0.01 g bromophenol blue, and 1 ml glycerol and completed to a final volume of 10 ml with ddH_2O). Samples in 600 µl were then boiled in a 100°C water bath for 10 minutes, centrifuged for 5 minutes at 12,000 rpm at room temperature to remove cellular debris, and the supernatant collected in a sterile 1.5 ml microfuge tube and stored at –20°C.

Proteins were separated by sodium dodecyl sulphate polyacrylamide gel electrophoresis (SDS-PAGE) using the protocol described by Sambrook *et al.* (1980). The protein running buffer contained 25 mM Tris base, 250 mM glycine, and 0.5% SDS for a 5X solution. Prior to loading the samples onto the gels, they were thawed and boiled for 5 minutes to ensure denaturation. Protein loading was standardized by three repetitions of densitometric analysis using Alpha Imager 1220 software (version 5.04;

Alpha Innotech Corporation) and the amount of each sample loaded for the Western blot analysis was adjusted to equalize protein concentration. Gels contained two phases including a 5% acrylamide stacking phase and a 12% acrylamide resolving phase. Proteins were separated using the Mini-PROTEAN II Electrophoresis Cell (Bio-Rad) at 100 volts until the loading buffer ran off the end of the gel. For the densitometric analysis, proteins were visualized by staining with Coomassie solution as described by Sambrook *et al.* (1980). Gels were destained by washing in the same solution in the absence of Coomassie Blue.

The Mini Trans-Blot® Electrophoretic Transfer Cell (Bio-Rad) was used for the Western transfer according to the manufacturer's instructions. Immobilon-P™ membranes (Millipore Corporation, Nepean, ONT) were washed in methanol for 15 seconds then in ddH_20 for 2 minutes prior to equilibration in transfer buffer (Sambrook *et al.,* 1980) for 15 minutes. The SDS-PAGE gels were similarly washed with transfer buffer for 15 minutes prior to the transfer to remove salts. The transfers took place for 1 hour at 100 V at room temperature. $MinC_{Ng}$ was detected as described by the instructions of the Immune-Blot® Assay Kit (Bio-Rad) with the exception that 3% skim milk was used for the blocking solution and antibody buffer instead of gelatin. The primary antibody, rabbit polyclonal anti-$MinC_{Ng}$, was previously prepared in our laboratory (Ramirez-Arcos *et al.,* 2001a). Dilutions varying from 1:100 to 1:1000 of the primary antibody were used depending on the antibody preparation. The secondary antibody was goat anti-rabbit IgG conjugated to alkaline phosphatase (Bio-Rad) and was diluted 1:3000. The Atto Phos Plus Kit (JBL Scientific, San Luis Obispo, CA) was used to develop the blot and results were visualized under UV light after 5 and 30 minute

exposure intervals. The membrane was photographed using Alpha Imager (Alpha Innotech Corporation) as described above.

Purified protein samples from the nickel affinity chromatography were diluted to 2 µl sample:800 µl PBS, added to 200 µl loading buffer and boiled for 10 minutes prior to loading the gel. Western blot analysis was the same as for the samples prepared from cell lysates.

2.7 Protein purification

$MinC_{Ng}$ proteins were purified for circular dichroism analysis of protein structure. Plasmids pHLCC, pET30aG138D, pET30aG157D, pET30aG164S, pET30aG174ED, and pET30aCh were transformed by heat shock into *E. coli* C41(DE3). 500 ml log-phase cultures (with optical densities at 600 nm [OD 600] greater than 0.4 as determined spectrophotometrically using the Beckman DU-640B) were induced with 0.4 mM IPTG for 0.5 h at 37°C with shaking at 250 rpm. Protein purification was completed using the procedure described by Szeto *et al.* (2001). Briefly, the cultures were centrifuged in the Sorvall RC 5C+ centrifuge (Sorvall) at 5000 rpm and the resultant pellet resuspended with binding buffer [prepared as described by Novagen (2002) and containing 5 mM imidazole, 0.5 M NaCl, and 20 mM Tris-HCl (pH 7.9)] containing 0.1 mg/ml of lysozyme (Sigma-Aldrich) and left at room temperature for 30 minutes. Samples were then sonicated in a Fisher Scientific 60 Sonic Dismembrator (Fisher Scientific) and centrifuged at 25,000 rpm in a Beckman L8 55M ultracentrifuge (Beckman Coulter) for 20 minutes at 4°C. The lysate was decanted into a polypropylene column (QIAgen) that had been loaded with Novagen His-Bind Resin and charged with a $NiSO_4$ solution as

described in the Novagen pET30a System Manual (2002) and allowed to flow by gravity at a rate of one drop per three seconds. The column was then washed with 30 ml binding buffer, 30 ml wash buffer (same composition as binding buffer but with 30 mM imidazole), and eluted with the elution buffer (containing 250 mM imidazole).

Protein concentration was determined by the method of Bradford (Bradford, 1976) using the Bio-Rad Protein Assay Kit II containing 450 ml dye reagent concentrate and bovine serum albumin (BSA) standard (Bio-Rad). In brief, known concentrations of BSA were serially diluted and dyed with a Coomassie blue-based reagent to generate a standard curve on which the unknown could be placed based on optical densities of the samples. Optical density was determined spectrophotometrically in plastic cuvets using the Beckman DU-640B.

2.8 Circular dichroism analysis

For purposes of this $MinC_{Ng}$ investigation, circular dichroism is used to predict whether or not the structure of a $MinC_{Ng}$ mutant is grossly affected by the introduction of a mutation. CD spectroscopy was performed by collaborators Dr. J. Wang and D. Fan (Southern Illinois University) using an AVIV Model 62DS CD spectrometer (AVIV Instruments, Lakewood NJ). A 1 mm path length quartz cell was used and experimentation took place at 20°C. The temperature of the sample was computer controlled to within 0.2°C. For the wild-type protein and each mutant, far-UV CD spectra were recorded at a protein concentration of 0.1-0.2 mg/ml in 10 mM ammonium bicarbonate buffer. All CD experiments were repeated three times to ensure

reproducibility. Following the baseline subtraction, the CD data were normalized to the protein concentration and were expressed as molar ellipticity.

2.9 Gonococcal transformations

N. gonorrhoeae strain F62 was transformed with pVG12, pVG13, and pVG14 using the spot transformation technique described by Gunn *et al.* (1996) for use in future gonococcal Min protein localization experiments. Piliated T2 colonies (Kellogg *et al.*, 1963) from these strains were selected for all transformations. These colonies were resuspended to a turbidity of 0.5 using the MacFarland standard in GCMBK broth (Gunn *et al.*, 1996). Cells were then diluted 10^4, 10^5, and 10^6 times in GCMBK broth and mixed with 100 ng of plasmid DNA. The mixtures were incubated at 35°C with 5% CO_2 for 30 minutes to promote DNA uptake. Mixtures were then spotted onto agar plates and incubated for 18 hours after which individual colonies were isolated and subcultured by streaking onto GCMBK agar containing kanamycin. Cultures were incubated for an additional 18 hours, following which colonies were screened by cracking and subcultured on GCMBK agar containing kanamycin. Plasmids from these colonies were purified using the QIAgen HiSpeed Plasmid Midi-prep Kit (QIAgen). Purified plasmids were screened by PCR amplification of the *gfp*-containing amplicon using primer pairs GFP-1/GFP-2 (pVG12), GFP-1/GFP-3 (pVG13), and GFP-4/GFP-5 (pVG14).

2.10 Yeast two-hybrid screening

The yeast two-hybrid system is an assay that enables the determination of protein-protein interactions (Fields and Song, 1989; Chien *et al.*, 1991). The

Saccharomyces cerevisiae transcriptional activator GAL4 is composed of two subunits, the activation domain (AD) and DNA binding domain (BD). When these units are brought within close proximity, transcription of *lacZ* (encoding β-galactosidase) occurs. The yeast two-hybrid system elegantly exploits the bipartite nature of this system to determine intermolecular protein interactions between suspected and unknown protein partners. In brief, the gene for the protein of interest is fused to the yeast GAL4 AD (this protein is the "bait") and the protein to be tested (a suspected partner of the bait or unknown cDNA) is fused to the GAL4 BD in two separate plasmids. These are transformed into *S. cerevisiae*, and if protein-protein interaction occurs, transcription of *lacZ* will result. Transcription is detected by the colormetric change that occurs when β-galactosidase enzymatically metabolizes IPTG, a galactose-like substrate, in the presence of the indicator X-gal. Both liquid and colony lift assays can be employed to detect and quantify this colour change from white (no interaction) to blue (positive interaction; Fields and Song, 1989).

To date, our laboratory has been unable to show self-interaction of $MinC_{Ng}$ and interaction of $MinC_{Ng}$ with $MinD_{Ng}$ using the yeast two-hybrid system (Matchmaker GAL4 Two-Hybrid System by Clontech) as has been demonstrated in *E. coli* Min proteins. Consequently, a chimera containing amino acids 1-99 of *E. coli* MinC and amino acids 103-237 of *N. gonorrhoeae* MinC has been constructed and has been shown to interact with $MinD_{Ng}$ (Douglas, 2002; Ramirez-Arcos *et al.*, 2003; Table 4). In this study, chimeric MinC containing the E144I mutation (encoding the protein $MinCCh_{E144I}$ in pPF2) was constructed from pPF1 (*min*C_{Ng}E144I) and pSRBD-Ch (Ramirez-Arcos *et al.*, 2003; Table 2). A 425 bp fragment encoding amino acids 103-237 of *min*C_{Ng}E144I

Table 4. Summary of functionality of $MinC_{Ec}$ and MinCh mutants.

Protein	Mutation	Morphology in *E. coli* PB103	Interaction	
			MinC	MinD
$MinC_{Ec}$	wild-type	Filamentous	+	+
	G135D	short rods	+	-
	G154D	short rods	+	-
	G161S	short rods	-	+
	G171E	short rods	weak	-
	P141A[b]	Filamentous	+	+
MinCCh	wild-type	Filamentous	-	+
	G135D	short rods	NT[a]	-
	G154D	short rods	NT	-
	G161S	short rods	NT	+
	G171E	short rods	NT	-
	E141I[b]	Filamentous	NT	+

a) NT : Not tested. Since a self-interaction of wild-typeMinCCh was not detected, we did not test self-interactions of the MinCCh mutants

b) These experiments were performed in this study; data from H. Douglas, 2002 and Ramirez-Arcos *et al.*, 2003

from pPF1 was amplified with primer pair CNg-up/min29 containing *Spe*I (NEB) and *Bam*HI restriction sites at their 5' and 3' ends, respectively (Table 3). This *minC*$_{Ng}$E144I fragment was digested and ligated as described above into pSRBD-Ch that had been previously digested with *Spe*I and *Bam*HI, generating pPF2. Plasmids were purified with the by miniprep (QIAgen) and integrity and frame of the fusion gene were confirmed by DNA sequencing.

pGAD*minC*$_{Ec}$C and pGBT*minC*$_{Ec}$C, the C-terminal domain of *minC*$_{Ec}$ fused with the GAL4 activation and binding domains, were constructed by amplification of from pSR32 which contains *minC*$_{Ec}$ (Table 2; Ramirez-Arcos *et al.*, 2003) using primer pair EcCh-up1/EcMinC-down (Table 3). This amplicon was digested with *Eco*RI and *Bam*HI and ligated as above into the similarly digested pGAD4T4 (AD) and pGBT9 (BD). Recombinant plasmids were confirmed by restriction endonuclease digestion with *Eco*RI and *Bam*HI to release the insert and by DNA sequencing.

Plasmids were transformed into *S. cerevisiae* SFY526, singly as a negative control, or in pairs to test for protein-protein interactions, using the lithium acetate (LiAc) method (Clontech, 1999). Double transformants included pPF2 with MinD$_{Ng}$ (to test interactions of the neutral mutation in MinC$_{Ng}$) and pGADMinC$_{Ec}$C with pGADMinC$_{Ec}$C (to determine MinC$_{Ec}$ termini can self interact). Interactions of the other MinC$_{Ng}$ mutants expressed as chimeras had been previously tested in the laboratory (Ramirez-Arcos *et al.*, 2003; Table 4). Yeast transformants were assayed for β-galactosidase activity, with IPTG as a substrate, using the colony-lift method (Clontech, 1999). Briefly, yeast colonies transformed with one or both plasmids were transferred to sterilized filter paper disks, frozen in liquid nitrogen and thawed, and developed

overnight in Z-buffer (Clontech, 1999) containing the X-gal indicator. Assays were performed in triplicate, at least twice, for each interaction.

2.11 Protein alignment and modeling

MinC sequences from 36 different prokaryotic microorganisms were obtained from the National Center for Biotechnology Information (NCBI) web site (www.ncbi.nlm.nih.gov) and 28 of these sequences were selected representing different genera (Figure 10). As sequences from different species of the same genus were usually 100% identical, 8 sequences were omitted. Sequences were aligned using Clustal W software (www.searchlauncher.bcm.tmc.edu/multi-align/multi-align.html).

The structures of MinC from *Thermotoga maritima* (Tm; Cordell *et al.,* 2001) and MinD from Pyrococcus furiosus (Pf; Hayashi, *et al.,* 2001) were used as templates for protein modeling of gonococcal Min proteins. To obtain predicted three-dimensional (3D) structures of $MinC_{Tm}$ and $MinD_{Pf}$, the $MinC_{Tm}$ and $MinD_{Pf}$ sequences were submitted for automated protein modeling using SWISS-MODEL (www.expasy.org/swissmod/SWISS-MODEL.html). All images were retrieved using Swiss Viewer PDB. $MinD_{Pf}$ has been previously modeled as a dimer using the dimeric structure of the iron protein NifH (dinitrogenase reductase; Lutkenhaus and Sundaramoorthy, 2003). A similar approach was employed and $MinD_{Pf}$ was superimposed on NifH to obtain a $MinD_{Pf}$ dimer where the exposed α-7 helix was localized. All hydrophobic amino acids within the helix were localized as being exposed on the surface or to the interior. The $MinD_{Pf}$ dimer was aligned with the C-terminus of a $MinC_{Tm}$ monomer in a position where a $MinC_{Tm}$-$MinD_{Pf}$ interaction might occur

between the $MinD_{Pf}$ α-7 helix and the B/C surface junction of $MinC_{Tm}$. Two views were analyzed corresponding to a 90° rotation to observe the interaction face of the proteins.

RESULTS

3.1 Mutation of four conserved C-terminus glycines causes loss of $MinC_{Ng}$ functionality

3.1.1 Four conserved glycines are selected for site-directed mutagenesis

Multiple alignment of MinC from 36 prokaryotic species revealed the complete conservation of five amino acids (Figure 10). These residues correspond to *N. gonorrhoeae* R136, G138, G157, G164, and G174. In *E. coli*, the corresponding glycine residues are G135, G154, G161, and G171 (Figure 10). Mutagenesis of the conserved R136 residue was previously performed (Greco, 2001) by introduction of a nonsense mutation at this codon resulting in a non-functional protein as determined by morphological analyses. The four conserved glycines were of paramount interest in the present investigation.

Glycines were radically mutagenized to G136D, G157D, G164S, G174E, and E144I by IPCR, generating plasmids pVG4, pVG6, pVG8, pVG10, and pPF1 (Table 2). Radical mutations were expected to have the greatest impact on protein function (Labie *et al.*, 1990; Mulder *et al.*, 1992). To assay the effect of a radical mutation in a non-conserved residue, E144 was mutagenized to E144I generating pPF1. Construction of one plasmid, pVG8 (G164E), is depicted in Figures 11 and 12. The amplified, linear product of the IPCR reaction using pSR2 as a template and mutagenic primers minCG164-1 and minCG164-2 generating pVG8 is shown Figure 11A. The product is 3,410 bp, the size of the progenitor plasmid pSR2. A sample of the cracking procedure used to screen transformants is depicted in Figure 11B. Lanes containing a suspected recombinant plasmid (later named pVG8) include lanes 5 through 10, 14, and 15; the

Figure 10: Multiple alignment of the conserved C-terminus of prokaryotic MinC. A: Multiple alignment of 36 MinC sequences. Ng, *N. gonorrhoeae*; Nm, *N. meningitidis*; Ec, *E. coli*; Sf, *S, flexneri;* St, *S. typhi*; Yp, *Y. pestis*; Kp, *K. pneumoniae;* B, *Buchnera;* Vc, *V. cholerae*; Xf, *X. fastidiosa*; Xc, *X. campestris*; At, *A. tumefaciens;* Sm, *Sinorhizobium*; Bj, *Bradyrizobium japonicum;* Sy, *Synechocistis* sp.; Ta, *T. elongatus*; So, *S. oneidensis*; Ml, *Mesorhizobium*; Pa, *P. aeruginosa*; Dr, *D. radiodurans*; Tt, *T. tengcongensis*; Cp, *C. perfringens;* Bs, *B. subtilis;* Oh, *O. iheyensis*; Lm, *L. monocytogenes;* Lp, *L. plantarum;* Tm, *T. maritima*; Hp, *H. pylori*. Black boxes highlight residues that are completely conserved while gray boxes show related amino acids. Asterisks indicate the location of the four conserved glycine residues investigated in the present study. B: Three-dimensional structure of the C-terminus β-helix of MinC from *Thermotoga maritima*.

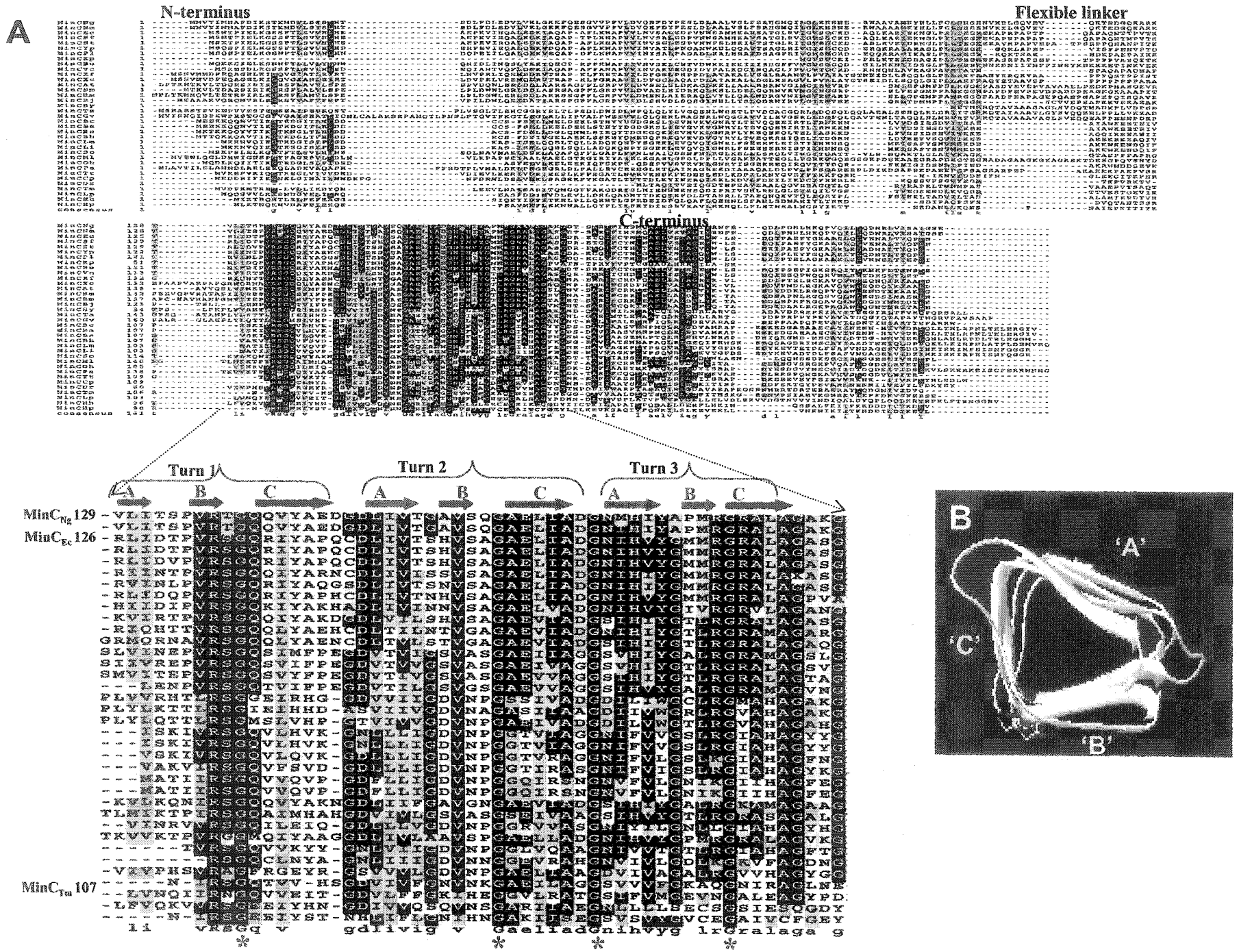
A
N-terminus
Flexible linker
C-terminus
Turn 1
Turn 2
Turn 3
A
B
C
MinC$_{Ng}$ 129
MinC$_{Ec}$ 126
MinC$_{Tm}$ 107
B
'A'
'B'
'C'

Figure 11: Inverse PCR and screening of pVG8 ($MinC_{Ng}$ with G164D). A: Amplification of pSR2 by IPCR. Lane 1 – 1 kb ladder; lane 2 – linear pVG8. B: Screening of pVG8 transformants by cracking.

A.

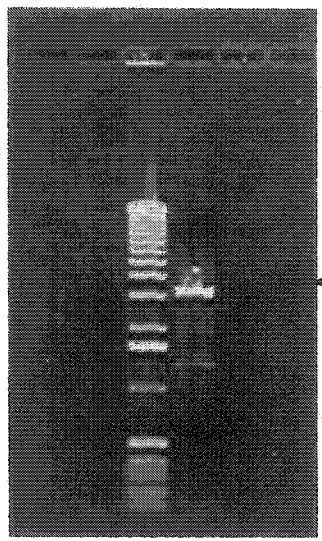

B.

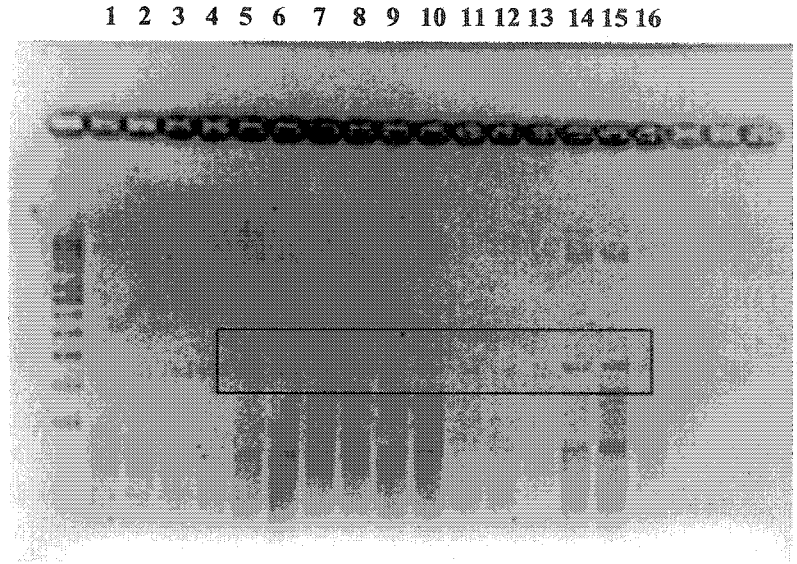

Figure 12: Screening of pVG8 transformants for introduction of the G164D mutation. A: *minC*$_{Ng}$ is amplified from cell suspensions of the transformants. Lane 1 – 1 kb ladder; lane 2 – amplification of *minC*$_{Ng}$ from pSR2 (wild-type *minC*$_{Ng}$) transformants; lanes 3-7 – amplification of *minC*$_{Ng}$ from pVG8 transformants. B: *TaqI*α digestion of amplicons from (A). Lane 1 – 1 kb ladder; lane 2 and lane 3 – digests of pVG8 clones that are positive for the G164D mutation; lanes 4 to 6 – digests of negative pVG8 clones; lane 7 – digest of *minC*$_{Ng}$ from pSR2 (negative control).

A.

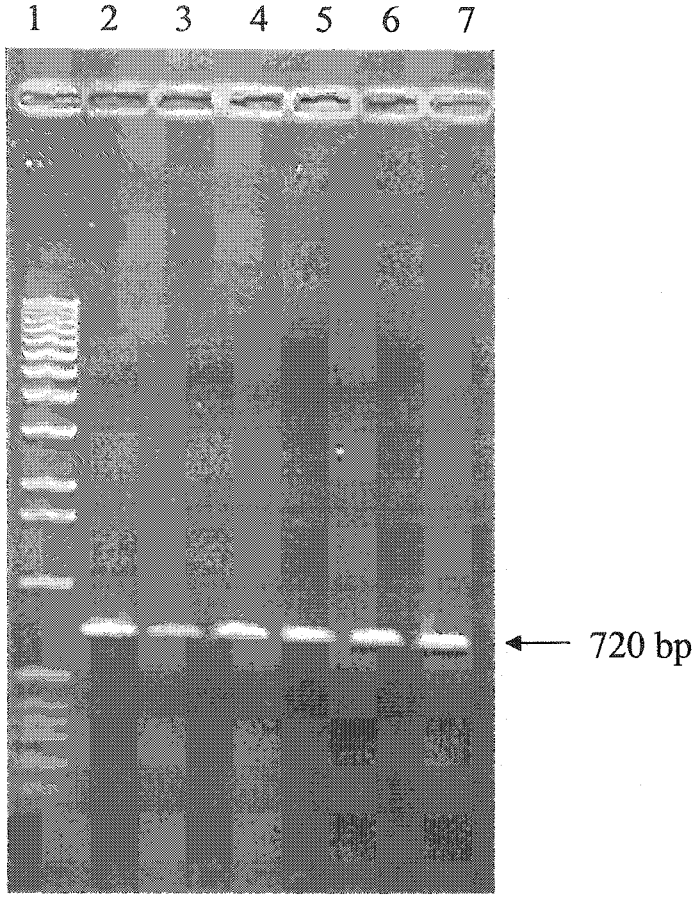

B.

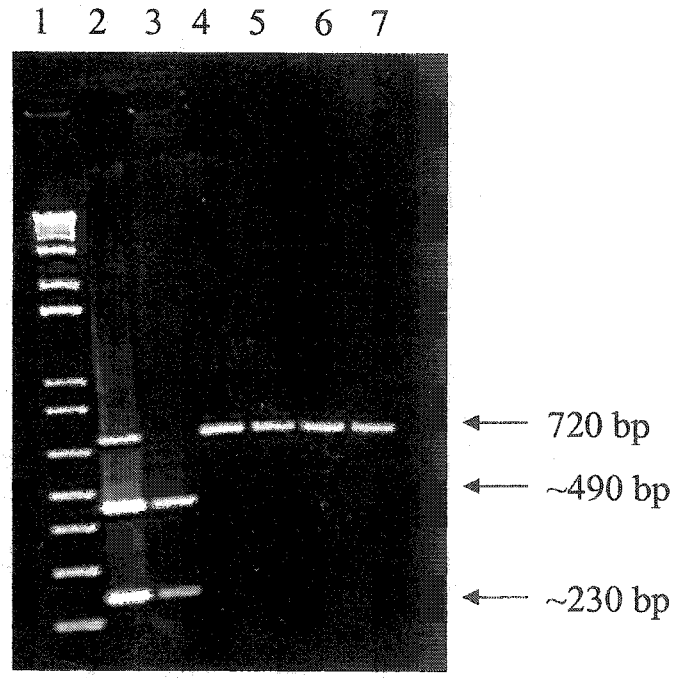

supercoiled 3,410 bp supercoiled plasmid is emphasized with a box. Amplification of *minC*$_{Ng}$ from cell suspensions of these colonies using primer pair min10/min29 is shown in Figure 12A; the resultant amplicon (*minC*$_{Ng}$) is 720 bp in length. Figure 12B demonstrates the difference in restriction endonuclease patterns between pVG8 positive clones (lanes 2 and 3) and negative clones (lanes 4 to 6) when *minC*$_{Ng}$ amplicons from these clones was digested with *Taq*Iα. Digestion with *Taq*Iα results in the cleavage of the G164S mutant *minC*$_{Ng}$ into 490 bp and 230 bp fragments, while the wild-type gene lacks this site and remains 720 bp. The DNA sequence of the mutated *minC*$_{Ng}$ gene was obtained for verification of the mutation and fidelity. An example of a site-directed mutant sequence from pVG8 is shown in Figure 13 in which a glycine residue has been changed to a serine residue. A section of the DNA sequencing results from pVG8 is shown in Figure 14.

3.1.2 Conserved glycine residues are mapped to the C-terminus of MinC$_{Tm}$

The mutated glycine and control residues were mapped to specific surfaces of the 12-standed β-barrel of the C-terminus of MinC$_{Tm}$ based on the solved structure by Cordell *et al.* (2001). It was found that G138$_{Ng}$, G157$_{Ng}$, and G174$_{Ng}$ lie on or within close proximity to the B and C surface junction and that G164$_{Ng}$ is located near the A surface (Figure 15). The non-conserved amino acid E144$_{Ng}$ is located on the C face near the A and C junction. Cordell *et al.* speculate that the A face is responsible for self-interaction; it was predicted that A face glycine MinC$_{Ng}$ mutant G164S would lose self-interaction. However, the surface responsible for MinD$_{Ng}$-MinC$_{Ng}$ interaction has yet to be identified.

Figure 13: Site-directed mutation G164S in *minC*$_{Ng}$ in pVG8. Upper sequence is from the pSR2 template; lower sequence is from the linear pVG8 product containing the mutation. Nucleotide numbers are indicated and correspond to those of the gene in the NCBI database.

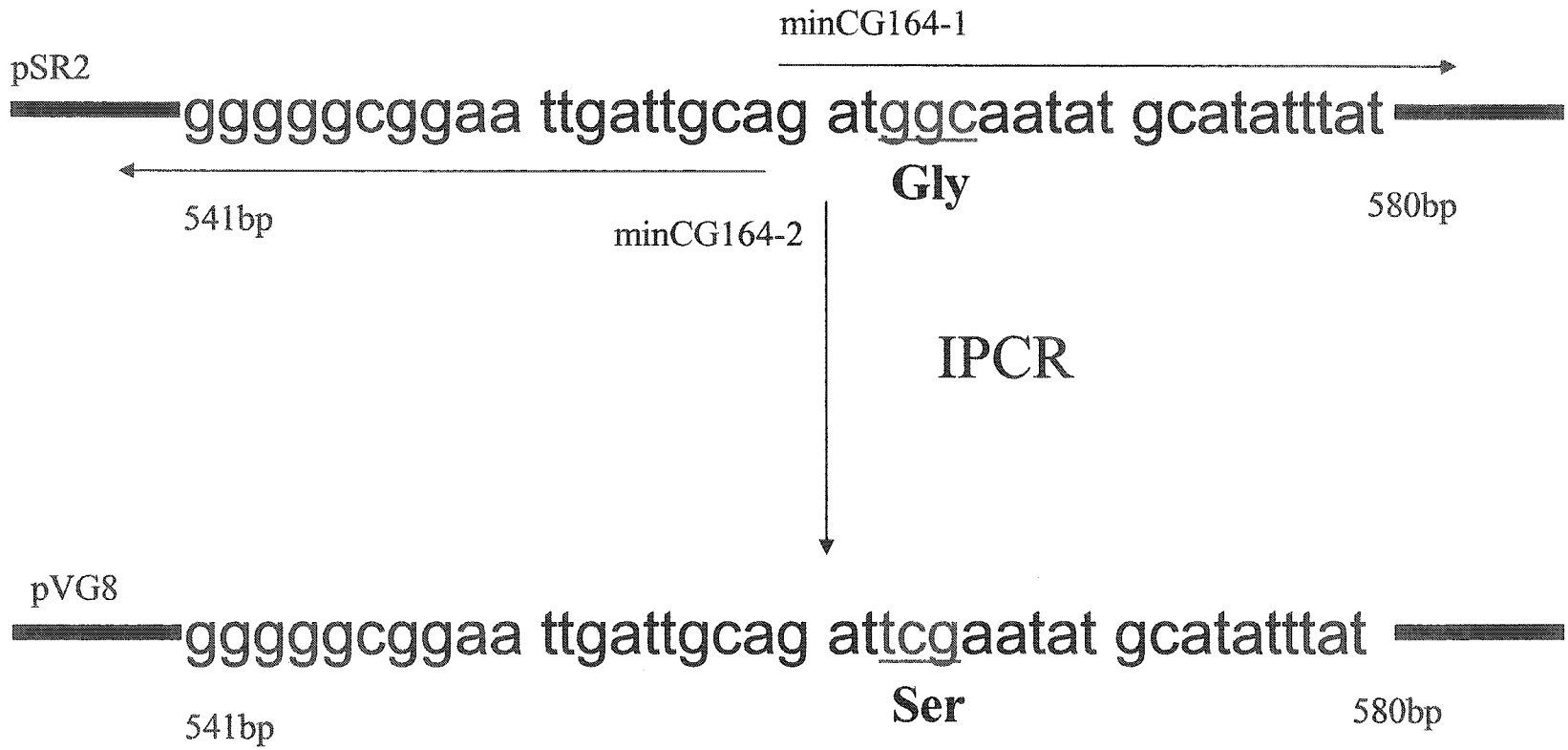
minCG164-1
pSR2
ggggggcggaa ttgattgcag atggcaatat gcatatttat
Gly
541bp
580bp
minCG164-2
IPCR
pVG8
ggggggcggaa ttgattgcag attcgaatat gcatatttat
Ser
541bp
580bp

Figure 14: Excerpt of the automated DNA sequencing results for pVG8 (G164S). The complementary strand was sequenced and is illustrated in the 5'→ 3' orientation. The mutagenized codon is indicated with a box.

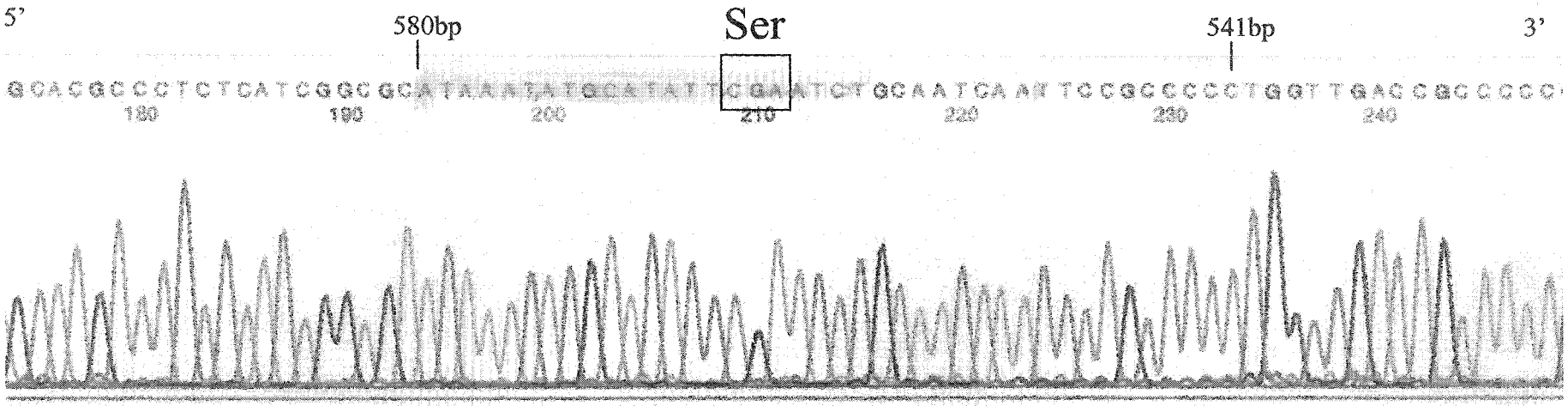
5'
580bp
Ser
541bp
3'
180
190
200
210
220
230
240

Figure 15: Location of mutagenized C-terminus residues of $MinC_{Ng}$ mapped to the C-terminus of *Thermotoga maritima* MinC. *T. maritima* structure from Cordell *et al.*, 2001. Red arrows indicate the position of the radical glycine mutations in $MinC_{Ng}$ and blue arrows represent the mutation in a non-conserved glutamic acid residue in $MinC_{Ng}$.

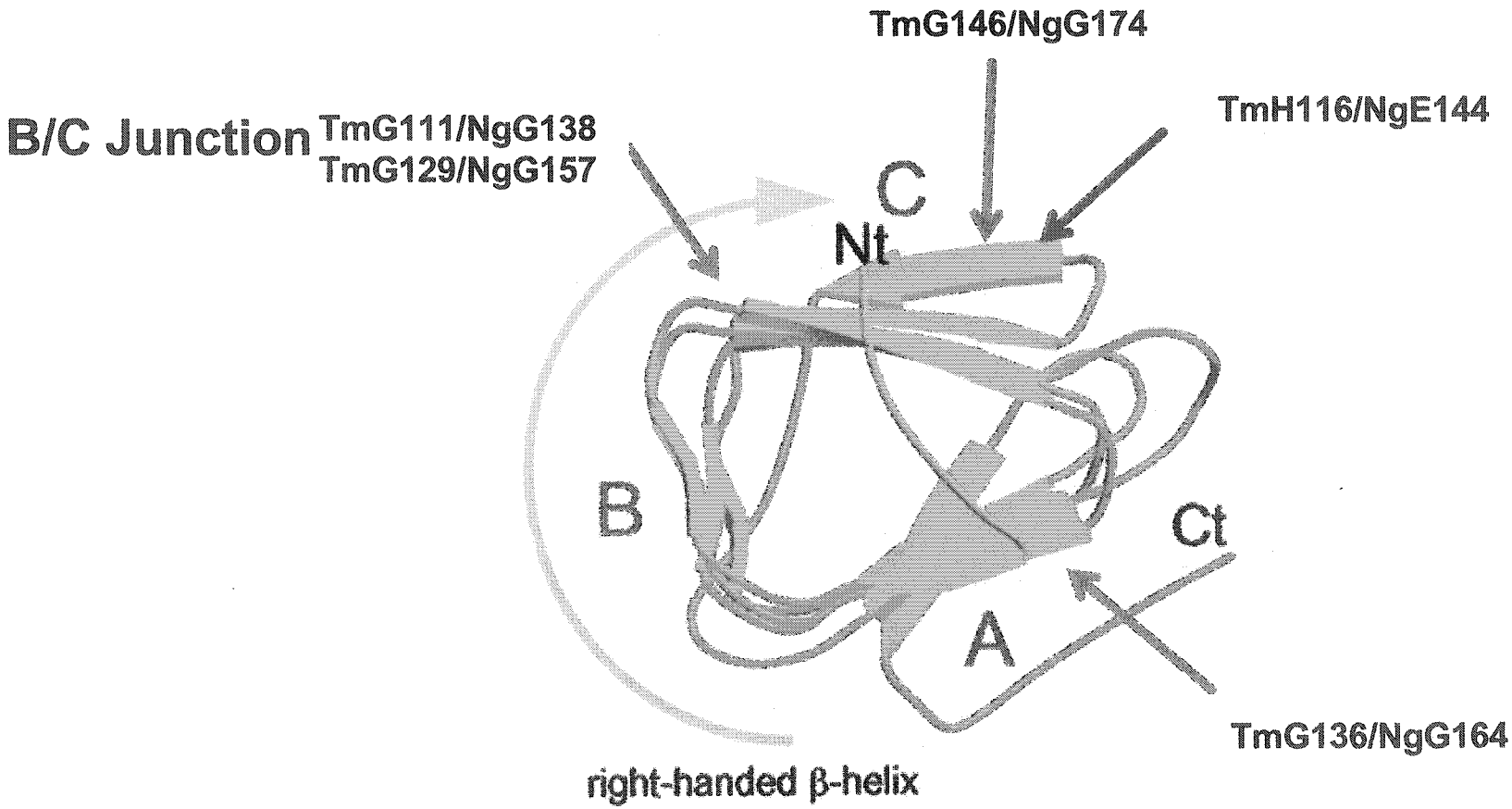
TmG146/NgG174
TmH116/NgE144
B/C Junction TmG111/NgG138
TmG129/NgG157
C
Nt
B
Ct
A
TmG136/NgG164
right-handed β-helix

3.1.3 Glycine mutants are non-functional as determined by inability to induce filamentation in *E. coli* PB103

Phase contrast microscopy was employed to determine the cellular morphology of the indicator *E. coli* strain PB103 when expressing the mutant variants of $MinC_{Ng}$ constructed in this study. Morphology is an indicator of $MinC_{Ng}$ functionality since this protein is heterologously expressed in *E. coli* and induces filamentation when overexpressed (Ramirez-Arcos *et al.*, 2001a). Figure 16 demonstrates cellular populations captured at the 100X oil emersion level. Cells that were at least six times the wild-type length (2-3 μm) were considered filamentous. Ten fields of >100 cells were for each of the transformants. The negative control transformed with pUC18 (Figure 16A), demonstrated 100% standard-sized short rods (~3 μm in length). These cells were used to determine a gate (Gate A) around wild-type sized populations of cells in the flow cytometric analysis (Figure 16A'). In contrast, the positive control transformed with pSR2 encoding wild-type $MinC_{Ng}$ (Figure 16B) was 95.3 ± 3.1% filamentous, with the presence of a few "ghost" (lysed) cells. Gate B was determined using these cells for flow cytometric analysis (Figure 16B'). Filamentous cells were seen that exceeded 50 μm in length. The neutral E144I mutant exhibited the characteristics of the positive control, with 77.6 ± 7.6% filamentation (Figure 16C). The corresponding flow cytometry data is shown in Figure 16C', in which a large amount of the population of cells are found in Gate B, corresponding to the filamentous phenotype (see below).

E. coli PB103 cells transformed with plasmids containing the four mutations in conserved $MinC_{Ng}$ glycine residues, pVG4 (G138D), pVG6 (G157D), pVG8 (G164S), and pVG10 (G174E) retained the characteristics of the wild-type $MinC_{Ng}$-expressing

Figure 16: Microscopy and flow cytometry of $MinC_{Ng}$ controls when expressed in *E. coli* PB103. Phase contrast micrographs were taken using 100X oil immersion objective. A: pUC18 transformant exhibits wild-type cellular morphology. B: Division inhibition due to overexpression of wild type $MinC_{Ng}$ from pSR2 results in extreme filamentation. C: Mutation in non-conserved $MinC_{Ng}$ E144I residue does not inhibit division inhibition function of this protein as demonstrated by filamentation. A'- C': Flow cytometric scatter graphs corresponding to each $MinC_{Ng}$ control. Gate A represents wild-type sized cells and Gate B represents filamentous cells.

A.

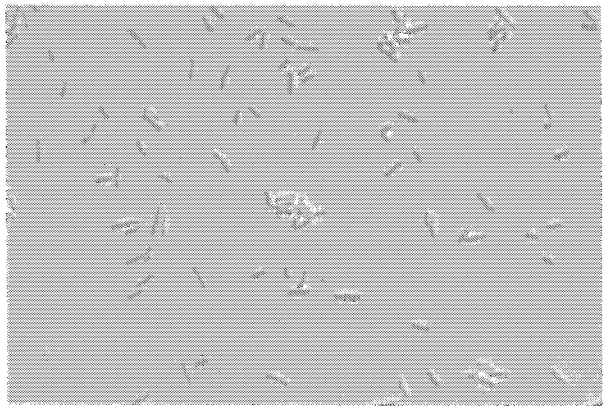

A'.

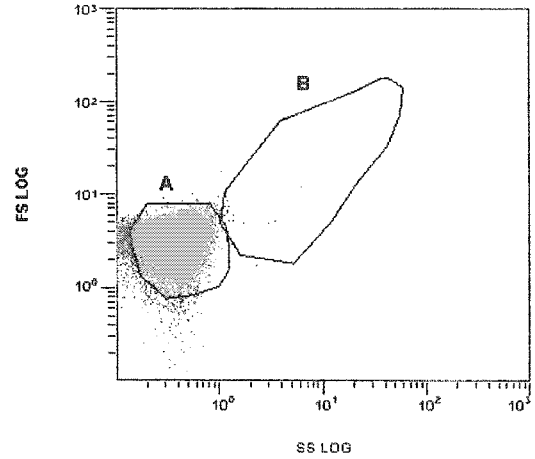

B.

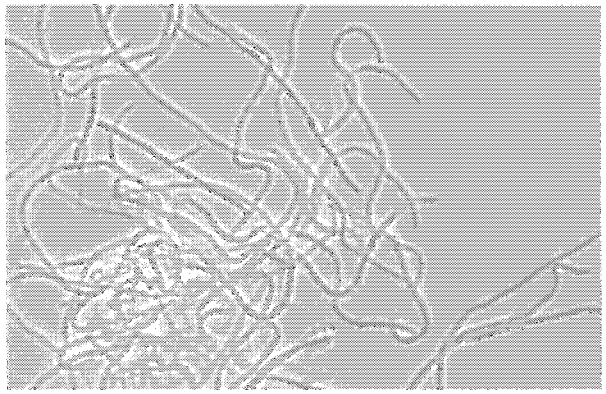

B'.

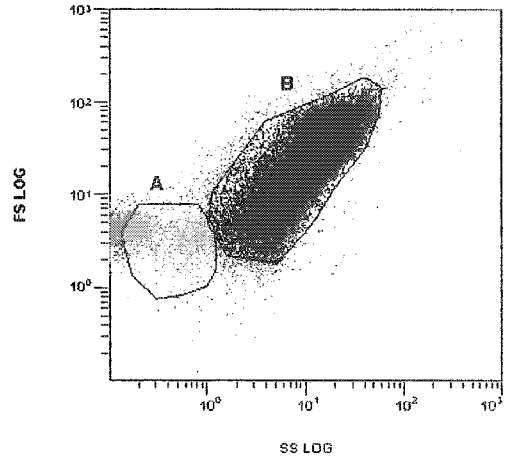

C.

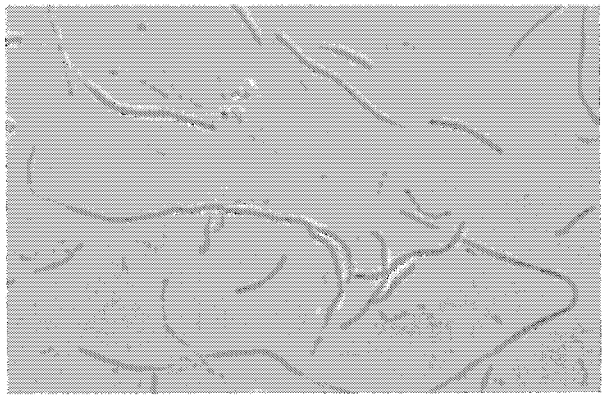

C'.

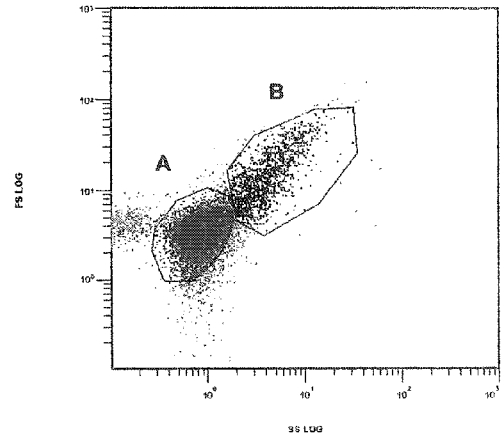

cells (Figures 17 and 18). The G138D (Figure 17A) and G157D (Figure 17B) transformants comprised exclusively short rods as well as the presence of lysed cells (examples are indicated with boxes). Lysed cells are ruptured and devoid of cellular contents; these are also known as ghost cells. Non-lysed cells exhibited a typical length of 3 to 6 μm. Some lysed cells were elongated (~6 to 10 μm in length). Inclusion bodies were also present in these two transformants. Corresponding flow cytometry scatter graphs are shown in Figures 17A' and 17B', in which it is evident that the majority of the cells are gated as wild-type sized. The remaining two mutants, G164S and G174E (Figures 18A and 18B, respectively) were comprised heterogeneously of short rods (~2 to 3 μm in length). Flow cytometric scatter graphs show that the both mutants are gated in the wild-type GateA (Figure 18A' and 18B'). The population size dynamics were studied more intensely using flow cytometric technology.

3.1.4 Glycine mutants are unable to induce filamentation in *E. coli* PB103 as determined by flow cytometry.

Flow cytometry was employed in this study to discriminate between different populations of cells based on size. Filaments appear in a different population than wild-type sized rods when sorted using this technique. Figure 19 depicts the percent of filamentation of the *E. coli* PB103 transformants as assessed using this method.

The wild-type $MinC_{Ng}$ transformants (pSR2) induced the highest amount of filamentation (87.81 ± 13.61%) with only the E144I mutation (pPF1) being comparable to this extent of filamentation (64.5 ± 14.84%). All $MinC_{Ng}$ mutants with mutations in conserved glycine residues exhibited little or no filamentation (>0.15%), similar to the

Figure 17: Microscopy and flow cytometry of the G138D and G157D $MinC_{Ng}$ mutants expressed in *E.coli* PB103. Phase contrast micrographs were taken using 100X oil immersion objective. A: Microscopy of G138D mutant; B: G157D mutant. Both mutants exhibit normal cellular morphology. Examples of ghost cells present in the G138D and G157D mutants are indicated with a box. A'and B': Flow cytometric scatter graphs corresponding to each $MinC_{Ng}$ mutant. Gate A represents wild-type sized cells and Gate B represents filamentous cells.

A.

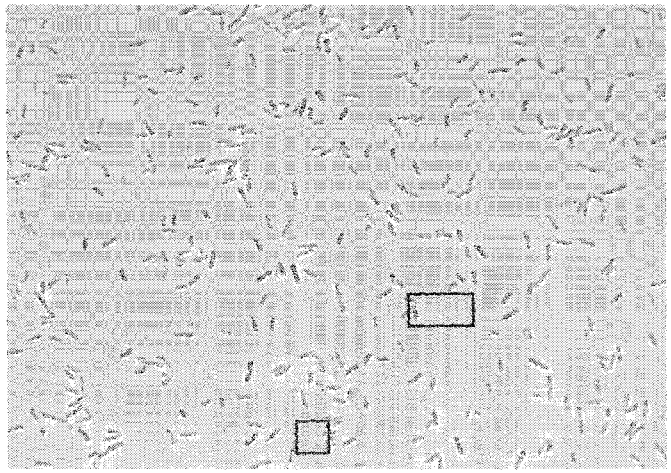

A'.

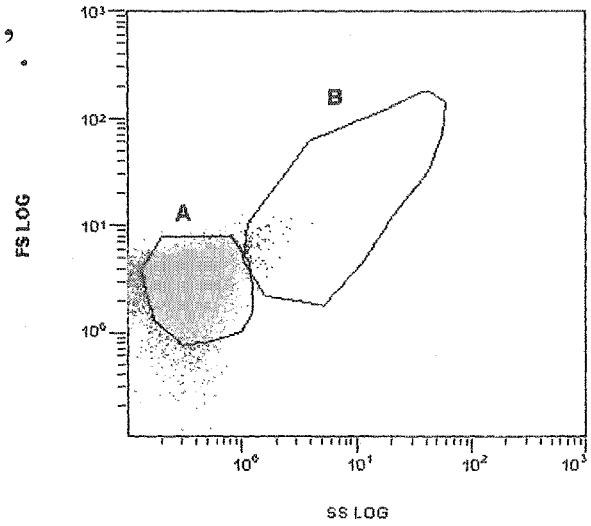

B.

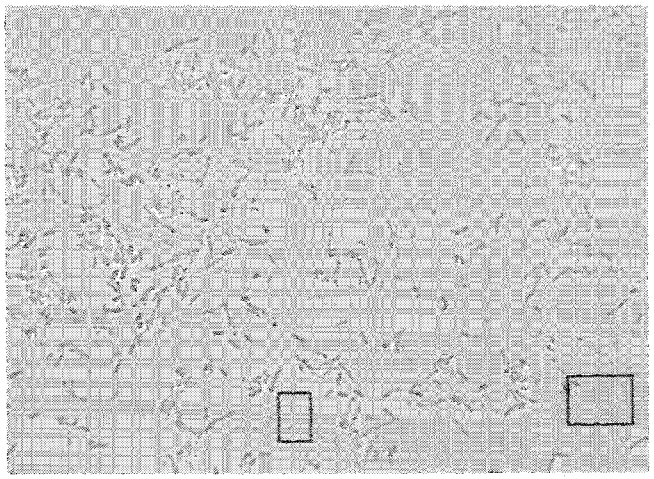

B'.

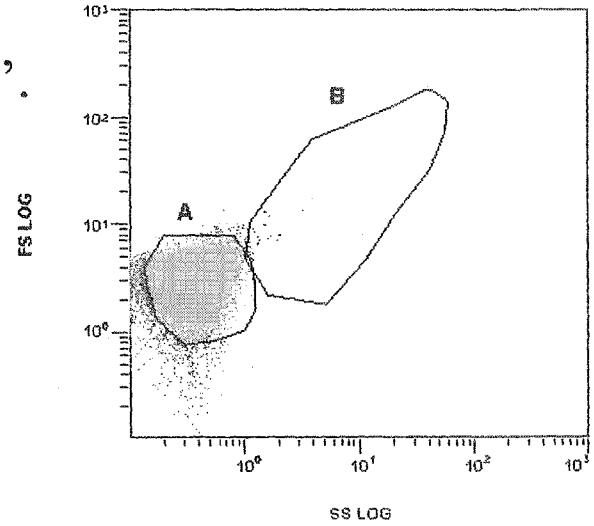

Figure 18: Microscopy and flow cytometry of the G164S and G174E $MinC_{Ng}$ mutants expressed in *E.coli* PB103. Phase contrast micrographs were taken using 100X oil immersion objective. A: Microscopy of G164S mutant; B: G174E mutant. Both mutants exhibit normal cellular morphology. A'and B': Flow cytometric scatter graphs corresponding to each $MinC_{Ng}$ mutant. Gate A represents wild-type sized cells and Gate B represents filamentous cells.

A.

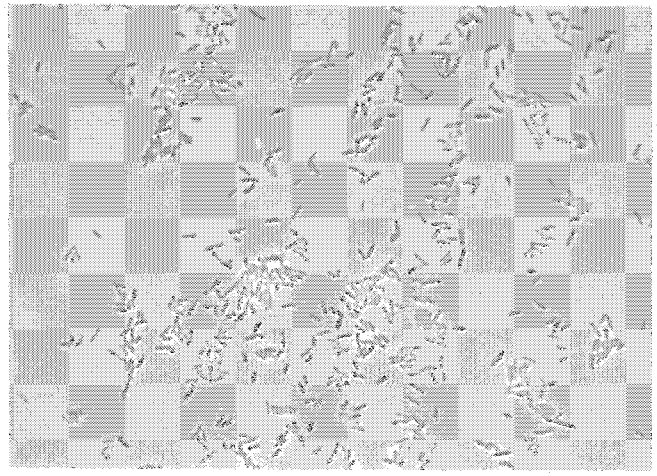

A'.

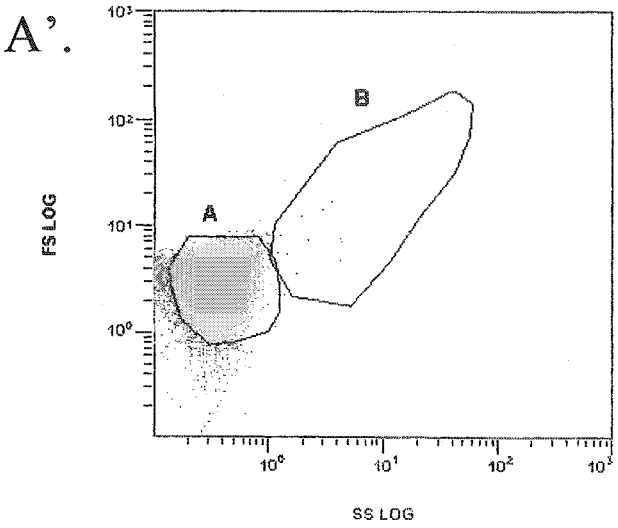

B.

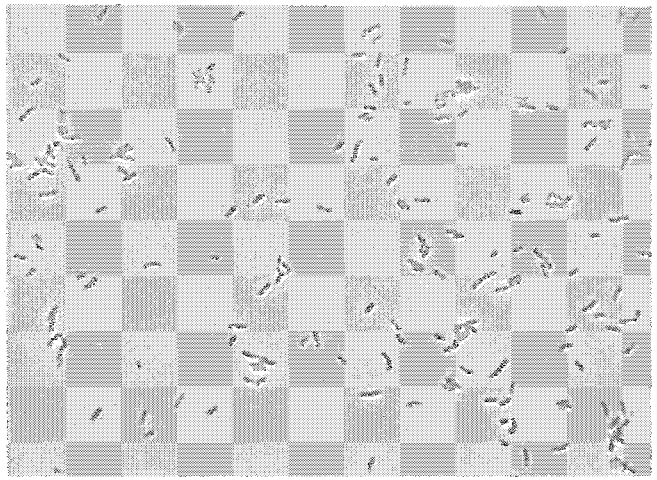

B'.

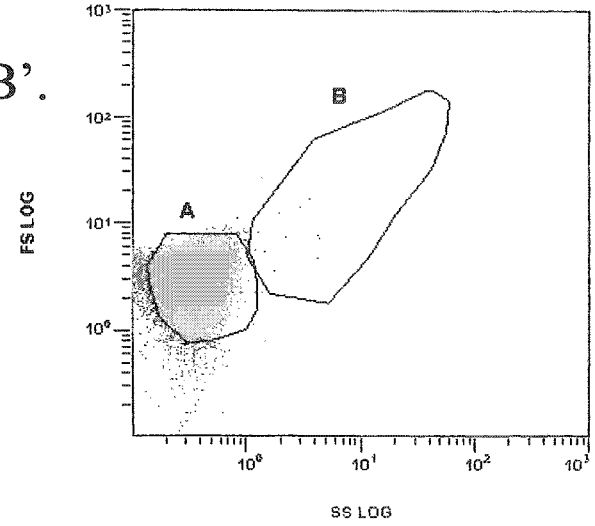

Figure 19: Flow cytometric analysis of $MinC_{Ng}$ mutants expressed in *E. coli* PB103. Data is shown with a standard deviation that is almost imperceptible in some mutants.

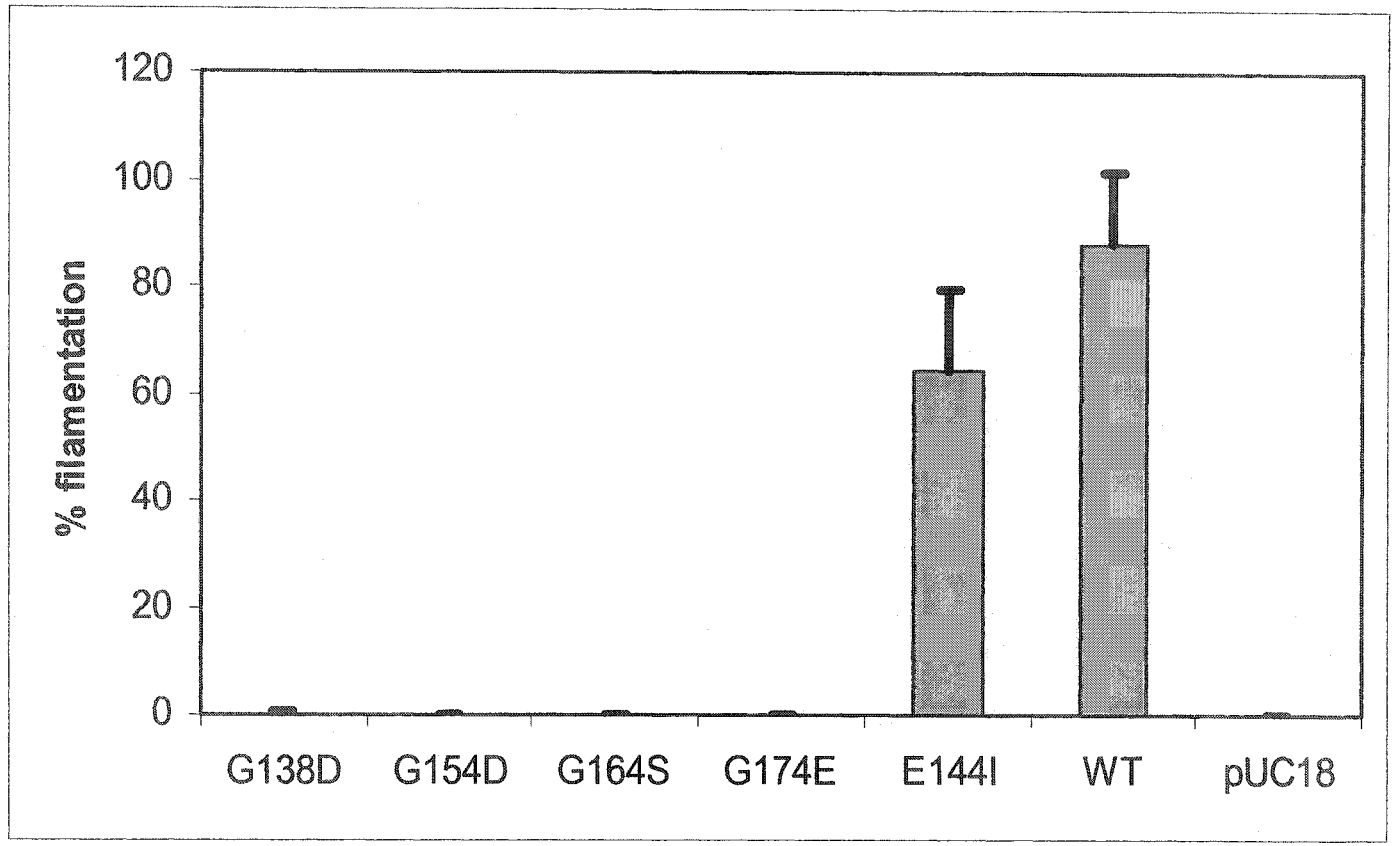
% filamentation
120
100
80
60
40
20
0
G138D
G154D
G164S
G174E
E144I
WT
pUC18

pUC18 negative controls (0.0%, used to establish Gate A, the wild-type morphological population). The glycine mutants and pUC18 transformants were uniform in population size and were grouped almost exclusively into Gate A, whereas various sizes of filaments were detected for the pSR2 (wild-type $MinC_{Ng}$, positive control) and pPF1 (neutral mutant) transformants. Some filaments were detected outside of Gate A, but not within Gate B, the limit set for the detection of filamentous cells, so it is possible that more aberrantly-sized cells were present within these populations that were not detected due to abnormal size. These results substantiate the above findings that $MinC_{Ng}$ is non-functional as a cell division inhibitor when conserved glycine residues are radically altered.

3.1.5 $MinC_{Ng}$ mutants are expressed in *E. coli* PB103

Western blot analysis was performed to ensure that the mutant $MinC_{Ng}$ proteins were being expressed in PB103. Western blots were performed in triplicate; an example of one such blot is shown in Figure 20. All mutants, including the four glycine mutants, the neutral mutant, and the chimera containing the neutral mutation (for use in yeast two-hybrid analyses) were expressed. Trace amounts of wild-type $MinC_{Ec}$ were detected from pUC18 transformants (lane 1); levels of wild-type $MinC_{Ng}$ were ~ 1.8 fold higher (lane 2). The glycine mutants G138D (lane 3) and G164S (lane 5) were expressed with the similar abundance as wild-type $MinC_{Ng}$ from pSR2 (lane 2). The G157D mutant (lane 3) was expressed at levels 25 % greater than wild-type $MinC_{Ng}$. Additionally, the migration of this mutant was retarded on the SDS-PAGE gel as compared to wild-type $MinC_{Ng}$ and the other glycine mutants. The G174E mutant protein expression was reduced 33% as compared to wild-type $MinC_{Ng}$. The E144I and $MinCCh_{E144I}$ mutants

Figure 20: Mutant $MinC_{Ng}$ is expressed in *E. coli* PB103 as determined by Western blot analysis. A: Lane 1- pUC18 transformant (negative control); lane 2 - $MinC_{Ng}$ from pSR2 transformant (positive control); lane 3 - $MinC_{Ng}$ G138D mutant; lane 4 - $MinC_{Ng}$ G157D mutant; lane 5 - $MinC_{Ng}$ G164S mutant; lane 6 - $MinC_{Ng}$ G1174E mutant. Note the overexpression of the G157D mutant and the retarded migration due to replacement of an aliphatic residue by a charged residue. B: Lane 1 - $MinC_{Ng}$ (positive control); lane 2 - $MinC_{Ng}$ E144I mutant; lane 3 - MinCCh E144I mutant.

A.

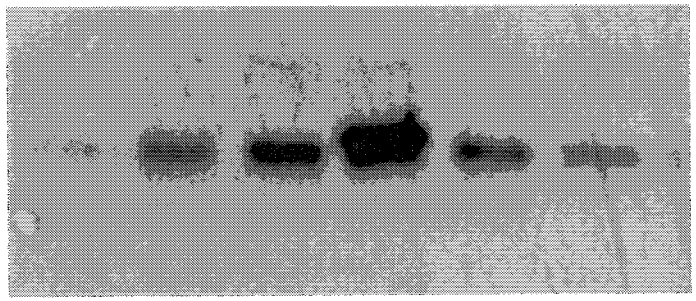
pUC18
MinC$_{Ng}$
G138D
G157D
G164S
G174E
1
2
3
4
5
6

B.

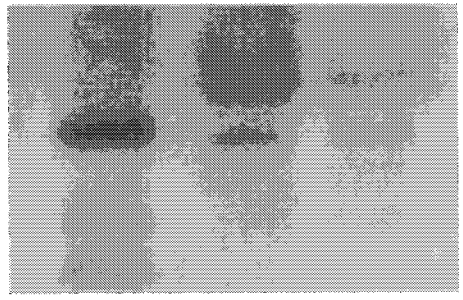
MinC$_{Ng}$
E144I
MinCCh
E144I
1
2
3

(Figure 20B, lanes 2 and 3, respectively) were not expressed to the same extent as the wild-type protein; they were expressed at levels ~2.0 fold less than the wild-type $MinC_{Ng}$ protein. Despite reduced expression as compared to wild-type $MinC_{Ng}$ from pSR2, the E144I mutant was still capable of inducing filamentation in *E. coli* PB103 (Figure 16C) whereas the conserved glycine mutants $MinC_{Ng}$ were not (Figures 17 and 18). This phenomenon indicates the complete non-functionality of the conserved glycine mutants as inhibitors of cell division.

3.2 Neutral $MinC_{Ng}$ chimeric mutant retains interaction with $MinD_{Ec}$

Since $MinC_{Ng}$ and $MinD_{Ng}$ have not been demonstrated to interact using the yeast two-hybrid system, chimeric MinC containing the N-terminal region and linker of $MinC_{Ec}$ (amino acids 1-99) and the C-terminal region of $MinC_{Ng}$ (amino acids 103-237) was constructed (MinCCh; Ramirez-Arcos *et al.*, 2003). Interactions of this chimera and chimeras containing mutations in conserved glycine residues have been previously performed in our laboratory (Table 4). The neutral mutation was not previously examined, therefore MinCCh containing the E144I mutation ($MinCCh_{E141I}$) was constructed and ligated in frame with the yeast GAL4 activation domain (pPF2) for yeast two-hybrid analysis. MinCCh does not self interact, therefore the interaction between $MinCCh_{E141I}$ and MinCCh was not tested. Interaction between the $MinCCh_{E141I}$ and $MinD_{Ng}$ was tested by co-transforming yeast with both the $MinCCh_{E141I}$/AD fusion and the $MinD_{Ng}$/BD fusions (plasmids pPF2 and pGBT9minD, respectively) and performing the colony lift assays. When single transformation of pPF2 alone was performed, no interaction was detected since all transferred colonies were white (Figure 21A). This was the anticipated negative reaction from this control. However, when the

Figure 21: Chimeric MinC with the E144I mutation maintains interaction with $MinD_{Ng}$. A: pGADMinC_{Ng} (MinC_{Ng}) + pPF2 (MinCCh$_{E144I}$); B: pGADMinD_{Ng} and pPF2.

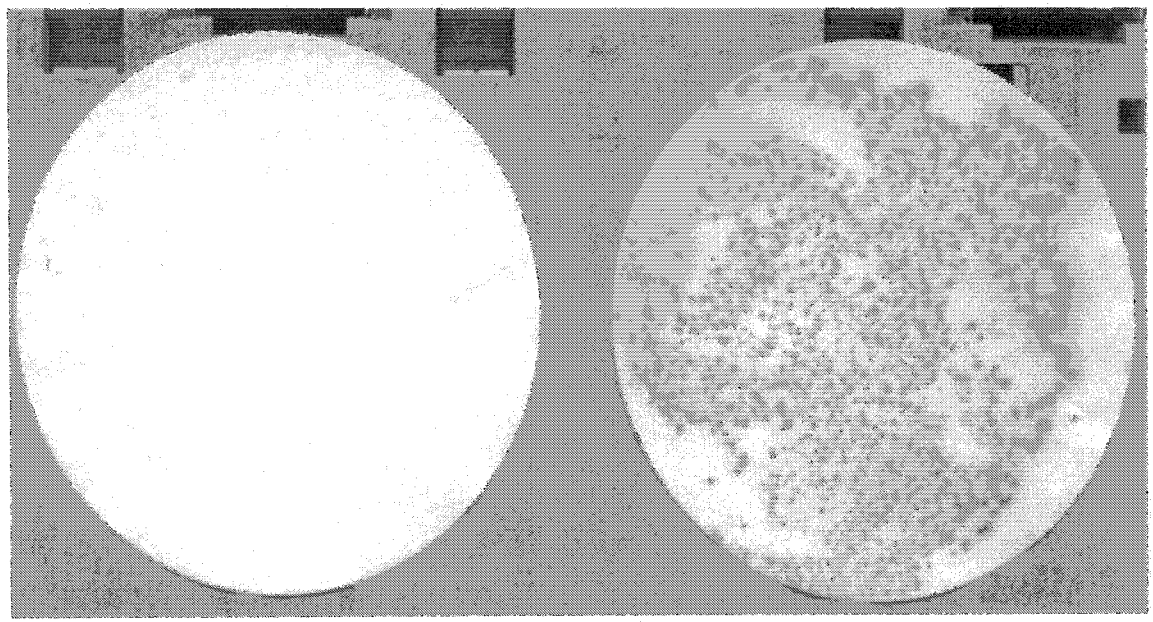

A. B.

two plasmids were co-transformed, all blue colonies were present, indicating the interaction of $MinCCh_{E141I}$ with $MinD_{Ng}$ (Figure 21B), which is the case with MinCCh (Table 4). Experiments were performed in triplicate to confirm these data.

3.3 $MinC_{Ng}$ is purified at high concentration from *E. coli* C41

Plasmids containing $MinC_{Ng}$ and mutant variants fused to a 6X His tag were transformed into the expression strain *E. coli* C41 and assayed to determine in which cell fraction $MinC_{Ng}$ was expressed (Figure 22A). C41 is used as an expression strain as it encodes the T7 RNA polymerase under control of a galactose-inducible promoter; pET30a fusion genes are transcribed by the T7 polymerase. This system is ideal for protein expression since fusion proteins are not expressed in the strains used for cloning (which reduces toxicity in cloning strains), and the galactose-sensitive nature of the system enables tight control over gene expression. The majority of the $MinC_{Ng}$ was determined to be located in the insoluble fraction of induced C41 cultures (Figure 22A, lane 5; $MinC_{Ng}$ is indicated with an arrow). Utilizing this information, a protocol was developed for the purification of $MinC_{Ng}$. $MinC_{Ng}$ was optimally eluted at 250 mM imidazole following extensive washing of the affinity column (see Materials and Methods). Wild-type and glycine mutant $MinC_{Ng}$ proteins were purified in high yield (in quantities in excess of 10 μg/ml) as shown in Figure 22B. Bradford analysis was used to determine protein concentration; a sample Bradford curve used in the determination of a wild-type $MinC_{Ng}$ sample is shown in Figure 23 in which 10.8 μg/ml purified protein was recovered. MinCCh was also purified in high yield using the same methodologies as were employed

Figure 22: Nickel affinity column purification of $MinC_{Ng}$ and mutant $MinC_{Ng}$ proteins. A: $MinC_{Ng}$ is determined to be in the insoluble protein fraction. Lane1 – molecular weight marker; lane 2 – pre-induction soluble fraction; lane 3 – pre-induction insoluble fraction; lane 4 – post-induction soluble fraction; lane 5 – post-induction insoluble fraction. $MinC_{Ng}$ is determined to be most abundant in the induced insoluble fraction and is indicated with an arrow. B: $MinC_{Ng}$ mutants are purified. Lane 1 – molecular weight marker; lane 2 – G138D mutant; lane 3 – G157D mutant; lane 4 – G164S mutant; lane 5 – G174E mutant; lane 6 – wild type $MinC_{Ng}$. C: Purification of E144I $MinC_{Ng}$ mutant. Lane 1 – molecular weight marker; lane 2 – cell lysate; lane 3 – 100 mM imidazole eluted fraction; lane 4 – 250 mM imidazole eluted fraction.

A.

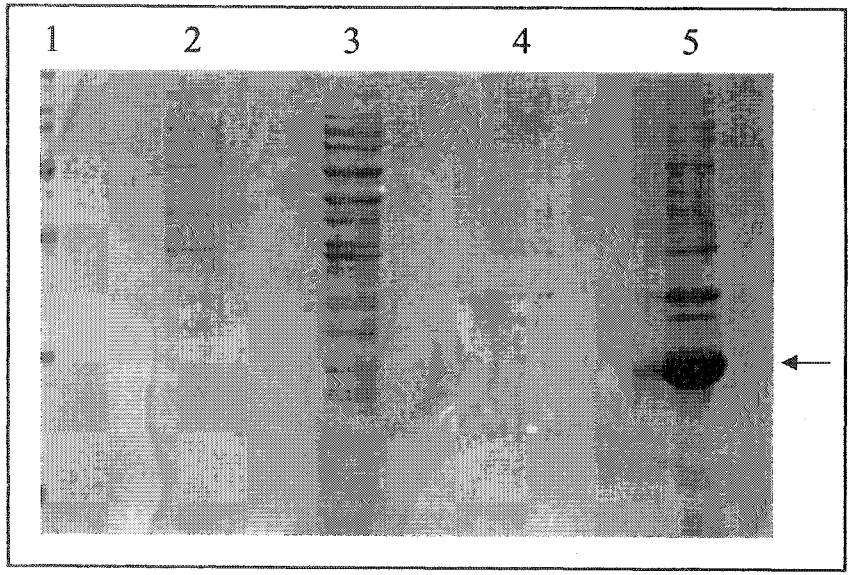

B.

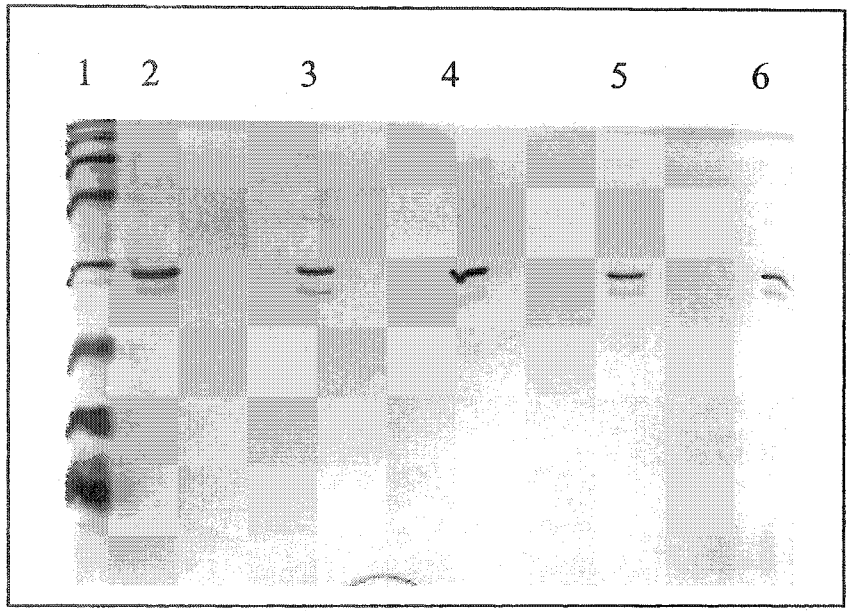

C.

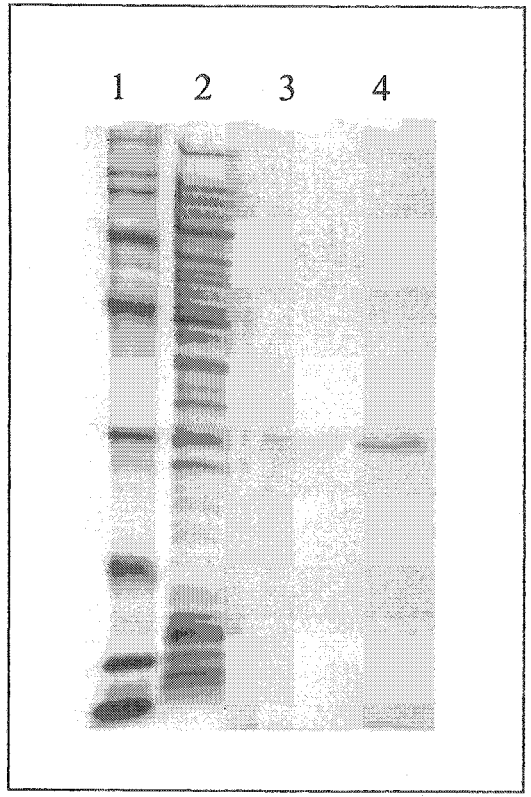

Figure 23: Determination of wild-type $MinC_{Ng}$ protein concentration using the Bradford assay. Concentration of $MinC_{Ng}$ is marked with an "x".

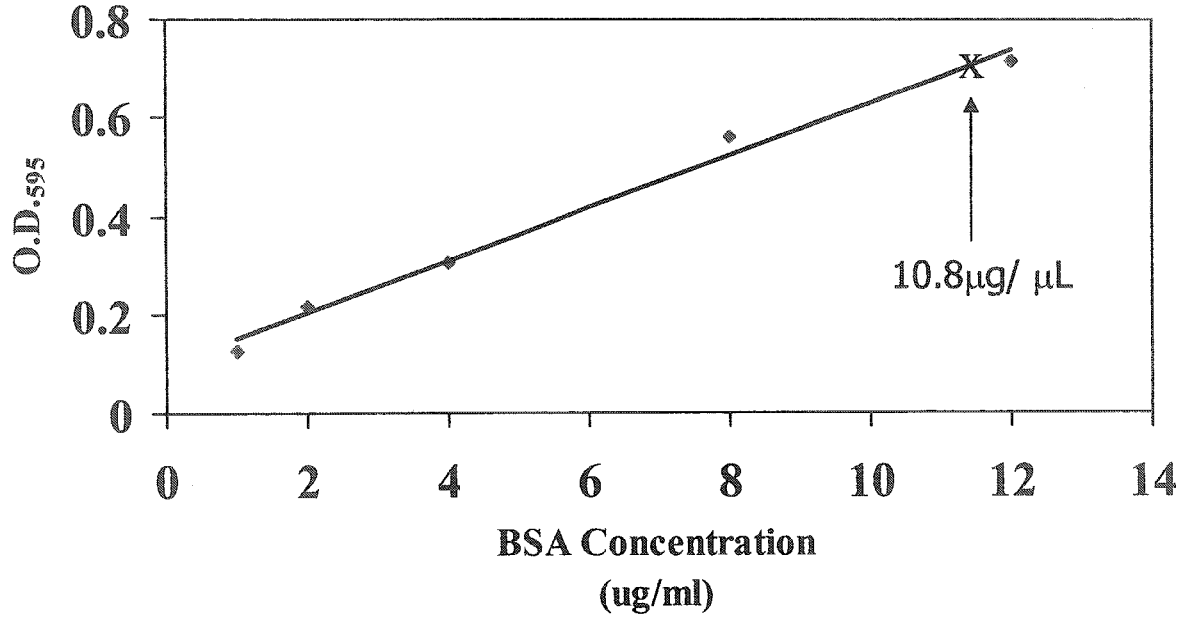

$y = 0.0535x + 0.0956$

for the wild-type and mutant $MinC_{Ng}$ samples (Figure 22C). Purified protein was subsequently used for circular dichroism analysis.

3.4 Circular dichroism analysis reveals that the $MinC_{Ng}$ structure is preserved in the glycine mutants

Far-UV circular dichroism spectra indicated that all four of the $MinC_{Ng}$ glycine mutants retained their structure as compared to the wild-type $MinC_{Ng}$ (Figure 24). The calculated α-helix contents of wild-type, mutants G138D, G157D, G164S and G174E were 53.6%, 54.3%, 52.8%, 54.1%, and 54.4%, respectively. These data confirm that the overall secondary structure of the $MinC_{Ng}$ mutants was conserved. MinCCh ($MinC_{Ec}^{1-99}MinC_{Ng}^{103-237}$) was also analyzed and was determined to be similar to wild-type $MinC_{Ng}$ in structure (Figure 25). Spectra differed slightly as three amino acids from the flexible linker of $MinC_{Ec}$ were deleted in this protein. Additionally, three-dimensional analysis of the chimera using the protein modeling software SWISS-MODEL showed that an additional ß-sheet appears near the beginning of the C-terminal domain, increasing the size of the ß-helix. These studies demonstrate that structure of $MinC_{Ng}$ mutants is conserved and that abrogation of function due to mutation is not a result of protein misfolding or structural deficiency or change and that MinCCh is structurally similar enough to $MinC_{Ng}$ to be useful for protein-protein interaction studies.

Figure 24: Circular dichroism spectra of four conserved glycine $MinC_{Ng}$ mutants. Far UV circular dichroism spectra indicated that all of the single glycine mutations did not change the overall secondary structure of $MinC_{Ng}$. The calculated a-helix contents of the wild type, mutants G138D, G157D, G164S, and G174E are 53.6%, 54.3%, 52.8%, 54.1%, and 54.4%, respectively. Wavelength is measured in nm. All samples were dissolved in 10 mM ammonium bicarbonate buffer and all measurements were made at 20°C.

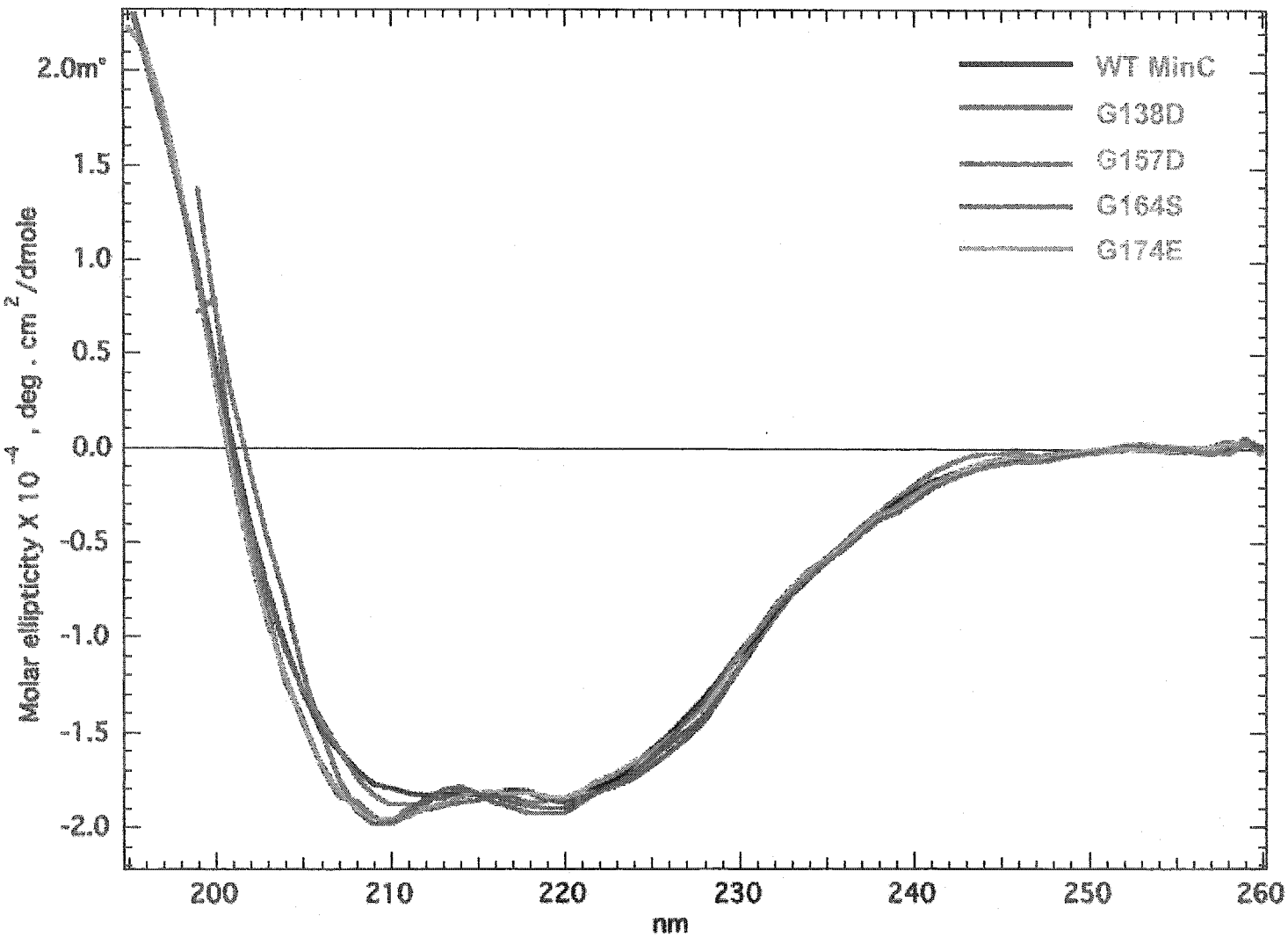
WT MinC
G138D
G157D
G164S
G174E
2.0m°
1.5
1.0
0.5
0.0
-0.5
-1.0
-1.5
-2.0
Molar ellipticity X 10 -4 , deg . cm 2 /dmole
200
210
220
230
240
250
260
nm

Figure 25: Circular dichroism spectra of chimeric MinC. Far UV circular dichroism spectra indicated that the chimera has the same overall secondary structure as $MinC_{Ng}$. All samples were dissolved in 10 mM ammonium bicarbonate buffer and all measurements were made at 20°C.

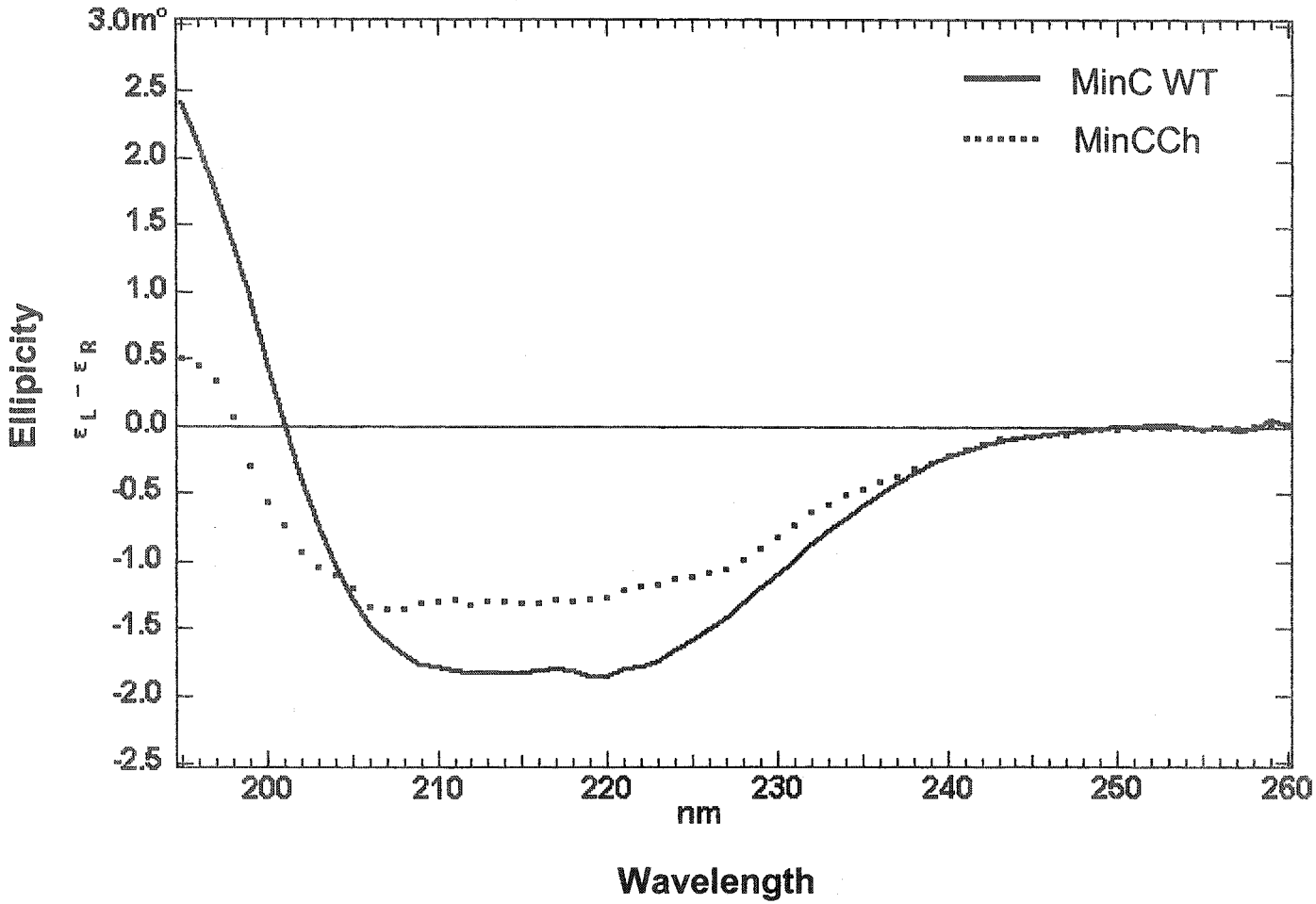
3.0m°
2.5
2.0
1.5
1.0
0.5
0.0
-0.5
-1.0
-1.5
-2.0
-2.5
Ellipicity
ε L − ε R
MinC WT
MinCCh
200
210
220
230
240
250
260
nm
Wavelength

3.5 The N-terminus of $MinC_{Ng}$ is essential for inhibition of cell division

3.5.1 Disruption of α-helical structural motifs in the N-terminus of $MinC_{Ng}$ result in loss of protein function

N-termini of MinC proteins are not conserved across species as determined by multiple alignment analysis (Ramirez-Arcos *et al.*, 2001a; Figure 10), but structural motifs, two α-helices in particular, are preserved and are thus expected to be integral to protein function. The N-terminal domain of $MinC_{Ec}$ interacts with FtsZ (Hu and Lutkenhaus, 2000) to promote $FtsZ_{Ec}$ polymer destabilization (Hu *et al.*, 1999). It thus suspected that alteration of the N-terminus of $MinC_{Ng}$ will lead to abrogation of $MinC_{Ng}$ function by annihilating this interaction. It has been demonstrated that proline disrupts α-helices and subsequently abrogates or alters protein function (Marin *et al.*, 2002; Nilsson *et al.*, 1998). Alteration of the helices by inserting proline, a helix-disrupting amino acid, in place of leucine, a aliphatic residue, was performed in the L35P and L68P mutants encoded by pVG15 and pVG16, respectively. Division inhibition was impaired in both of these mutants as indicated by inability to induce filamentation when over-expressed in *E. coli* PB103 (Figure 26). The L35P mutant was characterized by the presence of elongated rods (~10 to 15 μm) accounting for 50.7 ± 7.0% of the population (Figure 26A). The L68P mutant exhibited longer filaments (~30 to 50 μm) accounting for 34.0 ± 8.0% of the population (Figure 26B). These mutations were not sufficient to completely render $MinC_{Ng}$ inactive as demonstrated morphologically by the presence of filaments. Ten fields containing a minimum of 100 cells were examined.

Figure 26: Microscopy of N-terminus site-directed and truncated $MinC_{Ng}$ mutants. Phase contrast micrographs were taken using 100X oil immersion objective. A: L35P mutant demonstrates some ability to induce filamentation, as does the L68P mutant (B). C: 10aa truncated $MinC_{Ng}$ mutant induces filamentation. D: 13aa truncated mutant loses ability to function as a division inhibitor by failing to induce filamentation.

A.

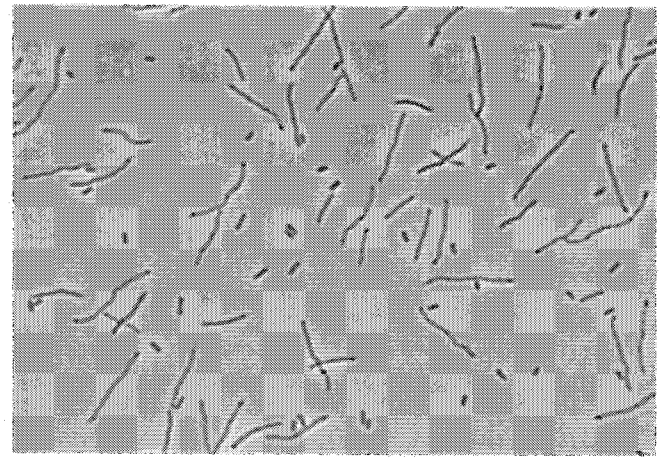

B.

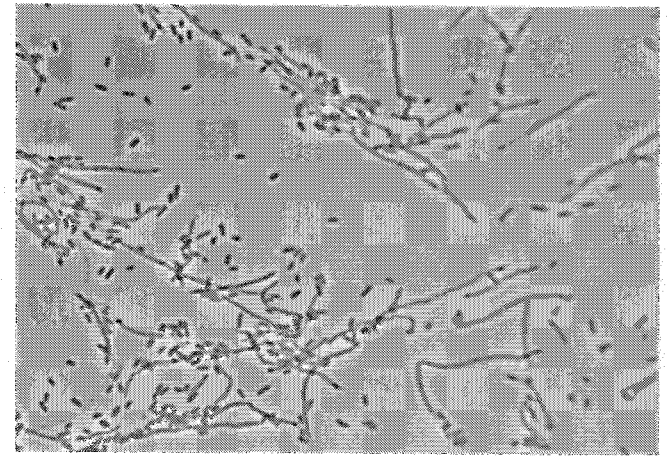

C.

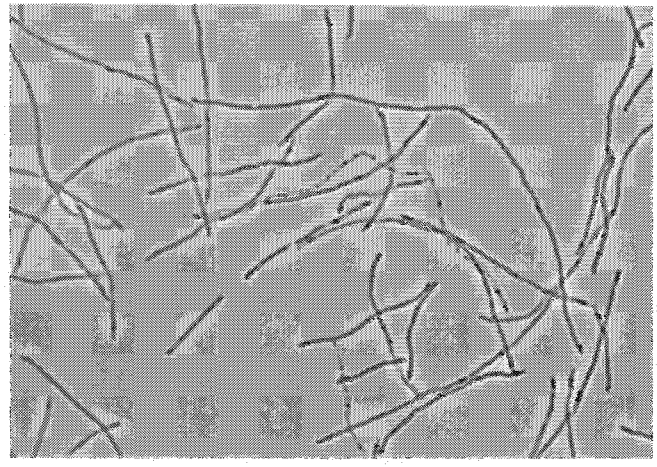

D.

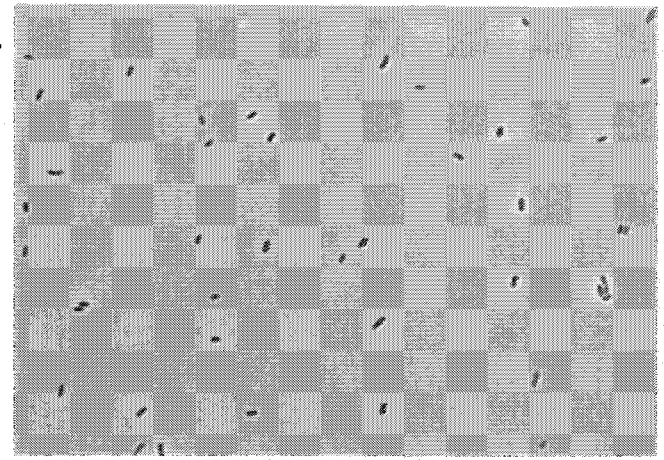

3.5.2 The 13th amino acid of $MinC_{Ng}$ is critical to protein function

The minC19 mutation in *E. coli* (G10D) renders $MinC_{Ec}$ non-functional (Labie *et al.*, 1990; Table 1). The corresponding residue is the 13th amino acid of $MinC_{Ng}$, and it was thus speculated that this residue would be critical to protein function. Truncations at this site (pVG17) and at the 10th amino acid (pVG18) were constructed to determine how much of the N-terminus is necessary for protein function, and *E. coli* PB103 was transformed with these truncated mutants (Figure 26). The 10 aa truncation retained its functionality as 99.3 ± 1.2% of cells were filamentous (Figure 26C) and the phenotype was indistinguishable from that of the pSR2 (wild-type $MinC_{Ng}$) transformants. In contrast, the 13 aa truncation was completely non-functional, as no filaments were present in the transformant cell population (0.0% filamentous; Figure 26D) and the phenotype was comparable by microscopy to the negative control pUC18 transformants.

3.5.3 $MinC_{Ng}$ 10 aa-truncated mutant retains ability to induce filamentation as determined by flow cytometry

Flow cytometry was employed to determine the percent filamentation of large numbers of transformend cells as was performed for the C-terminus glycine mutants (Figure 27). The 10 aa truncated mutant was virtually indistinguishable from the wild-type $MinC_{Ng}$-transformed cells (80.5 ± 3.5% and 82.0 ± 2.8% of the population, respectively), while the L35P and L68P retained some protein functionality (19.5 ± 3.5% and 28.5 ± 6.4% of the population, respectively). The pUC18 negative control demonstrated 13.5 ± 4.9% filamentation; conservative gating did not encompass larger-sized pUC18 transformants, causing some larger cells to be counted as small filaments. The 13 aa truncated mutant only demonstrated 13.5 ± 2.1% filamentation, indicating abrogation of protein function

Figure 27: Flow cytometric analysis of N-terminus $MinC_{Ng}$ mutants. Only the 10 aa truncated mutant retains full ability to inhibit cell division resulting in the filamentous phenotype.

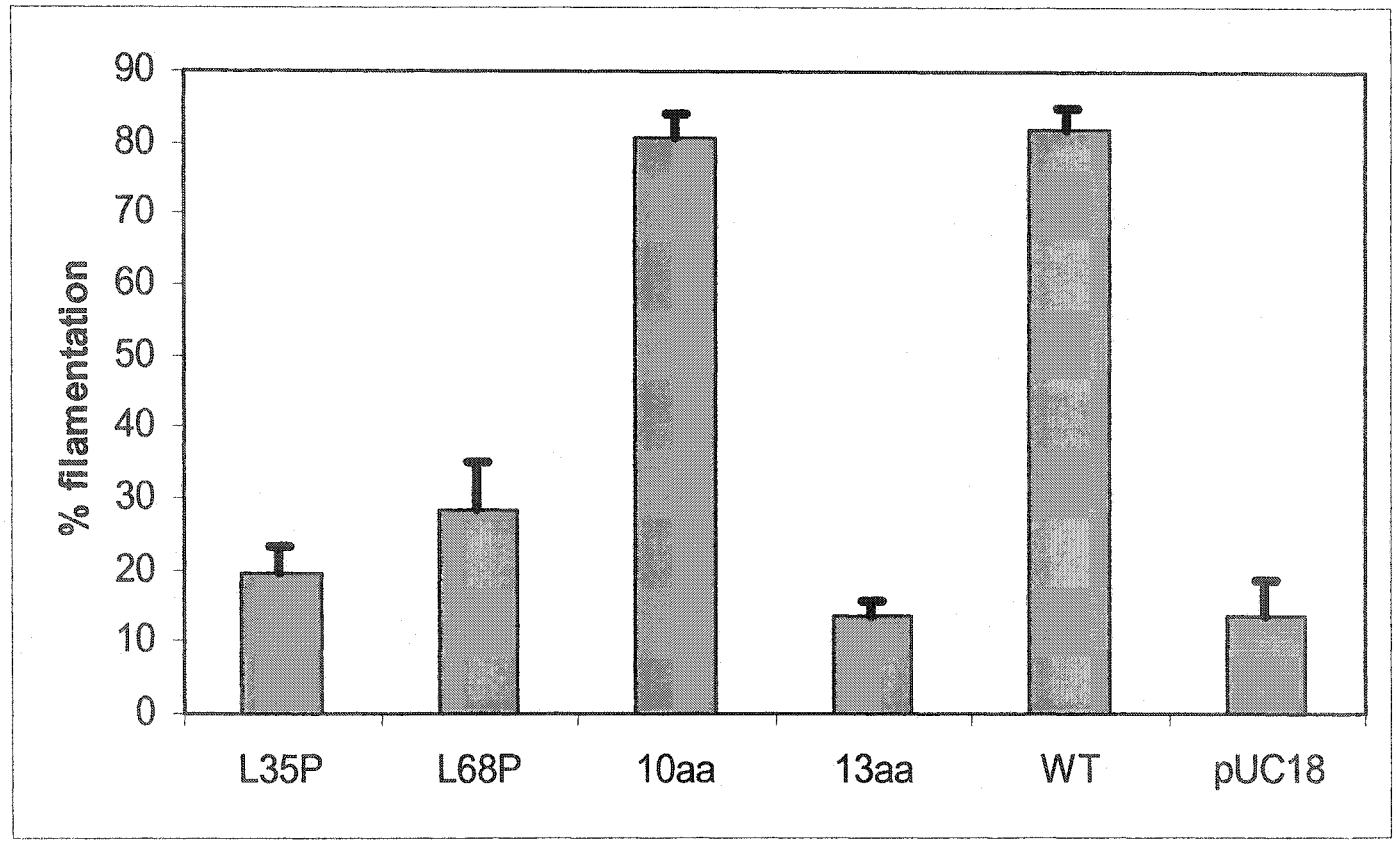
% filamentation
90
80
70
60
50
40
30
20
10
0
L35P
L68P
10aa
13aa
WT
pUC18

and confirming the findings of the microscopic analysis as this amount of filamentation is comparable to the pUC18 negative control. Flow cytometric analysis more accurately reflects the morphology of transformant cell populations than microscopy due to the large number of cells examined (100,000 cells per trial).

3.5.4 N-terminus truncations and mutants are expressed in *E. coli* PB103

Western blot assays were performed to ensure expression of the mutant and truncated constructs in *E. coli* PB103 (Figure 28). All proteins were expressed to the same extent as wild-type $MinC_{Ng}$ from pSR2 with the exception of pVG17, the 10 aa mutant, which was over expressed by ~ 30 % as determined by densitometric analysis (Figure 28, lane 5). Migration of this protein was also slightly retarded. Wild-type $MinC_{Ec}$ was barely detectable (Figure 28, lane 1). $MinC_{Ng}$ degradation products can be seen at the bottom of the lanes. Western analysis was performed in triplicate.

3.6 $MinC_{Ec}$ C-termini self interact but lose interaction with $MinD_{Ec}$

Future experimentation to assay the protein-protein interactions of N-terminus $MinC_{Ng}$ mutants will require the use of chimeric proteins with the N-terminus of $MinC_{Ng}$ and the C-terminus of $MinC_{Ec}$. To determine if the C-termini alone are capable of self-interaction and interaction with $MinD_{Ec}$, pGADMinC_{Ec}C and pGBTMinC_{Ec}C yeast two-hybrid vectors were constructed with the C-terminus of $MinC_{Ec}$ fused to the GAL4 activation and binding domains, respectively. The colony lift assay was performed in triplicate, and it was shown that the C-termini of $MinC_{Ec}$ lost interaction with $MinD_{Ec}$ but retained self interaction (data not shown). Single transformants of each construct were used as negative controls and did not display any interaction (data not shown).

Figure 28: N-terminus $MinC_{Ng}$ mutants are expressed in *E. coli* PB103 as determined by Western blot analysis. Lane 1 - pUC18 negative control; lane 2 -$MinC_{Ng}$ positive control; lane 3 - $MinC_{Ng}$ with L35P mutation; lane 4 - $MinC_{Ng}$ with L68P mutation; lane 5 - $MinC_{Ng}$ with 10aa truncation from the N-terminus; lane 6 - $MinC_{Ng}$ with 13aa truncation from the N-terminus. Note the overexpression of the 10aa truncated mutant pVG17.

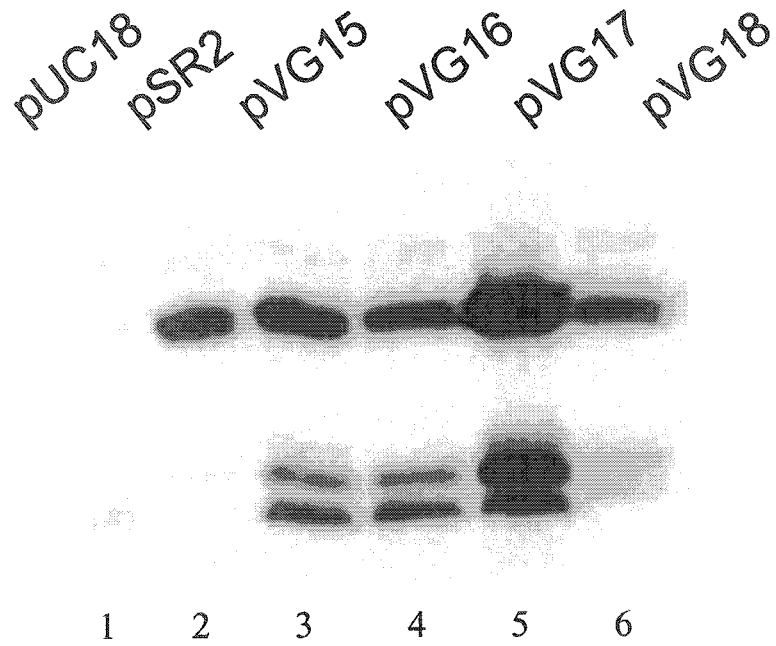
pUC18
pSR2
pVG15
pVG16
pVG17
pVG18
1
2
3
4
5
6

These data indicate that a chimeric MinC containing the N-terminus of $MinC_{Ng}$ and the C-terminus of $MinC_{Ec}$ could be used to determine if mutations in the N-terminal region of $MinC_{Ng}$ have any effect on interaction with $MinD_{Ng}$.

3.7 Construction of *gfp-minC*$_{Ng}$ and *gst-minC*$_{Ng}$ fusion vectors

Additional constructs for future studies were prepared during the duration of this study including GFP-$MinC_{Ng}$, GFP-$MinDE_{Ng}$, and $MinDE_{Ng}$-GFP encoding-constructs for protein localization in the *N. gonorrhoeae* and a GST-$MinC_{Ng}$ encoding-construct for use in immunoprecipitation and GST-pulldown assays to elucidate protein-protein interactions of $MinC_{Ng}$. Figure 29A schematically represents the pVG12 construct, *gfp-minC*$_{Ng}$ cloned into the low copy-number shuttle vector pFP20. Figure 29B depicts pVAL2, the *gst-minC*$_{Ng}$ fusion vector based constructed from pGEX 4T-3 (Table 2).

N. gonorrhoeae strain F62 was transformed with pVG12, pVG13, and pVG14 (containing *gfp-minC*$_{Ng}$, *gfp-minDE*$_{Ng}$, and *minDE*$_{Ng}$-*gfp*, respectively). Transformation was confirmed by recovery of plasmid DNA from transformants by miniprep and PCR amplification of the fusion genes. These constructs and transformants will consequently be available for study by our laboratory.

Figure 29: Schematic representation of pVAL2 and pVG12 vectors. A: pVAL2 is derived from pGEX 4T3 and will be used in GST pull down assays to detect protein-protein interactions of $MinC_{Ng}$. B: pVG12 is a derivative of pFP20 and will be used for fluorescence microscopy localization studies.

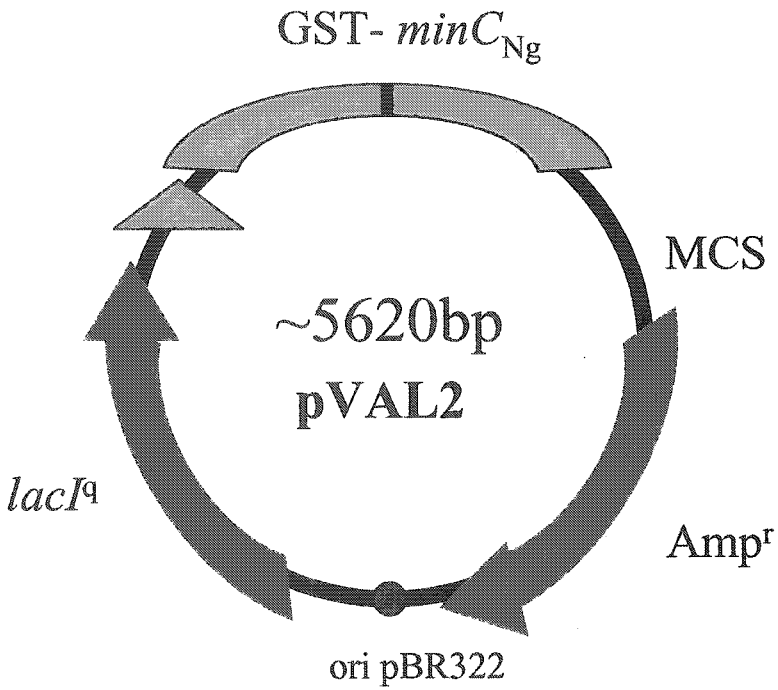
GST- $minC_{Ng}$
MCS
~5620bp
pVAL2
$lacI^q$
Amp^r
ori pBR322

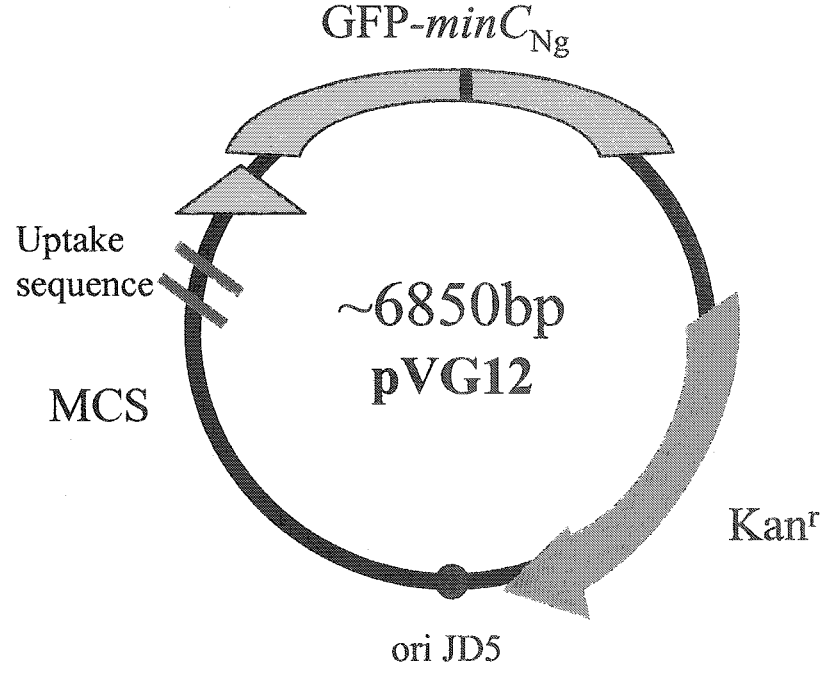
GFP-$minC_{Ng}$
Uptake sequence
MCS
~6850bp
pVG12
Kan^r
ori JD5

DISCUSSION

4.1 Conserved glycine residues in the C-terminus of $MinC_{Ng}$ are essential for protein function.

This research has demonstrated the necessity of conserved glycine residues of $MinC_{Ng}$ for protein functionality as an inhibitor of cell division. Replacement of these completely conserved glycine residues, G138, G157, G164, or G174, resulted in a protein that was non-functional as an inhibitor of cell division (i.e. could not induce filamentation) as determined by both microscopic and flow cytometric analyses. Due to the interspecies conservation of these glycines, these data can be extended to encompass MinC protein functionality in different bacterial species. Our laboratory has recently substantiated the involvement of these glycines in intermolecular interactions between $MinC_{Ec}$ and $MinD_{Ec}$ and itself (Ramirez-Arcos *et al.*, 2003). Circular dichroism analysis confirmed that abrogation of protein function resulted from the glycine substitutions and not from protein misfolding or alteration of secondary structure, implicating glycine as a critical amino acid involved in protein function. Together, these data present a comprehensive analysis of essential, conserved residues in the C-terminus of MinC that are imperative to protein function.

4.1.1 Flow cytometry as a tool for morphological analysis

This research employed flow cytometry to discriminate and quantify bacterial populations based on size. In the present study, filamentous cells were distinguished from short rods using novel flow cytometric protocol as an indicator of $MinC_{Ng}$ functionality. Flow cytometry has been shown to be an accurate and precise alternative

to the quantification of bacterial populations using microscopy alone (Bouvier *et al.*, 2001); up to 100,000 cells were quantified per experiment in the present study. Dr. Ramirez-Arcos and I designed a protocol for the quantification of microorganisms using flow cytometry based on size discrimination; previously, the small size of bacterial cells was considered an impediment to morphological analysis and cells were only studied using flow cytometry when they were sorted by fluorescent signal (Winson *et al.*, 2000). In the present research, flow cytometry was used to accurately and quantitatively corroborate the data obtained microscopically regarding the size of bacterial cells as an indicator of $MinC_{Ng}$ functionality and has proven to be an asset to this field of research. Correlation between the flow cytometric and microscopic data was good, and the flow cytometric analysis provided the means to assess vast numbers of cells, a limitation of microscopic techniques. Microscopic morphological data is subjective, whereas flow cytometry is capable of discriminating distinct populations of different-sized cells. The limitation of flow cytometry is that it is not possible to determine the actual size range of cells within a particular gated population, and gates are determined by the researcher and are arbitrary once established. However, taken together, microscopic and flow cytometric analysis accurately demonstrated the function of $MinC_{Ng}$ and mutant variants of this protein by indicating the presence of filamentous cells among transformant populations.

4.1.2 The G157D $MinC_{Ng}$ protein exhibits increased accumulation when expressed in *E. coli* PB103

All of the $MinC_{Ng}$ glycine mutant proteins were expressed at similar levels to the wild-type $MinC_{Ng}$ from pSR2 with the exception of the G157D mutant (Figure 20A).

Although all four of the radical glycine mutants of $MinC_{Ng}$ are non-functional, it is interesting to observe the extreme accumulation of the G157D $MinC_{Ng}$ (Figure 20A, lane 3). The complete non-functionality of this protein as a division inhibitor is evident by its inability to induce filamentation despite its extreme abundance. One explanation for the increased accumulation of the G157D $MinC_{Ng}$ protein is that the choice of amino acid substitution, an aspartic acid residue, conferred increased stability to this mutant. It has recently been demonstrated that substitution of various amino acids for aspartic acid results in increased protein stability and reduced susceptibility to catalysis as demonstrated by the D→N,E,Q mutations in human 8-oxyguanine glycosylase and the D→N mutation in mouse cathepsin D proteins (Norman *et al.*, 2003 and Partanen *et al.*, 2003, respectively). Additionally, halophilic archaea contain a high proportion of aspartic acid residues in most proteins (irrespective of function) to confer stability, and thermophilic bacteria also employ many acidic and basic residues in their proteins to confer thermostability (Fukuchi *et al.*, 2003). Aspartic acid has also been demonstrated to form salt bridges that confer protein stability (Speare *et al.*, 2003); since $MinC_{Ng}$ contains other aspartic acid residues, including a conserved aspartic acid at position 136, it is possible that these inter-residue interactions could occur to confer increased stability to this protein. It is thus possible that the addition of an aspartic acid residue at a conserved position of $MinC_{Ng}$ has the dual effect of abrogation of protein function based on the location of the mutation and increased stability due to the unique properties of this amino acid.

Alternatively, it is possible that this protein is less susceptible to proteases since more of the protein has accumulated as evident from the Western analysis and the presence of inclusion bodies (Figure 17B) and it has been demonstrated that alteration of

C-terminus residues of $MinC_{Ec}$ results in alteration of protease susceptibility (Sen and Rothfield, 1998). It is thus possible that alteration of this key residue not only abrogates protein function but might also reduce susceptibility to proteases. Since the *lacZ* promoter from pUC18 is utilized in all constructs for transcription of the $minC_{Ng}$ genes, it is unlikely that the extreme overexpression observed with this mutant occurs at the level of transcriptional control. This study has led to the speculation that much regulation of $MinC_{Ng}$ (and other MinC proteins) might occur at the level of protein stability and degradation. To ascertain whether or not this particular mutant is more susceptible to proteolytic degradation by the Lon protease, wild-type $MinC_{Ng}$ and G157D $MinC_{Ng}$ constructs can be transformed into both Lon+ and Lon- strains of *E. coli* and detected using Western blot protocol. Alternatively, nickel-affinity purified proteins can be subjected to various proteases, including the Lon protease, *in vitro* and then detected by Western blot.

The other $MinC_{Ng}$ glycine mutants, G138D, G164S, and G174E, were expressed at similar levels as wild-type $MinC_{Ng}$ and were all non-functional as division inhibitors. Since wild-type $MinC_{Ng}$ was capable of inhibiting cell division as determined flow cytometrically and microscopically by the ability to induce filamentation, it is evident that these mutant's non-functionality can be attributed to mutation and not low expression levels. Interestingly, the E144I mutant that contained a radical mutation in a non-conserved residue retained its ability to inhibit cell division despite its low expression as compared to wild-type $MinC_{Ng}$ expressed from pSR2 (Figure 20B, lane 2). Low abundance of this protein likely occurs due to mutational interference with C-terminus stability elements (Sen and Rothfield, 1998). Moderate overexpression of this protein is capable of causing the filamentous phenotype by preventing cell division. The

retention of function of this protein indicates the necessity of the conserved glycine residues, as compared to non-conserved residues, to $MinC_{Ng}$ functionality as a division inhibitor.

4.1.3 $MinC_{Ng}$ G138D and G157D protein accumulation results in inclusion formation in *E. coli* PB103.

In the case of both the $MinC_{Ng}$ G138D and G157D mutants, inclusion bodies were present and ghost (lysed) cells were found concomitantly (~10 % of the total cell population) with these inclusions. Inclusion bodies result from the accumulation of misfolded and aggregated proteins (Carrio and Villaverde, 2003). To reduce inclusion formation, it has been suggested that the temperature of bacterial cultures overexpressing a particular protein be lowered from 37°C to 30°C or room temperature; this maneuver has been determined to solublize inclusion proteins and has also been demonstrated to increase activity of certain proteins (Chalmers *et al.*, 1990; Kato and Asano, 2003). In these experiments, no change in inclusion formation was detected by changing growth conditions (temperature and agitation speed) of the bacterial cultures overexpressing $MinC_{Ng}$ (data not shown). Interestingly, both mutants that formed inclusions were G→D mutants and, as aforementioned, aspartic acid has been implicated in intra- and intermolecular protein interactions and stability (Speare *et al.*, 2003). Ergo, it is possible that due to the aspartic acid content of these mutants the resultant $MinC_{Ng}$ protein is less soluble, more stable, and tends to aggregate when overexpressed. Microscopy of these mutants demonstrated that the cells were overburdened by these inclusions and they might have contributed to cell lysis.

4.1.4. Radical mutation of a non-conserved residue in $MinC_{Ng}$ has no impact on protein function

Mutation of a conserved residue, E144, was selected to demonstrate the significance of the conserved glycines and illustrate that not every residue in the C-terminus of $MinC_{Ng}$ is critical for protein function. E144 has been mapped to the C/A junction of MinC, and radical alteration from E→I was anticipated to increase the hydrophobicity of this portion of the helix. If this residue was critical to protein function, this alteration should exert some effect on protein structure and/or functionality. However, no changes in $MinC_{Ng}$ function were detected with this mutation. Despite only moderate overexpression of this protein in *E. coli* PB103, it retained its ability to function as a division inhibitor, indicating the importance of the conserved $MinC_{Ng}$ glycine residues to protein function.

4.1.5 Homologous mutations in $MinC_{Ec}$ result in loss of protein-protein interactions

In concert with the present study, the role of conserved glycine residues was examined in $MinC_{Ec}$. Mutant variants of $MinC_{Ec}$ (G135D, G154D, G161S, and G171E) were constructed in the laboratory in parallel to the research presented in this study to confirm the importance of these residues across species. A neutral mutation in a non-conserved amino acid, P141A, was also constructed as a negative control. The selected residues correspond to $MinC_{Ng}$ residues G138, G157, G164, G174, and E144, respectively. Using microscopic and flow cytometric techniques to assess the morphology of transformants containing plasmids bearing these mutations in $MinC_{Ec}$, it was determined that only the neutral mutant (P141A, corresponding to E144I in $MinC_{Ng}$) retained function as a

division inhibitor as observed by the inability of the conserved glycine mutants to induce filamentation. These data corroborate the findings of the present study and implicate conserved glycines as being critical to MinC protein function across species.

Protein-protein interaction of these parallel $MinC_{Ec}$ mutants was determined by yeast two-hybrid analysis and results are shown in Table 4. The G135D, G154D, and G171E mutants all lost interaction with $MinD_{Ec}$ but retained interaction with MinCEc, while the G161S mutant interacted with $MinD_{Ec}$ but lost self-interaction. Chimeric MinC (MinCCh) containing the N-terminus of $MinC_{Ec}$ (amino acids 1 to 99) C-terminus of $MinC_{Ng}$ (amino acids 103 to 237) was mutagenized to determine protein-protein interactions between MinCCh containing the gonococcal glycine mutations and $MinD_{Ec}$ (Douglas, 2002; Ramirez-Arcos *et al.,* 2003). MinCCCh confers stability to $MinC_{Ng}$ in yeast and has enabled examination of gonococcal Min proteins using the yeast two-hybrid system. MinCCh has demonstrated interaction with $MinD_{Ec}$ (Ramirez-Arcos *et al.,* 2002, Ramirez-Arcos *et al.,* 2003, this study; Table 4). Since MinCCh does not self-interact, only interactions with $MinD_{Ng}$ can be assayed using this system. The present study contributed the analysis of the mutation in a non-conserved residue, $MinC_{Ng}$ E144I (corresponding to $MinCCh_{E141I}$); alteration of this residue did not affect the ability of MinCCh to interact with $MinD_{Ec}$ (Table 4).

The G135D, G154D, and G171E mutants of MinCCh (corresponding to $MinC_{Ng}$ mutants G138D, G157D, and G174E) all lost interaction with $MinD_{Ec}$ (Ramirez-Arcos *et al.*, 2003). The G161S mutant (corresponding to the $MinC_{Ng}$ G164S mutant) maintained interaction with $MinD_{Ec}$ (Ramirez-Arcos *et al.*, 2003). Mapping of these mutations to the structure of *T. maritima* (Figure 15) show that the residues responsible for self-interaction lie on the A-face (G164 in $MinC_{Ng}$), as predicted by Cordell *et al.*

(2001), and the residues responsible for MinD interaction lie on the B/C face junction and on the C-face (G138, G157, and G174 in $MinC_{Ng}$), a novel discovery in the determination of Min protein interactions. The neutral mutation in the chimera cannot be tested for self-interaction, but the equivalent $MinC_{Ec}$ mutant (P141A) did not lose interaction with $MinD_{Ec}$ and maps to the A/C junction, demonstrating that conservation of these residues is not paramount to protein function and that this region is not as critical as the more highly conserved areas. Together, these data demonstrate the significance of the glycine residues to protein function and intramolecular interactions in $MinC_{Ec}$ and in $MinC_{Ng}$. Due to the completely conserved nature of these glycine residues across species, this observation can be extended to MinC proteins in general.

4.1.6 Protein modeling predicts the location of $MinC_{Ng}$-$MinD_{Ng}$ interaction

Protein modeling was used to predict the protein-protein interactions of $MinC_{Ng}$ with $MinD_{Ng}$ based on the three-dimensional structures of $MinC_{Tm}$ (Cordell *et al.*, 2001) and $MinD_{Pf}$ (from *Pyrococcus furiosus*; Hayashi *et al.*, 2001). Predicted interaction of MinC with MinD is depicted in Figure 30. This model shows that the junction between the B and C surfaces of the MinC C-terminus, which contains the conserved glycines, would be exposed and might be available to directly interact with the α-7 helix of MinD, a structural motif that has been previously implicated in interaction with MinC (Hayashi *et al.*, 2001). In the present model, part of the α-7 helix of the $MinD_{Pf}$ dimer is exposed and would be available for interaction with MinC. $MinD_{Pf}$ contains three hydrophobic amino acids in the α-7 helix, L148, M152, and I156, and these residues would be surface-exposed once a MinD dimer has been formed. However, multiple sequence alignment of

Figure 30: Model of MinC-MinD interaction using the solved structures of *Thermotoga maritima* MinC and *Pyrococcus furiosus* MinD. A: The MinD monomers in the $MinD_{Pf}$ dimer are blue and green, while $MinC_{Th}$ is white. The α-7 helix of $MinD_{Pf}$ is shown in yellow with the exposed residues L148, M152, and I156 highlighted in pink. The conserved glycines in $MinC_{Tm}$ (G111, G129, and G146) are shown in red. The putative zone of interaction is enclosed in a white square and hydrophobic interactions are represented by pointed yellow lines. B: Magnification showing the zone of $MinC_{Tm}$ and $MinD_{Pf}$ interaction. Exposed residues are labeled in pink in the α-helix of $MinD_{Pf}$ and in red in the β-sheet of $MinC_{Tm}$.

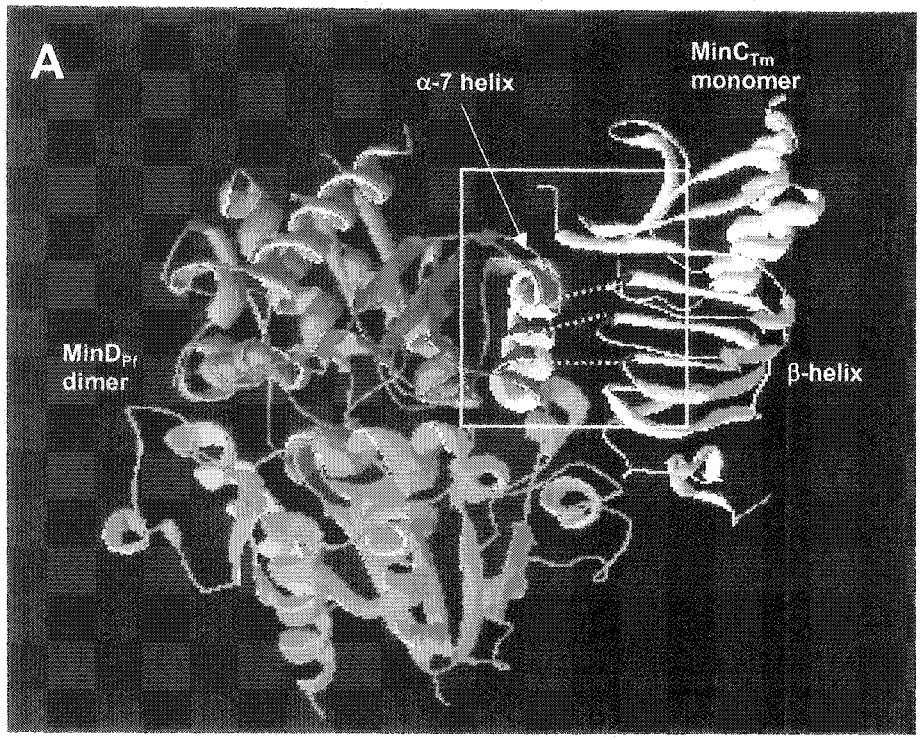
A
α-7 helix
MinC$_{Tm}$
monomer
MinD$_{Pf}$
dimer
β-helix

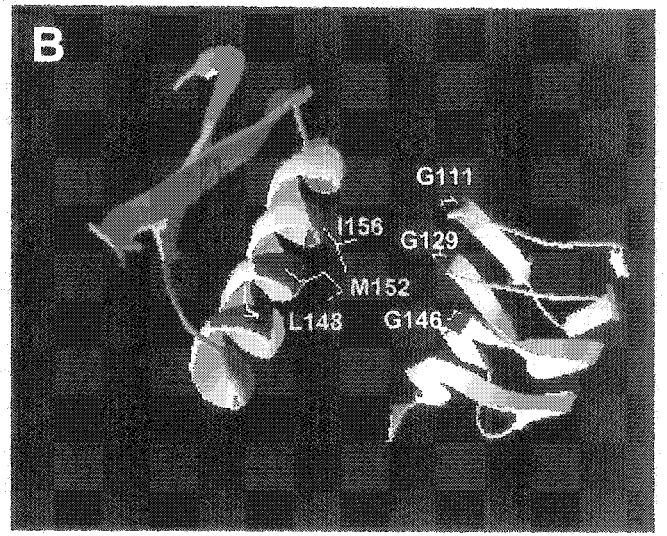
B
G111
I156
G129
M152
L148
G146

MinD has shown that only L148 and I156 of $MinD_{Pf}$ consistently have aliphatic residues conserved at these positions. Residues aligned to L148 are typically valines or isoleucines, while those aligned to I156 are glycines, including $MinD_{Ng}$ and $MinD_{Ec}$. Hydrophobic interactions between these amino acids and conserved glycines in $MinC_{Tm}$ (G111 and G129) could subsequently occur and be responsible for the intermolecular interactions of these proteins.

Mutations in amino acids S146 and D150 of $MinD_{Pf}$ and their homologues in $MinD_{Ec}$, which are part of the α-7 helix of MinD, have been shown to be involved in MinC-MinD interaction since mutation abrogates $MinC_{Ec}$-$MinD_{Ec}$ interaction (Hayashi *et al.,* 2001). In our model, this would enable the MinC-MinD complex formation. These interactions would account for the stabilization of the MinD-ATP-MinC complex that has been proposed to occur in the cytoplasm and be essential to inhibit ATPase activity of MinD before it reaches the cell membrane (Lutkenhaus and Sundaramoorthy, 2003; Ramirez-Arcos *et al.,* 2003). This model could be experimentally proven by solving the structure of a MinC-MinD complex using X-ray crystallography or nuclear magnetic resonance analysis.

4.1.7 Possible roles of conserved glycine residues in $MinC_{Ng}$ in intermolecular interactions

Both the conserved position of the glycine residues in the C-terminus of $MinC_{Ng}$ and the biochemistry of the glycine residue are critical to their impact on protein function in $MinC_{Ng}$. Dogovski *et al.* (2003) recently demonstrated a correlation between glycine conservation and biological importance in the phenylalanine and tyrosine transporter

PheP protein in *E. coli*. Glycine is a principal component of the β-sheet, a protein secondary structural motif, and confers flexibility due to the nature of its small side chain consisting of a sole hydrogen atom (Dogovski *et al.,* 2003). It is the only non-chiral amino acid (i.e. does not have four different molecular groups attached to the central carbon; has hydrogen as a side chain) and glycine content is subsequently extremely important for local flexibility in the protein (available online at www.whatislife.com/reader/protein/protein.html). β-sheets are proline- and glycine-rich, and these residues appear frequently at the β-turns, which must be flexible to confer this structure on the peptide sequence (Alix, 2001). The residues in the turn are stabilized by their ability to hydrogen bond (Alix, 2001).

The mutagenized glycine residues in $MinC_{Ng}$ in the present study occur at the β-helix surface junctions where a β-turn is present (Figure 12). Reduced stability through loss of hydrogen bonding and protein rigidity likely contribute to loss of $MinC_{Ng}$ mutant function. Since the C-terminus of MinC is comprised of a β-sheet that forms a helix, it is understandable that glycine residues are not only important for β-sheet formation but also for the structure of the helix itself. Conserved glycine residues within α-helices have also been recently demonstrated to be integral to helix capping, helix flexibility, and mediation of helix-helix interactions (Dogovski *et al.*, 2003), all of which seem to be congruent with the role of the conserved glycines of $MinC_{Ng}$.

Flexibility is essential for intermolecular interactions. $MinC_{Ec}$ has been demonstrated to interact with $MinD_{Ec}$, $FtsZ_{Ec}$, $DicB_{Ec}$, and itself (Hu *et al.,* 1999; Hu and Lutkenhaus, 2000; Cordell *et. al.*, 2001). Other potential intermolecular interactions of MinC cannot be excluded since many protein-protein interactions involve hydrophobic

interactions. Sprinzak and Margalit demonstrated that the *Cap-Gly* domain which contains several conserved glycine residues is necessary for protein-protein interactions (2001). The glycine-rich *Cap-Gly* domain is present in numerous cytoskeletal-associated elements that interact with microtubules of the tubulin and FtsZ families (Sprinzak and Margalit, 2001). From the present study, it has been shown that MinC also contains several conserved glycines located in close proximity to each other, and it is thus possible that these conserved glycines play a role in intermolecular interactions. To further corroborate this idea, Heinrichs and Baker (1997) have demonstrated that the glycine-rich domain of *Drosophila* mRNA splicing regulator RBP1 is essential for protein function by modulating interaction with both splicing factor TRA-2 and itself. Only non-radical substitution (G→A) was necessary to abrogate the regulatory function of RBP1. Once again, protein conformational changes and reduced expression were not the cause of this loss of activity. It can be speculated that these glycine residues are either directly involved in protein-protein interaction or that they are necessary to confer flexibility to the protein and prevent steric hindrance so that the correct stereochemistry for interaction can be achieved.

Glycine-containing motifs have been demonstrated to confer stability through hydrophobic interactions, van der Waals forces, and hydrogen bonding with intramolecular motifs containing isoleucine and valine residues (Kleiger and Eisenberg, 2002). Glycine can also hydrophobically interact with methionine to regulate protein function (Ren *et al.*, 2003). It has been demonstrated that the properties of a protein, such as desensitization of the N-methyl-d-aspartate receptor in eukaryotes, can be dramatically affected by the positioning of a hydrophobic residue at a specific location

within a protein, and that hydrophobic interactions are critical to protein function (Ren *et al.*, 2003).

In addition to the lack of protein stability and flexibility mentioned above, introduction of a charged residue would impair the hydrophobic interactions necessary for $MinC_{Ng}$ to undergo intermolecular interactions and, in this manner, render the protein non-functional. Addition of a charged molecule could cause repulsion of hydrophobic molecules and impede interaction between individual residues and subsequently other proteins. Aspartic acid also contains a bulkier side chain than glycine, which could cause steric disturbances that would render a protein incapable of function and protein-protein interaction. Shand *et al.* (2003) demonstrated a 30-fold reduction in the activity of rat insulin-like growth factor-binding protein 5 (ILGFBP5) when a critical glycine residue was substituted for glutamine. Of significance to this study is that, as in the case of the mutant $MinC_{Ng}$ proteins, alteration of this protein in ILGFBP5 did not confer any gross conformational change in the protein as a result of the substitution. Additionally, a mutant allele of the mitogen-activated protein kinase gene *SLT2(MPK1)* in yeast encodes a non-functional protein as the result of a G→D mutation (Martin *et al.*, 1996). These data, in concert with those presented in the present study, indicate that glycine itself, at conserved positions within a protein, are essential to protein function without alteration of protein structure. Glycine has been demonstrated to be so critical in certain positions, such as the β-turn, that even non-radical mutation such as glycine to alanine can eliminate protein stability and function (Kong *et al.*, 2003). It has been shown by Kong *et al.* (2003) that such a mutation does not alter protein structure, but might alter the transient substructure of a protein. This could affect protein function, especially by

abrogating protein-protein interactions. This seems to be the case in the present example of $MinC_{Ng}$.

It is thus speculated that the conserved glycine residues in $MinC_{Ng}$ are essential for protein function by affecting the ability of $MinC_{Ng}$ to undergo intramolecular interactions. It is not believed that the glycine residues investigated in the present research are the direct sites of intermolecular action but participate indirectly in the interaction in ways that are essential to protein function such as through van der Waals interactions. In agreement with these speculations, Bogan *et al* (1998) showed that the free energy of binding is not evenly distributed across protein-protein interfaces; instead single residues contribute specifically (>2kcal/mol) to these interfaces. In the case of glycine residues, it was determined that they can contribute weakly with 3.57 kcal/mol to a protein-protein interaction (Bogan *et al* 1998). Disruption of van der Waals interactions involving glycine residues unlikely results in complete disruption of a protein-protein interaction. Due to the position of the conserved glycine residues in β-turns of the C-terminus of MinC, these residues are not likely to be directly involved in MinC-MinD association. Instead, these glycines may have a structural role, conferring stability and/or flexibility to the protein that is critical for its function as a cell division inhibitor. Mutation of these residues would result in altered spatial orientation of the protein preventing protein-protein interactions.

Due to the conserved nature of the glycine residues examined and the similar results achieved in *E. coli* and *N. gonorrhoeae* MinC experiments, the findings of this research can be extended to other MinC proteins and might demonstrate the mechanism by which MinC undergoes intermolecular interactions in most bacterial species. Of

paramount interest is the mapping of MinC-MinD interaction to the B/C surface of MinC, an interaction that, to date, has not been examined in great detail. The role of glycine residues in protein function has also been expanded through this research.

4.2 *gfp-minC*$_{Ng}$ and *gst-minC*$_{Ng}$ fusion constructs will further investigations of MinC$_{Ng}$ localization and protein-protein interactions.

Another goal of the present study was to construct plasmid vectors for use in localization studies of the gonococcal Min proteins both heterologously and in *N. gonorrhoeae*. In this study, shuttle vectors containing *gfp-min*$_{Ng}$ fusions were constructed for the three gonococcal Min proteins. The low copy-number nature of these vectors is hoped to more closely mimic the actual levels of the Min$_{Ng}$ proteins in bacterial cells than would be observed when expressed from a high copy-number vector. It is hoped that both localization and oscillation of Min$_{Ng}$ proteins will be observed in gonococcal cells using these constructs.

Additionally, a *gst-minC*$_{Ng}$ fusion was constructed for the performance of GST-pulldown assays to elucidate suspected and novel MinC$_{Ng}$ interacting proteins. Proteins that found to interact with MinC$_{Ng}$ using this assay can then be identified by Western blot analysis (for suspected partners such as MinD$_{Ng}$ and FtsZ$_{Ng}$) and nuclear magnetic resonance analysis (NMR; for novel interacting partners whose interaction is not suspected). The constructs created in the present study are hoped to greatly further investigations of the gonococcal Min proteins in our laboratory.

4.3 The N-terminus of $MinC_{Ng}$ contains determinants that are essential to protein function

4.3.1 $MinC_{Ng}$ function is largely dependent on the structural integrity of the N-terminus α-helices.

The α-helix is a well-characterized and ubiquitous structural motif that is involved in numerous aspects of protein function. Insertion of proline residue in the α-helix disrupts the structure as it prevents hydrogen bonding between adjacent residues, ultimately resulting in loss of structural integrity and abrogation of protein function. Marin *et al.* (2002) demonstrated that alteration of an α-helix in eukaryotic transducin resulted in reduced protein function. In a similar study, Nilsson *et al.* (1998) illustrated the helix-disrupting properties of proline in transmembrane α-helices. In prokaryotes, the necessity of key α-helical residues was demonstrated by Simmons *et al.* (2003) when they showed that alteration of certain residues in the α-helix of DnaA, a replication initiator, caused loss of protein function by inability to oligomerize. In the case of the present study, the L35P and L68P α-helical site-directed $MinC_{Ng}$ mutants retained some activity as division inhibitors as indicated by the presence of populations of filamentous cells when overexpressed in *E. coli* PB103. The mutant $MinC_{Ng}$ proteins remained marginally functional within certain populations as demonstrated microscopically and flow cytometrically by the presence of short filaments (L35P) and long filaments (L68P).

There are several possible explanations for the quasi-functional nature of these mutant proteins. It is suspected that any lack of protein function in $MinC_{Ng}$ can be attributed to the predicted alteration of secondary structure of the α-helix due to proline

insertion. It has been shown that substitution of P47 with leucine in $MinC_{Ec}$ results in complete non-functionality of the protein as indicated by the mini-cell phenotype when expressed in single copy from the *E. coli* chromosome (Mulder *et al.* 1992; Table 1), and a similar phenotype is attained when $MinC_{Ec}$ is truncated after the 61st or 85th amino acid (Labie *et al.* 1990, Mulder *et al.* 1992; Table 1). However, in the present case, alteration of one residue might not be sufficient to completely abrogate protein function, explaining why short filaments (i.e. longer than wild-type sized cells but not in excess of 6X their length) are present in the L35P mutant and filamentous populations exist among L68P transformants (Figures 26A and 26B). It appears that the $MinC_{Ng}$ protein is active in a small percentage of these transformants, although the degree of activity is suspected to be lower than is observed in wild-type $MinC_{Ng}$ transformants due to the short nature of these filaments. In the L68P mutant, the protein appears completely active in a small population of the transformants as indicated by filamentation of some cells. It is possible that, as occurred in the case of the C-terminus $MinC_{Ng}$ mutants, the change of a single residue, in this case one that is semi-conserved, conferred altered properties on the local sequence of the protein resulting in loss of interaction with partners (i.e. $FtsZ_{Ng}$, a potential interacting partner). The α-helix is implicated in protein-protein interaction (Dogovski *et al.*, 2003) and alteration of the local sequence (Bogan *et al.*, 1998) might be sufficient to abrogate such interaction.

In the future, these N-terminus mutants can be overexpressed in *E. coli* C41, purified, and submitted for CD analysis to determine whether or not the secondary structure of the protein was altered by the introduced mutations. Information regarding protein secondary structure could thus be acquired and it could be definitively

determined if these introduced mutations cause alteration of the secondary structure of $MinC_{Ng}$ as was anticipated. If there is such a change, it is expected to be conservative as some protein function is retained. Additionally, constructs containing double mutations can be constructed to ascertain the degree of alteration necessary for complete loss of protein function.

4.3.2 Development of a system for the elucidation of protein-protein interactions of N-terminus $MinC_{Ng}$ mutants

When a suitable system for the determination of gonococcal division-related proteins becomes available, it will be possible to determine if alteration of semi-conserved residues in the N-terminal region causes a loss of protein-protein interactions. To facilitate the creation of this system, the present study involved the assessment of interaction between C-termini of $MinC_{Ec}$ to determine whether or not a chimera containing the N-terminus of $MinC_{Ng}$ and the C-terminus of $MinC_{Ec}$ would be as useful for these studies as the reverse chimera was for C-terminus analysis. It was determined that the C-termini of $MinC_{Ec}$ self interact but lose interaction with $MinD_{Ec}$. This information dictates that the chimera containing the N-terminus of $MinC_{Ng}$ will be useful for testing interaction of N-terminus mutants with $MinD_{Ec}$, but that self-interaction between chimeras will occur regardless of N-terminus alteration. However, the most significant partner that would potentially interact with the N-terminus of $MinC_{Ng}$ is $FtsZ_{Ng}$, an interaction which, to date, has not been demonstrated. It is suspected from the present study that alteration of the α-helices of the N-terminus of $MinC_{Ng}$ result in loss of protein function due to lack of $MinC_{Ng}$-$FtzZ_{Ng}$ interaction. This hypothesis can be

tested using the new chimeric MinC, which has been constructed by our laboratory (unpublished data).

4.3.3 Truncation of 13 N-terminus amino acids from $MinC_{Ng}$ renders the protein non-functional

Truncation of 10 and 13 amino acids from the N-terminus of $MinC_{Ng}$ was performed in this study. This research has demonstrated that the first 10 amino acids are not essential to $MinC_{Ng}$ function, although deletion of the 13^{th} amino acid renders the protein completely non-functional. Investigation of the 11^{th} and 12^{th} amino acids is ongoing, however preliminary evidence suggests that these two residues are likewise unessential for division inhibition function (data not shown).

Based on MinC sequence multiple alignment, it was determined that the 13^{th} amino acid of $MinC_{Ng}$ corresponds to the 10^{th} amino acid of $MinC_{Ec}$, a residue which has been implicated in protein function (Labie *et al.*, 1990). When the glycine residue at position 10 of $MinC_{Ec}$ is radically substituted for an aspartic acid residue, the resultant protein is incapable of inhibiting cell division, resulting in a minicell phenotype when expressed from the *E. coli* chromosome (Labie et al., 1990). It was thus anticipated that protein function would be lost through truncation at this residue in $MinC_{Ng}$. The results of this study collaborate the $MinC_{Ec}$ data implicating this residue as critical for protein function. A novel observation was made in terms of the ability of the 10 aa truncated mutant to be completely functional and to accumulate excessively in *E. coli* PB103. This property of the 10 aa truncated mutant was interesting in terms of the implication of N-terminus regulation of $MinC_{Ng}$ stability and turnover in the gonococcus and, potentially, in other bacterial species. It has been shown that the C-terminus contains elements that

confer stability to the Lon protease; alteration of C-terminus residues can lead to decreased protein stability (Sen and Rothfield, 1998). In contrast, it appears that the N-terminus contains elements that destabilize the protein; removal of the first 10 amino acids results in an overabundance of protein when expressed in *E. coli* PB103 as compared to the expression of wild-type $MinC_{Ng}$ in the same strain as indicated by Western blot analysis (Figure 28, lane 5). It thus appears as though the extreme N-terminus of $MinC_{Ng}$ contains destabilizing elements that, when removed, enable protein accumulation. Similar phenomena have been observed in other proteins. Most notably is the study by Manieri *et al.* which recently demonstrated that removal of the first 16 or 24 amino acids from the N-terminus of spinach ferredoxin:thioredoxin reductase (FTR) resulted in increased protein stability and intracellular accumulation. Protein function was not altered by these truncations. These data mimic those obtained in the present study. Additionally, Bernstein and Keck (2003) demonstrated that a 25 amino acid portion of the N-terminus of *E. coli* RecQ is susceptible to proteases. In the case of $MinC_{Ng}$ and as elucidated in the present study, it is likely that similar elements exist in this protein that, upon removal, impart greater stability to the protein. The present research is thus interesting in that a novel role of MinC concentration regulation might exist and that the N-terminus is involved in this process. Levels of intracellular MinC must be tightly regulated in order for the Min system to function; abundance of MinC results in inability to divide, while absence of MinC causes minicell division to occur because no inhibition of division is present at improper, polar septation sites. The present data illustrate the potential for the existence of complex mechanisms of tightly regulating MinC concentrations in the bacterial cell and implicate the extreme N-terminus of the protein as being one of the sites at which this regulation is exerted. To

determine the susceptibility of these N-terminus truncated mutants to proteases, experiments such as those outlined above can be employed in future research.

Further experimentation will be necessary to elucidate the role of the N-terminus in MinC function. As aforementioned, yeast two-hybrid analysis will be employed with these truncated mutants to determine their significance in protein-protein interactions, and whether or not it is the extreme N-terminus that interacts with FtsZ. Other methods of detecting intramolecular interactions between $MinC_{Ng}$ and the N- and C-terminus mutants are currently being developed, including the GST-pulldown assay for which a wild-type *gfp-minC*$_{Ng}$ fusion was constructed in this study. Once partners of $MinC_{Ng}$ have been determined, experimentation can be repeated with the mutant variants of this protein. Gel filtration analysis can also be employed to substantiate these findings. Lucet *et al.* (2000) successfully used this method to determine that sporulation factor SpoIIE and FtsZ from *B. subtilis* interacted in solution. High concentrations of purified $FtsZ_{Ng}$, $MinD_{Ng}$, and $MinC_{Ng}$ have been prepared in our laboratory and will facilitate the testing of these interactions. These methodologies will lead to an improved comprehension of the role of the N-terminus of $MinC_{Ng}$ in the inhibition of cell division.

4.4 The proposed model of gonococcal cell division

The culmination of this research and other investigations performed in our laboratory has lead to the proposal of a model for division site selection in *N. gonorrhoeae*. Following DNA replication, *N. gonorrhoeae* undergoes asymmetric invagination at a site opposite the replisome as previously discussed. $MinD_{Ng}$ binds ATP and dimerizes in the cytoplasm. $MinC_{Ng}$ likewise dimerizes in the cytoplasm and then becomes associated with the ATP-$MinD_{Ng}$ dimer. *The critical, conserved glycine residues in the C-terminus*

of $MinC_{Ng}$ facilitate these interactions. $MinD_{Ng}$ associates with the membrane, subsequently recruiting $MinC_{Ng}$. The localization of $MinD_{Ng}$ (and consequently $MinC_{Ng}$) is determined by $MinE_{Ng}$, which acts as a topological specificity factor. $MinD_{Ng}$ oscillates from end to end of the coccus perpendicular to the invagination, allowing $MinC_{Ng}$ to inhibit $FtsZ_{Ng}$ polymerization in these areas. The $FtsZ_{Ng}$ ring forms parallel to the invagination, and division into two separate daughter cells of equal size ensues. $MinD_{Ng}$ then oscillates parallel to the division plane in the daughter cells, and the above process is repeated to create another pair of daughter cells, resulting in tetrad formation. Research in the present study has been beneficial in elucidation of the role of $MinC_{Ng}$ in the process of cell division in the Gram-negative coccus and the mechanism by which $MinC_{Ng}$ functions at the molecular level to fulfill its role as an inhibitor of cell division.

Concluding Remarks

The present research has meticulously characterized the significance of specific amino acids and structural motifs in the function of the cell division inhibitor MinC from *N. gonorrhoeae*. Four conserved glycine residues in the C-terminus of $MinC_{Ng}$ have been demonstrated to be critical to protein function; alteration of these residues using site-directed mutagenesis results in abrogation of protein function as determined by the inability of these proteins to induce filamentation when heterologously expressed in *E. coli*. Both microscopic and flow cytometric techniques were used to assess and quantify these observations. Concurrent research has demonstrated that glycine mutants lose self interaction (G161S A face mutant) and interaction with MinD (G135D, G154D, and G171S B/C face mutants), which is likely responsible for the over-all lack of protein function. Since protein secondary structure was not altered in these mutants as

determined by circular dichroism analysis, the residues themselves must be significant to protein function. The critical glycines are implicated in maintenance of this protein-protein interaction indirectly, likely through participation in stabilizing the β-helix, maintaining local sequence integrity, or providing correct steric conformation.

The importance of the N-terminus α-helices was also investigated by site-directed mutagenesis of semi-conserved residues to proline, a known helix-disrupting residue. It was shown using the aforementioned analyses that these mutants lost a significant amount of division inhibition function, indicating the significance of these residues in $MinC_{Ng}$ function. Truncation of 10 amino acids had no effect on protein function, however truncation of 13 amino acids rendered the protein completely non-functional. It was also determined that the first 10 amino acids are important to protein stability, exerting a destabilizing effect and resulting in protein overabundance when heterologously expressed in *E. coli*. These data imply that complicated mechanisms for regulation of intracellular $MinC_{Ng}$ levels exist, and that determinants of protein stability reside not only in the C-terminus but also in the N-terminus.

Future research is necessary to completely determine the mechanism by which $MinC_{Ng}$ performs division inhibition. To facilitate these studies, a low copy-number *gfp-*$minC_{Ng}$ fusion vector was constructed to enable the visualization of intracellular localization of $MinC_{Ng}$ in both *N. gonorrhoeae* and *E. coli* live cells. A *gst-*$minC_{Ng}$ fusion construct was also made in order to discover and confirm both suspected and novel protein-protein interactions of $MinC_{Ng}$.

The present study is significant as it has elucidated residues that are requisite for $MinC_{Ng}$ division inhibition function, contributing to the knowledge of the mechanism of

action of this protein. It has also demonstrated the utility of glycine residues in protein function through their implicated role in protein-protein interactions; this role is likely not limited function in $MinC_{Ng}$ alone, and it is predicted that conserved residues are necessary to the proper functioning of other eukaryotic and prokaryotic proteins. Due to the conserved nature of these residues in MinC across species, this information can be applied to studies of MinC from various prokaryotic organisms. Additionally, evidence for protein-stabilizing determinants in the N-terminus of $MinC_{Ng}$ is a novel observation which can similarly be speculated for other MinC proteins as well as unrelated proteins. Through analysis of division-associated proteins such as $MinC_{Ng}$, it will eventually become possible to target antimicrobial agents to these proteins to impede cell division and control microbial growth.

STATEMENT OF COLLABORATION

The author of this study extends gratitude to all members of the laboratory of Dr. Jo-Anne Dillon for their advice and guidance during the course of the present study. All pVG- and pVAL- plasmids were constructed by V. Greco; other plasmids used in this research were constructed by those so accredited in Table 2. All pPF-plasmids were constructed by P. Fabre, a student completing an Honour's thesis, under the direct supervision of Dr. S. Ramirez-Arcos and V. Greco. Circular dichroism analysis of $MinC_{Ng}$ proteins was graciously performed by Dr. J. Wang and D. Fan (Southern Illinois University).

REFERENCES

Adler, H.I., W.D. Fisher, A. Cohen, and A.A. Hardigree. 1967. Miniature *Escherichia coli* cells deficient in DNA. PNAS. **57**: 321-326.

Aldea, M., T. Garrido, J. Pla, and M. Vicente. 1990. Division genes in *Escherichia coli* are expressed coordinately to cell septum requirements by gearbox promoters. EMBO J. 9: 3787-3794.

Alix, A.J. 2001. A turning point in the knowledge of the structure-function-activity relations of elastin. J. Soc. Biol. **195**:181-193.

Ayala, J.A., T. Garrido, M.A. De Pedro, M. Vicente. 1994. Molecular biology of bacterial septation. In: Hackenbec, R. and J.M. Ghuysen (eds). New comprehensive biochemistry bacterial cell wall, vol. 27. Elsevier, Amsterdam: pp. 73-101.

Ballicora, M.A., A.A. Iglesias, and J. Preiss. 2003. ADP-glucose pyrophosphorylase, a regulatory enzyme for bacterial glycogen synthesis. Microbiol. Mol. Biol. Rev. **67**: 213-225.

Begg, K.J. and W.D. Donachie. 1985. Cell shape and division in *Escherichia coli*: experiments with shape and division mutants. J. Bacteriol. **163**: 615-622.

Bernstein, D.A. and J.L. Keck. 2003. Domain mapping of *Escherichia coli* RecQ defines the roles of conserved N- and C-terminal regions in the RecQ family. Nucleic Acids Res. **31**: 2778-2785.

Bi, E. and J. Lutkenhaus 1991. FtsZ ring structure associated with division in *Escherichia coli*. Nature. **354:** 161-164.

Bogan, A.A. and K.S. Thorn. 1998. Anatomy of hot spots in protein interfaces. J. Mol. Biol. **280**: 1-9.

Bouvier, T., M. Troussellier, A. Anzil, C. Courties, and P. Servais. 2001. Using light scatter signal to estimate bacterial biovolume by flow cytometry. Cytometry. **44**:188-194.

Bradford, M.M. 1976. A rapid and sensitive method for the quantitation of microgram quantities of protein utilizing the principle of protein-dye binding. Anal. Biochem. 7: 248-54.

Bramhill, D. and C.M. Thompson. 1994. GTP-dependent polymerization of *Escherichia coli* FtsZ protein to form tubules. Proc. Natl. Acad. Sci. **91**: 5813-5817.

Cam, K., G. Rome, H.M. Krisch, and J.P. Bouche. 1996. RNAse E processing and essential cell division genes mRNA in *Escherichia coli*. Nucleic Acids Res. **24**: 3065-3070.

Carrio, M.M. and A. Villaverde. 2003. Role of molecular chaperones in inclusion body formation. FEBS Lett. **537**: 215-221.

Cha, J.H. and G.C. Stewart. 1997. The *div*IVA minicell locus of *Bacillus subtilis*. J. Bacteriol. **179**: 1671-83.

Chalmers, J.J., E. Kim, J.N. Telford, E.Y. Wong, W.C. Tacon, M.L. 1990. Effects of temperature on *Escherichia coli* over expressing beta-lactamase or human epidermal growth factor. Appl. Environ. Microbiol. **56**: 104-111.

Chien, C.T., P.L. Bartel, R. Sternglanz, And S. Fields. 1991. The two-hybrid system: a method to identify and clone genes for proteins that interact with a protein of interest. Proc. Natl. Acad. Sci. **88**: 9578-9582.

Clontech Laboratories, Inc. 1999. Matchmaker GAL4 Two-Hybrid System 3 & Libraries User Manual. BD Biosciences: Palo Alto, CA.

Cooperman, B.S., T. Wooten, D.P. Romero, and R.R. Traut. 1995. Histidine 229 in protein L2 is apparently essential for 50S peptidyl transferase activity. Biochem. Cell. Biol. **73**: 1087-1094.

Cordell, S.C., R.E. Anderson, and J. Lowe. 2001. Crystal structure of the bacterial cell division inhibitor MinC. EMBO J. **20**: 2454-2461.

Curtis, N.A., R.L. Eisenstadt, K.A. Turner, and A.J. White. 1985. Inhibition of penicillin-binding protein 3 of *Escherichia coli* K-12. Effects upon growth, viability, and outer membrane barrier function. J. Antimicrob. Chemother. **16**: 287-296.

Daniel, R.A. and J. Errington. 1993. DNA sequence of the *murE-murD* region of *Bacillus subtilis* 168. J. Gen. Microbiol. **139**: 361-370.

Daniel, R.A., A.M. Williams, and J. Errington. 1996. A complex four-gene operon containing essential cell division gene *pbpB* in *Bacillus subtilis*. J. Bacteriol. **178**: 199-230.

de Boer, P.A.J., R.E. Crossley, and L.I. Rothfield. 1988. Isolation and properties of *minB*, a complex genetic locus involved in correct placement of the division site in *Escherichia coli*. J. Bacteriol. **176**: 2106-2112.

de Boer, P.A.J., R.E. Crossley, and L.I. Rothfield. 1989. A division inhibitor and topological specificity factor coded for by the minicell locus determine proper placement of the division septum in *E. coli*. Cell **56**: 641-649.

de Boer, P.A.J., R.E. Crossley, and L.I. Rothfield. 1992. Roles of MinC and MinD in the site-specific septation block mediated by the MinCDE system of *Escherichia coli*. J. Bacteriol. **174**: 63-70

Dewar, S.J., V. Kagan-Zur, K.J. Begg, and W.D. Donachie. 1989. Transcriptional regulation of cell division genes in *Escherichia coli*. Mol. Microbiol. **3**: 1371-1377.

Dewar, S.J. and R. Dorazi. 2000. Control of division gene expression in *Escherichia coli*. FEMS Microbio. Lett. 187: 1-7.

Dillon, J.R. 1983. Laboratory methods for *Neisseria gonorrhoeae*. Publication H47-58/1983E, Health and Welfare Canada, Ottawa, Ontario.

Dogovski, C., J. Pi, and A.J. Pittard. 2003. Putative interhelical interactions within the PheP protein revealed by second-site suppressor analysis. J. Bacteriol. **185**: 6225-6232.

Donachie, W.D. and K.J. Begg. 1970. Growth of the bacterial cell. Nature (London). **227**: 1220-1224.

Donachie, W.D. 1993. The cell cycle of *Escherichia coli*. Annu. Rev. Microbiol. **47**: 199-230.

Douglas, H. 2002. Functional analysis of the conservd C-terminal residues of *Escherichia coli* MinC and of MinC proteins from *Escherichia coli* MinC and *Neisseria gonorrhoeae*. Department of Biology. University of Ottawa, Ontario. Honours Thesis.

Edwards, D.H. and J. Errington. 1997. The *Bacillus subtilis* DivIVA protein targets to the division septum and controls site specificity and cell division. Mol. Microbiol. **24**: 905-915.

Errington, J., R.A. Daniel, and D.J. Scheffers. 2003. Cytokinesis in bacteria. Microbiol. Mol. Biol. Rev. **67**: 52-65.

Fadda, D., C. Pischedda, F. Caldara, M.B. Whalen, D. Anderluzzi, E. Domenici, and O. Massida. 2003. Charachterization of *divVA* and other genes located in the chromosomal region downstream of the *dcw* cluster in *Streptococcus pneumoniae*. J. Bacteriol. **185**: 6209-6214.

Fields, S. and O. Song. 1989. A novel genetic system to detect protein-protein interactions. Nature. **34**: 245-246.

Fitz-James, P. 1964. Thin sections of dividing *Neisseria gonorrhoeae*. J. Bacteriol. **87**: 1477-1482.

Fox, K.K., J.S. Knapp, K.K. Holmes, E.W. Hook III, F.N. Judson, S.E. Thompson, J.A. Washington, and W.L. Whittington. 1997. Antimicrobial resistance in *Neisseria gonorrhoeae* in the United States, 1988-1994: The emergence of decreased susceptibility to the fluoroquinolones. J. Infect. Dis. **175**: 1396-1403.

Francis, F., S. Ramirez-Arcos, H. Salimnia, C. Victor, and J.R. Dillon. 2000. Organization and transcription of the division cell wall (*dcw*) cluster in *Neisseria gonorrhoeae*. Gene. **251**: 141-151.

Frazer, A.C. and R. Curtis III. 1975. Production, properties, and utility of bacterial minicells. Curr. Top. Microbiol. Immunol. **69**: 1-84.

Fukuchi, S., K. Yoshimune, M. Wakayama, M. Moriguchi, and K. Nishikawa. 2003. Unique amino acid composition of proteins in halophilic bacteria. J. Mol. Biol. **327**: 347-357.

Greco, V.S. 2001. Site-directed mutagenesis of the division inhibitor *minC* from *Neisseria gonorrhoeae* results in loss of protein functionality when heterologously expressed in *Escherichia coli*. University of Ottawa, Ontario. Honours Thesis.

Greco, V.S., L.K. Ng, R. Catana, H. Li, and J.R. Dillon. 2003. Molecular epidemiology of *Neisseria gonorrhoeae* isolates with plasmid-mediated tetracycline resistance (TRNG) in Canada: temporal and geographical trends (1986-1997). Microbial Drug Res. In press.

Greenfield, N. and G.D. Fasman. 1996. Computer circular spectra for the evaluation of protein conformation. Biochem. **8**: 4108.

Gunn, J. S. and D.C. Stein. 1996. Use of a non-selective transformation technique to construct a multiply restriction/modification-deficient mutant of *Neisseria gonorrhoeae*. Mol. Gen. Genet. **251**: 509-517.

Harry, E.J. and P.J. Lewis. 2003. Early targeting of Min proteins to the cell poles in germinated spores of *Bacillus subtilis*: evidence for division apparatus-independent recruitment of Min proteins to the division site. Mol. Microbiol. **47**: 37-48.

Hayashi, I., T. Oyama, and K. Morikawa. 2001. Structural and functional studies of MinD ATPase: implications for the molecular recognition of the bacterial cell division apparatus. EMBO J. **20**:1819-1828.

Health Canada. Canadian STD Guidelines - 1998 Edition. 1998. ISBN 0-662-27208-0. Health Canada Division of STD Prevention and Control, Ottawa, Canada.

Heinrichs, V. and B.S. Baker. 1997. *In vivo* analysis of the functional domains of the *Drosophila* splicing regulator RBP1. Proc. Natl. Acad. Sci. **94**: 115-120.

Hu, Z., A. Mukherjee, S. Pichoff, and J. Lutkenhaus. 1999. The MinC component of the division site selection system in *E. coli* interacts with FtsZ to prevent polymerization. Proc. Natl. Acad. Sci. **96**: 14819-14824.

Hu, Z. and J. Lutkenhaus. 2000. Analysis of MinC reveals two independent domains involved in interaction with MinD and FtsZ. J. Bacteriol. **182**: 3965-3971.

Hu, Z., A.P. Gogol, and J. Lutkenhaus. 2002. Dynamic assembly of MinD on phospholipid vesicles regulated by ATP and MinE. PNAS **99**: 6761-6766.

Hu, Z., C. Saez, and J. Lutkenhaus. 2003. Recruitment of MinC, an inhibitor of Z-ring formation, to the membrane in *Escherichia coli*: role of MinD and MinE. J. Bacteriol. **185**: 196-203.

Ison, C.A. 1996. Antimicrobial agents and gonorrhea: therapeutic choice, resistance and susceptibility testing. Genitourin. Med. 72: 253-257.

Ison, C.A., J.A. Dillon, and J.W. Tapsall. 1998. The epidemiology of global antibiotic resistance among *Neisseria gonorrhoeae* and *Haemophilus ducreyi*. Lancet. Suppl. **3**: 8-11.

Jaffe, A., R. D'Ari, and S. Hiraga. 1988. Minicell-forming mutants of *Escherichia coli*: production of minicells and anucleate rods. J. Bacteriol. **170**: 3094-3101.

Kato, Y. and Y. Asano. 2003. High-level expression of a novel FMN-dependent heme-containing lyase, phenylacetaldoxime dehydratase of *Bacillus* sp. strain OxB-1, in heterologous hosts. Protein Expr. Purif. **28**: 131-139.

Kellogg, Jr. D. S. W.L. Peacock, Jr., W.F. Deacon, L. Brown, and C. I. Pirkle. 1963. *Neisseria gonorrhoeae* I. Virulence genetically linked to clonal variation. J. Bacteriol. **85**: 1274-1279.

Klieger, G. and D. Eiserberg. 2002. GXXXG and GXXXA motifs stabilize FAD and NAD(P)-binding Rossman folds through C(alpha)-H... O hydrogen bonds and van der Waals interactions. J. Mol. Biol. **323**: 69-76.

Kong, G.K., G. Polekhina, G., W.J. McKinstry, M.W. Parker, B. Dragani, A. Aceto, D.R. Principe, B. Mannervik, and G. Stenberg. 2003. Contribution of glycine 146 to a conserved folding module affecting stability and refolding of human glutathione transferase p1-1. J. Biol. Chem. **278**: 1291-1302.

Krieg, N.R. and J.G. Holt. 1984. Bergey's Manual of Systematic Bacteriology, Vol. 1. Baltimore, MD: Williams & Wilkins.

Johnson, J.E., L.L. Lackner. and P.A. de Boer. 2002. Targeting of (D)MinC/MinD and (D)MinC/DicB complexes to septal rings in *Escherichia coli* suggests a multistep mechanism for MinC-mediated destruction of nascent FtsZ rings. J. Bacteriol. **184**: 2951-2962.

Johnson, S.R. and S.A. Morse. 1988. Antibiotic resistance in *Neisseria gonorrhoeae*: genetics and mechanisms of resistance. Sex. Transm. Dis. **15**: 217-24.

Knapp, J.S., K.K. Fox, D.L. Trees, and W.L. Whittington. 1997. Fluoroquinolone resistance in *Neisseria gonorrhoeae.* Emerg. Infect. Dis. **3**: 33-39.

Labie, C., F. Bouche, and J.P. Bouche. 1990. Minicell-forming mutants of *Escherichia coli*: suppression of both DicB- and MinD-dependent division inhibition by inactivation of the *minC* gene product. J. Bacteriol. **172**: 5852-5855.

Lackner, L.L., D.M. Raskin, and P.A.J. de Boer. 2003. ATP-dependent interactions between *Escherichia coli* Min proteins and the phospholipid membrane *in vitro*. J. Bacteriol. **185**: 735-749.

Levin, P.A., P.S. Margolis, P. Setlow, R. Losick, and D. Sun. 1992. Identification of the *Bacillus subtilis* genes for septum placement and shape determination. J. Bacteriol. **174**: 6717-6728.

Levin, P.A. and R. Losick. 1996. Transcription factor SpoOA switches the localization of the cell division protein FtsZ from a medial to bipolar pattern in *Bacillus subtilis*. Genes Dev. **10**: 478-488.

Lo Leggio, L. and S. Larsen. 2002. The 1.62 A structure of *Thermoascus aurantiacus* endoglucanase: completing the structural picture of subfamilies in glycoside hydrolase family 5. FEBS Lett. **523**: 103-108.

Lucet, I., A. Feucht, M.D. Yudkin, and J. Errington. 2000. Direct interaction between the cell division protein FtsZ and the cell differentiation protein SpoIIE. EMBO J. **19**: 1467-1475.

Lutkenhaus, J. and S. Addinall. 1997. Bacterial cell division and the Z ring Annu. Rev. Biochem. **66**: 93-116.

Lutkenhaus, J. and M. Sundaramoorthy. 2003. MinD and role of the deviant Walker A motif, dimerization and membrane binding in oscillation. Mol. Microbiol. **48**: 295-303.

Manieri, W., L. Franchini, L. Raeber, S. Dai, A.L. Stritt-Etter, and P. Schurmann. 2003. N-terminal truncation of the variable subunit stabilizes spinach ferredoxin:thioredoxin reductase. FEBS Let. **549**: 167-170.

Marin, E.P., A.G. Krishna, and T.P. Sakmar. 2002. Disruption of the alpha5 helix of transducin impairs rhodopsin-catalyzed nucleotide exchange. Biochem. **41**: 6988-6994

Margolin, W. 2001. Spatial regulation of cytokinesis in bacteria. Curr. Opin. Microbiol. **4**: 647-652.

Margolin, W. 2003. Bacterial division: the fellowship of the ring. Curr. Biol. **13**: R16-R18.

Marston, A.L., H.B. Thomaides, D.H. Edwards, M.E. Sharpe, and J. Errington. 1998. Polar localization of the MinD protein of *Bacillus subtilis* and its role in selection of the midcell division site. Genes Dev. **12**: 3417-3430.

Marston, A.L. and J. Errington. 1999. Selection of the mid-cell division site in *Bacillus subtilis* through MinD-dependent polar localization and activation of MinC. Mol. Microbiol. **33**: 84-96.

Martin, H., M.C. Castellanos, R. Cenamor, M. Sanchez, M. Molina, and C. Nombela. 1996. Molecular and functional characterization of a mutant allele of the mitogen-activated protein-kinase gene *SLT2(MPK1)* rescued from yeast autolytic mutants. Curr. Genet. **29**: 516-522.

Massidda, O., D. Anderluzzi, L. Friedli, and G. Feger. 1998. Unconventional organization of the division and cell wall gene cluster of *Streptococcus pneumoniae*. Microbiol. **144**: 3069-3078.

Meinhardt, H. and P.A. de Boer. 2001. Pattern formation in *Escherichia coli*: a model for the pole to pole oscillations of Min proteins and the localization of the division site. Proc. Natl. Acad. Sci. **98**: 14202-14207.

Migocki, M.D., M.K. Freeman, R.G. Wake, and E.J. Harry. 2002. The Min system is not required for precise placement of the midcell Z ring in *Bacillus subtilis*. EMBO reports. **3**: 1163-1167.

Miroux, B. and Walker, J.E. 1996. Over-production of proteins in *Escherichia coli*: mutant hosts that allow synthesis of some membrane proteins and globular proteins at high levels. J. Mol. Biol. **19**: 289-298.

Morse, S.A., S.R. Johnson, J.W. Biddle, and M.C. Roberts. 1986. High level tetracycline resistance in *Neisseria gonorrhoeae* is result of acquisition of streptococcal TetM determinant. Antimicrob. Agents Chemother. **30**: 664-670.

Mulder, E., C.L. Woldringh, F. Tetart, and J.P. Bouche. 1992. New *minC* mutations suggest different interactions of the same region of division inhibitor MinC with proteins specific for *minD* and *dicB* combination pathways. J. Bacteriol. **174**: 35-39.

Nanninga, N. and C.L. Woldringh. 1985. Cell growth, genome duplication, and cell division. Molecular cytology of *Escherichia coli*. London, UK: Academic Press.

Nilsson, I., A. Saaf, P. Whitley, G. Gafvelin, C. Waller, and G. von Heijne. 1998. Proline-induced disruption of a transmembrane alpha-helix in its natural environment. J. Mol. Biol. **284**: 1165-1175.

Norman, D.P., S.J. Chung, G.L. Verdine. 2003. Structural and biochemical exploration of a critical amino acid in human 8-oxoguanine glycosylase. Biochemistry. **42**:1564-1572.

Novagen. 2002. pET System Manual. Novagen: Madison, WI.

Osteryoung, K.W. and E. Vierling. 1995. Conserved cell and organelle division. Nature. **376**: 473-474.

Pagotto, F.J., H. Salimmia, P.A. Totten, and J.R. Dillon. 2000. Stable shuttle vectors for *Neisseria gonorrhoea, Haemophilus* spp. and other bacterial species based on a single origin of replication. Gene. **244**: 13-9.

Partanen, S., S. Storch, H.G. Loffle, A. Hasilik, J. Tyynela, and T. Braulke. 2003. A replacement of the active-site aspartic acid residue 293 in mouse cathepsin D affects its intracellular stability, processing and transport in HEK-293 cells. Biochem. J. **369**: 55-62.

Picard, F. J. and J. R. Dillon. 1989. Biochemical and genetic studies with arginine and proline auxotypes of *Neisseria gonorrhoeae*. Can. J. Microbiol. **35**: 1069-1075.

Pichoff, S., B. Vollrath, C. Touriol, and J.P. Bouche. 1995. Deletion analysis of gene *minE* which encodes the topological specificity factor of cell division in *Escherichia coli*. Mol. Microbiol. **18**: 321-329

Pucci, M.J., J.A. Thanassi, L.F. Discotto, R.E. Kessler, and T.J. Dougherty. 1997. Identification and characterization of cell wall-cell division gene clusters in pathogenic Gram-positive cocci. J. Bacteriol. **179**: 5632-5635.

QIAgen. 2001. HighSpeed™ Plasmid Purification Handbook. QIAgen: Mississauga, ONT.

QIAgen. 2002. QIAquick® Spin Handbook. QIAgen: Mississauga, ONT.

QIAgen. 2003. QIAprep® Miniprep Handbook. QIAgen: Mississauga, ONT.

Ramirez-Arcos, S., J. Szeto, T.J. Beveridge, C. Victor, F. Francis, and J.R. Dillon. 2001a. Deletion of the cell-division inhibitor MinC results in lysis of *Neisseria gonorrhoeae*. Microbiol. **147**: 225-237.

Ramirez-Arcos, S., H. Salimnia, I. Bergevin, M. Paradis, and J.R. Dillon. 2001b. Expression of *Neisseria gonorrhoeae* cell division genes *ftsZ, ftsE*, and *minD* is influenced by environmental conditions. Res. Microbiol. **152**: 781-791.

Ramirez-Arcos, S., J. Szeto, J.R. Dillon, and W. Margolin. 2002. Conservation of dynamic localization among MinD and MinE orthologs: oscillation of *Neisseria gonorrhoeae* proteins in *Escherichia coli*. Mol. Microbiol. **46**: 493-504.

Ramirez-Arcos, S., V. Greco, H. Douglas, and J.R. Dillon. 2003. Four conserved glycines in the C-terminus of MinC mediate protein-protein interactions essential for controlling bacterial cell division. In Preparation.

Ren, H., Y. Honse, B.J. Karp, R.H. Lipsky, and R.W. Peoples. 2003. A site in the fourth membrane-associated domain of the N-methyl-D-aspartate receptor regulates desensitization and ion channel gating. J. Biol. Chem. **278**: 276-283.

Rothfield, L.I. and S.S. Justice. 1997. Bacterial cell division: the cycle of the ring. Cell. **88**: 581-584.

Salimnia, H., A. Radia, S. Bernatchez, T.J. Beveridge, and J.R. Dillon. 2000. Characterization of the *ftsZ* cell division gene of *Neisseria gonorrhoeae*: expression in *Escherichia coli* and *N. gonorrhoeae*. Arch. Microbiol. **173**: 10-20.

Sambrook, J., E.F. Fritschand, and T. Maniatis. 1980. Molecular Cloning, 2nd ed. A Laboratory Manual. Cold Spring Harbour, NY: Cold Spring Harbour Press.

Sanchez, M., A. Valencia, M.J. Ferrandiz, C. Sander, and M. Vincente. 1994. Correlation between the structure and biochemical activities of FtsA, an essential cell division protein of the actin family. EMBO J. **13**: 4919-4925.

Sarwal, S., T. Wong, C. Sevigny, and L.K. Ng. 2003. Increasing incidence of ciprofloxacin-resistant *Neisseria gonorrhoeae* infection in Canada. CMAJ. **168**: 872-3.

Sen, M. and L.I. Rothfield. 1998. Stability of the *Escherichia coli* division inhibitor protein MinC requires determinants in the carboxy-terminal region of the protein. J. Bacteriol. **180**: 175-177.

Sefton, A.M. 2002. Mechanisms of antimicrobial resistance: their clinical relevance in the new millennium. Drugs. **62**: 557-66.

Shand, J.H., J. Beattie, H. Song, K. Phillips, S.M. Kelly, D.J. Flint, and G.J. Allen. 2003. Specific amino acid substitutions determine the differential contribution of the N- and C-terminal domains of insulin-like growth factor (IGF)-binding protein-5 in binding IGF-1. J. Biol. Chem. **278**: 17859-17866.

Shih, Y.L., X. Fu, G.F. King, T. Le, and L. Rothfield. 2002. Division site placement in *E. coli*: mutations that prevent formation of the MinE ring lead to loss in the normal midcell arrest of growth of polar MinD membrane domains. EMBO J. **21**: 3347-3357.

Shih, Y.L., T. Le, and L. Rothfield. 2003. Division site selection in *Escherichia coli* involves dynamic redistribution of Min proteins within coiled structures that extend between the two cell poles. Proc. Natl. Acad. Sci. **100**: 7865-7870.

Simmons, L.A., M. Felczak, J.M. Kaguni. 2003. DnaA Protein of *Escherichia coli*: oligomerization at the *E. coli* chromosomal origin is required for initiation and involves specific N-terminal amino acids. Mol. Microbiol. **49**: 849-858

Slatko, B.E. 1994. Thermal cycle dideoxy DNA sequencing. Methods Mol. Biol. **31**: 35-45.

Snyder, L.A., N.J. Saunders, and W.M. Shafer. 2001. A putatively phase variable gene (*dca*) required for natural competence in *Neisseria gonorrhoeae* but not *Neisseria meningitidis* is located within the division cell wall (*dcw*) gene cluster. J. Bacteriol. **183**: 1233-1241.

Snyder, L.A., W.M. Shafer, and N.J. Saunders. 2003. Divergence and transcriptional analysis of the division cell wall (*dcw*) gene cluster in *Neisseria* spp. Mol. Microbiol. **47**: 431-42.

Sparling, P.F., F.A. Sarubbi Jr., and E. Blackman. 1975. Inheritance of low-level resistance to penicillin, tetracycline, and chloramphenicol in *Neisseria gonorrhoeae*. J. Bacteriol. **124**: 740-749

Speare, J.O., T.S. Rush III, M.E. Bloom, and B. Caughey. 2003. The role of helix 1 aspartates and salt bridges in the stability and conversion of prion protein. J. Biol. Chem. **278**: 12522-12529

Spratt, B.G. 1988. Hybrid penicillin-binding proteins in penicillin-resistant strains of *Neisseria gonorrhoeae*. Nature. **32**: 173-176.

Sprinzak, E. and H. Margalit. 2001. Correlated sequence-signatures as markers of protein-protein interaction. J. Mol. Biol. **311**: 681-692.

Sullivan, S.M. and J.R. Maddock. Bacterial cell division: finding the dividing line. Curr. Biol. **10**: R249-R252.

Sun, Q. and W. Margolin. 2001. Influence of the nucleoid on placement of FtsZ and MinE rings in *Escherichia coli*. J. Bacteriol. **184**: 1413-1422.

Szeto, J., S. Ramirez-Arcos, C. Raymond, L.D. Hicks, C.M. Kay, and J.R. Dillon. 2001. Gonococcal MinD affects cell division in *Neisseria gonorrhoeae* and *Escherichia coli* and exhibits novel self-interaction. J. Bacteriol. **183**: 6253-6264.

Tamames, J., M. Gonzales-Moreno, J. Mingorance, A. Valencia, and M. Vicente. 2001. Bringing gene order to bacterial shape. Trends Genetics. **17**: 124-126.

Teather, R.M., J.F. Collins, and W.D. Donachie. 1974. Quantal behaviour of a diffusible factor which initiates septum formation at potential division sites in *Escherichia coli*. J. Bacteriol. **118**: 407-413.

Varley, A.W. and G.C. Stewart. 1992. The *divIVB* region of the *Bacillus subtilis* chromosome encodes homologs of *Escherichia coli* septum placement (MinCD) and cell shape (MreBCD) determinants. J. Bacteriol. **174**: 6729-6742.

Vicente, M., S.R. Kushner, T. Garrido, and M. Aldea. 1991. The role of the "gearbox" in the transcription of essential genes. Mol. Microbiol. **5**: 2085-2091.

Vicente, M., M.J. Gomez, and J.A. Ayala. 1998. Regulation of transcription of cell division genes in the *Escherichia coli dcw* cluster. Cell Mol. Life Sci. **54**: 317-324.

Weiss, D. S., J.C. Chen, J.M. Ghigo, D. Boyd, and J. Beckwith. 1999. Localization of FtsI (PBP3) to the Septal Ring Requires Its Membrane Anchor, the Z Ring, FtsA, FtsQ, and FtsL. J. Bacteriol. **181**: 508-520.

West, S. E. and V. L. Clark. 1989. Genetic loci and linkage associations in *Neisseria gonorrhoeae* and *Neisseria meningitidis*. Clin. Microbiol. Rev. 2: S92-S103.

Westling-Häggström, B. T. Elmros, S. Normark, and B. Winblad. 1977. Growth pattern and cell division in *Neisseria gonorrhoeae*. J. Bacteriol. **29**: 333-342.

Winson, M.K. and H.M. Davey. 2000. Flow cytometric analysis of microorganisms. Methods. **21**: 231-240.

Ye S., X. Su, Q. Wang, Y. Yin, X. Dai, H. Sun. 2002. Surveillance of antibiotic resistance of *Neisseria gonorrhoeae* isolates in China, 1993-1998. Sex. Transm. Dis. 29: 242-245.

Yura, T., H. Mori, H. Nagai, T. Nagata, A. Ishihama, N. Fujita, K. Isono, K. Mizobuchi, and A. Nakata. 1992. Systemic analysis of the *Escherichia coli* genome: analysis of the 0-2.4 min region. Nucleic Acids Res. **20**: 3305-3308.

Zhao, C.R., P.A. de Boer, and L.I. Rothfield. 1995. Proper placement of the *Escherichia coli* division site requires two functions that are associated with different domains of the MinE protein. Proc. Natl. Acad. Sci. **92**: 4313-4317.

Valerie Suzanne Greco

Education

2001 – 2004: M.Sc. (Biochemistry, Microbiology, and Immunology), University of Ottawa. Thesis title: Structural and functional analysis of the division inhibitor MinC from *Neisseria gonorrhoeae*.
Thesis supervisor: Dr. J. R. Dillon.

1997 – 2001 B.Sc. (Biology) with Honours Biotechnology option (Suma Cum Laude) University of Ottawa.
Honours project: Site-directed mutagenesis of essential residues of MinC from *Neisseria gonorrhoeae* results in loss of protein functionality.
Thesis supervisor: Dr. J. R. Dillon.

Work Experience

2001
Undergraduate NSERC summer scholarship recipient
Dr. J. R. Dillon, University of Ottawa

- Performed research involving the cell division protein FtsZ from *Neisseria gonorrhoeae.*
- Studies involved construction of a FtsZ-polyhistidine containing construct, optimizing a protein purification protocol, SDS-PAGE electrophoresis, Western blot analysis, and preliminary crystallization techniques.

2000
Undergraduate NSERC summer scholarship recipient
Dr. V. L. Trudeau, University of Ottawa

- Performed research involving the identification of novel glutamic acid decarboxylase (GAD) sequences from elasmobranches to elucidate GAD phylogeny.
- Research included basic molecular biology techniques to locate novel GAD sequences and intense bioinformatic analysis for sequence identification and phylogenetic tree construction.

1999 – 2000 (Part time)
Laboratory technician
Synthaid Biotechnology Institute
Dr. G. Alvarado

- Synthesized custom oligonucleotide primers and assisted with the synthesis of peptide sequences.
- Responsible for laboratory maintenance and product purchasing.
- Performed office duties including reception, processing and shipping/delivering orders, and account management.

1999 – 2000 (Part time)
Laboratory technician
Dr. I. Altosaar, University of Ottawa

- Responsible for general laboratory maintenance, product purchasing, and media and reagent preparation.
- Assisted with research of graduate students in various areas of plant molecular biology.

1999
Careers Canada summer research award recipient
Dr. I. Altosaar, University of Ottawa

- Learned basic molecular biology principals and assisted graduate student and post-doctoral fellows with various research projects involving transgenic tobacco and rice.
- Responsible for general laboratory maintenance, journal club presentations, and product purchasing.

Related Work Experience

Fall 2001 and 2002
Teaching assistant of general microbiology undergraduate course
University of Ottawa, Faculty of Biology

- Assisted lesson and test preparation, maintained course web page, and answered student questions.
- Evaluated tests, entered and submitted grades, and proctored examinations.

1997-1998
Co-operative education student and hospital technician
Navan Veterinary Hospital

- Responsible for general hospital maintenance, animal care, and customer service/administration.

- Laboratory technician with duties including blood, skin, and urinalysis, bacterial staining and culture, microscopy of biological samples, serological analysis, automated endocrinological analysis, and antimicrobial susceptibility testing.

Other Skills

- ***Microbiology:*** culture, isolation and identification of bacterial species using biochemical and growth-dependant assays as well as commercially-available products, preparation of culture media, antimicrobial susceptibility testing, light and phase-contrast microscopy.
- ***Molecular biology:*** DNA and RNA isolation, Polymerase Chain Reaction (PCR) and Reverse Transcriptase (RT) – PCR, DNA and RNA gel electrophoresis (agarose and SDS-PAGE), plasmid construction, protein SDS-PAGE electrophoresis, Northern, Southern, and Western blot analysis, antibody purification, protein purification, oligonucleotide and peptide synthesis.
- ***Computer:*** All Windows operating systems, Microsoft Word, Powerpoint, Excel, Wordperfect, Netscape Navigator and Internet Explorer, web-based bioinformatic tools (BLAST, sequence analysis, restriction mapping, multiple alignment, phylogenetic tree construction), protein structural analysis (CN3D), molecular biology software (Primer Design).

Peer-Reviewed Publications

Lariviere, K., MacEachern, L., **Greco, V.,** Majchrzak, G., Chiu, S., Drouin, G., and Trudeau, V. 2002. GAD_{65} and GAD_{67} isoforms of the glutamic acid decarboxylase gene originated before the divergence of cartilaginous fish. Mol. Biol. Evol. 19: 2325-2329.

Greco, V., Ng, L.K., Catana, R., Li, H., and Dillon, J.R. 2003. Molecular Epidemiology of *Neisseria gonorrhoeae* Isolates with Plasmid-mediated Tetracycline Resistance (TRNG) in Canada: Temporal and Geographical Trends (1986-1997). Microbial Drug Resistance. In press.

Ramirez-Arcos, S., **Greco, V.,** Douglas, H., and Dillon, J.R. 2003. Four conserved glycines in the C-terminus of MinC mediate protein-protein interactions essential for controlling bacterial cell division. J. Bacteriol. In Press.

In Preparation

Greco, V., Ramirez-Arcos, S., and J. R. Dillon. 2003. Truncation of 13 amino acids from the N-terminal of MinC from *Neisseria gonorrhoeae* results in abrogation of protein function. Manuscript in preparation.

Conference Posters and Presentations

Greco, V. and I. Altosaar. 1999. Expression of antimicrobial peptides from *Sarcophaga peregrina* in transgenic rice. Internation Rice Research Institute Annual Conference. Ottawa, Canada.

Lariviere, K., L. MacEachern, **V. Greco**, and V. L. Trudeau. 2000. Multiple forms of GAD likely arose prior to the divergence of Chondrichtheys. 20th Conference of European Comparative Endocrinology. Faro, Portugal.

Dillon, Jo-Anne R., S. Ramirez-Arcos, P. Thibault, J. Szeto, and **V. Greco**. 2001. Cell division proteins MinC and MinD from *Neisseria gonorrhoeae* as potential antimicrobial targets. Center for Research in Biopharmaceuticals. University of Ottawa, Ottawa, Canada.

Ramirez-Arcos, S., **V. Greco**, H. Douglas, and J. R. Dillon. 2002. Four conserved glycines in the C-terminus of MinC are essential for protein functionality. International Pathogenic Neisseria Conference. Madrid, Spain.

V. Greco and J. R. Dillon. 2003. Structural and functional analysis of the division inhibitor MinC from *Neisseria gonorrhoeae*. Graduate student seminar presentation, Department of Biochemistry, Microbiology, and Immunology, University of Ottawa.

V. Greco, L. K. Ng, R. Catana, H. Li, and J. R. Dillon. 2003. Molecular Epidemiology of *Neisseria gonorrhoeae* Isolates with Plasmid-mediated Tetracycline Resistance (TRNG) in Canada: Temporal and Geographical Trends (1986-1997). 2003 ISSTDR Congress. Ottawa, Canada.